MARTIN MARIETTA ENERGY SYSTEMS LIBRARIES
3 4456 0361365 9

CENTRAL RESEARCH LIBRARY
DOCUMENT COLLECTION

PAH

ORNL-2676
Reactors-Power

cy-125

GAS-COOLED REACTOR PROJECT

SEMIANNUAL PROGRESS REPORT

FOR PERIOD ENDING DECEMBER 31, 1958

CENTRAL RESEARCH LIBRARY
DOCUMENT COLLECTION
LIBRARY LOAN COPY
DO NOT TRANSFER TO ANOTHER PERSON
If you wish someone else to see this document, send in name with document and the library will arrange a loan.

OAK RIDGE NATIONAL LABORATORY
operated by
UNION CARBIDE CORPORATION
for the
U.S. ATOMIC ENERGY COMMISSION

Printed in USA. Price $3.00 Available from the

Office of Technical Services
U. S. Department of Commerce
Washington 25, D. C.

LEGAL NOTICE

This report was prepared as an account of Government sponsored work. Neither the United States, nor the Commission, nor any person acting on behalf of the Commission:

A. Makes any warranty or representation, express or implied, with respect to the accuracy, completeness, or usefulness of the information contained in this report, or that the use of any information, apparatus, method, or process disclosed in this report may not infringe privately owned rights; or

B. Assumes any liabilities with respect to the use of, or for damages resulting from the use of any information, apparatus, method, or process disclosed in this report.

As used in the above, "person acting on behalf of the Commission" includes any employee or contractor of the Commission to the extent that such employee or contractor prepares, handles or distributes, or provides access to, any information pursuant to his employment or contract with the Commission.

ORNL-2676

Reactors - Power
TID-4500 (14th ed., Rev.)

Contract No. W-7405-eng-26

GAS-COOLED REACTOR PROJECT

SEMIANNUAL PROGRESS REPORT

for Period Ending December 31, 1958

Staff

Oak Ridge National Laboratory

DATE ISSUED
MAR 2 1959

OAK RIDGE NATIONAL LABORATORY
Oak Ridge, Tennessee
operated by
UNION CARBIDE CORPORATION
U.S. ATOMIC ENERGY COMMISSION

MARTIN MARIETTA ENERGY SYSTEMS LIBRARIES

3 4456 0361365 9

GAS-COOLED REACTOR PROJECT SEMIANNUAL PROGRESS REPORT

INTRODUCTION AND SUMMARY

This report is the initial report in a series of semiannual reports on gas-cooled reactor research and development at the Oak Ridge National Laboratory. It covers the accomplishments during the 10-month period since the issuance of the report, The ORNL Gas-Cooled Reactor, ORNL report 2500. The program is divided into two principal parts: design investigations and materials research and testing. Most of the activities described were initiated in support of the prototype gas-cooled power reactor (GCPR) designed by Kaiser Engineers-ACF Industries. Some advanced reactor design studies were made, and basic design studies required to facilitate design review work were completed that have application beyond the limited review objective.

In furtherance of an assigned responsibility for providing the fuel elements for the GCPR, methods for fabricating and testing fuel elements were developed. Tests of mechanical properties were undertaken as required to obtain the information needed in the development of the fuel elements. In-pile and out-of-pile tests of the components and materials of the reactor core were also initiated.

PART I. DESIGN INVESTIGATIONS

1. REACTOR SYSTEMS

The possibility of developing graphite-moderated Th-U^{233} breeder reactors that would satisfy the demands of an expanding power economy was investigated. In order to achieve this goal, systems that could produce their entire inventory in 5 to 10 years would be required. The results of multigroup calculations, which depended on the normalization of η for U^{235}, showed very little net breeding of U^{233}.

A reactor capable of utilizing fuel elements that would operate at 1800°F or above was considered. Since refractory materials would have to be used for such fuel elements and such materials are not capable of complete retention of fission products, the activation of the primary coolant

would be significant. In order to study such a system, a preliminary design of a 3095-Mw (thermal) helium-cooled graphite-moderated reactor employing graphite-UO_2 fuel elements was prepared. In estimating the cost of such a plant it was considered that maintenance would be performed by remote removal and replacement of components followed by remote maintenance work on the failed component in a hot cell. An operating charge to maintenance of 0.75 mill/kwhr was assigned, and the plant load factor was reduced to 0.75. The capital cost of such a power station per electrical kilowatt would be about $220, and the production cost of electrical power would be 7.8 mills/kwhr.

The possibility of coupling a reciprocating engine to a gas-cooled nuclear reactor was investigated and found to be promising for power outputs up to 30,000 bhp. A single gas is used as both the reactor coolant and as the working fluid of the thermodynamic cycle, and thus much complicated pumping and heat exchange equipment is eliminated. The overall thermal efficiency of the plant is about 30% with a peak gas temperature of 1100°F.

2. DESIGN STUDIES

A study was made of the thermal performance of the seven-rod-cluster fuel element proposed for the gas-cooled reactors now being studied. Marked circumferential variations in the rod surface temperatures as a result of channeling of the coolant stream were indicated by numerical calculations. The analysis also revealed the possibility of thermal instability of the fuel elements. The temperature variations in the cluster could cause bowing of the rods. An analysis is being made of an arrangement in which the channel wall is scalloped.

The design work on the GCR-2 system indicated the need for a thorough study of steam generators for gas-cooled reactor systems. Since the steam generators are a large factor in the cost of the system, detailed information is needed for plant optimization. Methods are being developed for coding the heat transfer and pressure drop characteristics for machine solution, and studies are under way of heat transfer and pressure drop correlations.

A steam system that would utilize 1500°F reactor outlet gas was investigated. It was found that scaled-up versions of the GCR-2 steam generators could remove 2.25 times as much heat per boiler with a 3-ft shorter tube matrix because of the higher gas-to-steam temperature difference.

In connection with the review of the support structure designed for the GCPR, equations for analyzing such a structure were derived. The equations include the effects of bending, shear, and torsion. Codes for solving the equations and evaluating the results were written for IBM calculation.

An experimental program was initiated at the University of Tennessee to study the effect of geometry and materials on the buckling of cylindrical shells, such as fuel capsules, at room temperature. The results of these studies will be correlated with the results of creep-buckling tests being conducted by the ORNL Metallurgy Division.

In connection with the study of a reactor that would employ graphite-UO_2 fuel elements, an estimate was made of the level of activity that could be expected in the primary coolant as a result of release of fission products from the fuel. It was found that the activity in the coolant would be about 0.2% of the activity generated in the fuel, with the difference being due to the ability of the fuel to hold up the release of the short-lived nuclides until they have decayed to daughters of longer life.

A survey was made of the costs of various reactor systems in order to obtain a basis for evaluating gas-cooled reactor costs. The survey showed that the most important factor affecting nuclear power plant capital costs is the net output capacity of the plant and that in the range of capacities above 125 Mw there is little difference between the many types of reactors on the basis of cost.

3. EXPERIMENTAL INVESTIGATIONS OF HEAT TRANSFER AND FLUID FLOW

The friction characteristics of a bare seven-rod fuel-element cluster of the GCR-2 geometry were established for two tube center-to-center spacings. No significant difference was observed between the results of

the two spacings. The friction data are being used to determine the contribution of spacers and hangers to the over-all pressure drop in a full-scale model of a GCR-2 fuel channel.

Methods are being studied for redistributing coolant flow in fuel element channels to minimize circumferential surface temperature asymmetries. Two entrance region swirl generator assemblies are being prepared.

Preliminary circumferential surface temperature profiles have been obtained for the central tube and one of the peripheral tubes of a seven-rod cluster in an electrical resistance-heated-tube apparatus. The similarity of the temperature patterns around the peripheral tube at varying axial positions indicated stable flow in the vicinity of this tube. The observed asymmetry in the profile is believed to reflect the specific entrance conditions of the apparatus. Lower surface temperature variations around the central tube suggested a more nearly uniform velocity distribution in this region. There also appeared to be a slight swirl to the flow around the central tube.

Qualitative visual observations were made of tube bowing by using an apparatus in which the tubes were internally heated. With the specific tube center-to-center spacing used, the peripheral tubes bowed outward. Initial experiments have been completed in which mass transfer from naphthalene rods arranged in a GCR cluster geometry to flowing air was measured. Calculations based on an analogy between the mass transfer and heat transfer indicated a strong effect of tube spacing on the circumferential variation of the local heat transfer coefficient.

4. ADVISORY SERVICE TO AEC ON PROTOTYPE EXPERIMENTAL GAS-COOLED POWER REACTOR

A detailed review was made of the Kaiser Engineers-ACF Industries design of the prototype experimental gas-cooled power reactor. Specific recommendations developed in the review were transmitted to the AEC.

An evaluation review was also made of the Sanderson and Porter and Alco Products Company Report, S and P 1963, The Pebble Bed Reactor. It was concluded that the pebble bed reactor shows promise of being

competitive with other gas-cooled power reactors if the fuel lifetime is adequate and the coolant contamination can be controlled sufficiently to permit economical maintenance of the system.

A survey was made of the Oak Ridge Area to identify possible sites for the construction of a gas-cooled reactor. In cooperation with the AEC Oak Ridge Operations Office and K-25 personnel, site evaluation reports were prepared for two sites.

Studies of plant control were made to facilitate the design review work. In these studies analog computations were performed to examine the variations in temperatures and nuclear power that would result from a severe drop in heat removal from the fuel or by a startup accident in which there was no heat removal and continuous withdrawal of the control rods.

A study of possible coolants for the GCPR limited the choice to CO_2 and helium. The compatibility of graphite and CO_2 at the temperatures of interest has not been established. The considerations with regard to helium were availability and cost. It was found that, if the proposed helium conservation program of the Bureau of Mines is implemented, there will be an adequate helium supply for a reactor power complex of substantial size. A general study was also made which showed the effect of coolant choice on power cost increment, and the effects of impurities on the induced activity in the various gases were examined. Preliminary studies were completed which showed that steam would have many advantages as a coolant, but means of preventing contact of the steam and graphite would have to be provided or a different moderator material would have to be used.

PART II. MATERIALS RESEARCH AND TESTING

5. METALLURGICAL DEVELOPMENTS

A process for the fabrication of UO_2 pellets was developed in which the number of operations is minimized in order to cut fuel costs. The process now being used in pilot-plant-scale production involves only granulation, forming by dry pressing, and sintering in an induction furnace.

The highly sinterable UO_2 powder required for this process is prepared from partially enriched UF_6 in a continuous process that can be integrated into a production facility that starts with UF_6 and ends with a finished UO_2 shape. Thermogravimetric and differential thermal analyses, followed by forming and sintering tests, provide the required quality control and evaluation of the UO_2 powder.

Uranium dioxide pellets for use in fuel capsule irradiation tests are being fabricated. The finished pellets are evaluated by a series of physical measurements.

The fabrication of highly dense UO_2 rods by extrusion is being investigated under a subcontract at the Electric Auto-Lite Company. The binders and plasticizers that can be used in the least amounts to produce the highest density are being sought.

Creep-buckling and tube-burst tests of the type 304 stainless steel tubing selected for fabrication of fuel capsules are being performed to evaluate the material experimentally. The integrity of the capsule is essential for the retention of fission gases.

The different modes of collapse of tubes under external pressure were determined, and the collapse of fuel capsule tubing by creep buckling was predicted. No failures were observed in any tests, even when complete collapse of a capsule without pellets occurred. The conditions necessary for uniform collapse of capsule tubing around the pellets were determined at temperatures ranging from 1300 to 1700°F. Since the required conditions would be difficult and expensive to achieve, the possibility of collapsing the tubing under controlled conditions of pressure and temperature before inserting the fuel element into the reactor is being evaluated as a means of preventing wrinkles and gaps and the resultant hot spots. The possible effects of cracks that might develop in the UO_2 during operation and the effect of a hot streak along the length of a capsule are also being studied.

The possibility of failure of a capsule from internal pressure is being studied in long-time burst tests. The end cap welds failed in the capsules tested initially, and new capsules prepared according to improved machining and welding specifications are now being tested.

The reactions of type 304 stainless steel with the impurities of helium and the contaminants that would be evolved by graphite during reactor operation were predicted. It was found that the principal impurities would be CO, CO_2, CH_4, H_2O, H_2, and other metastable gases derived from radiation effects. A program of tests of the individual gases and controlled mixtures of the gases was initiated to obtain the information required in the design of purification equipment for the reactor gases.

The procedures to be used in dye-penetrant and eddy-current inspections of tubing for fuel capsules were specified, and quality standards were established. Since tubing manufacturers are equipped to perform the necessary inspections, investigations of the effectiveness of such in-plant inspections are being made. It is hoped that the manufacturer's inspection will suffice.

Difficulty is being encountered in the eddy-current inspection of tubing because of the presence of anomalous conditions that are not detrimental. Attempts are being made to desensitize the eddy-current system to these conditions.

A number of experiments are being conducted to determine the optimum design for the fuel capsule end closure. Welding conditions were established for three types of closure: a butt weld, a plug weld, and an edge weld. Short-time, high-temperature burst tests of the three types of closures were not selective; in each case failure occurred in the tube wall. Long-time tests at lower pressures are now under way.

Suitable welding conditions were determined for fabricating end closures on machined beryllium tubes. Both edge-fusion and plug-weld designs were used successfully. These welds are brittle, but should be suitable for sealing capsules.

The compatibility of beryllium with TSF graphite and helium at 1400°F was studied in static pot tests. The beryllium specimens scaled badly, but the gas analysis of the system did not differ significantly from that of other tests with stainless and low-alloy steels.

6. IN-PILE TESTING OF COMPONENTS AND MATERIALS

A program of irradiation tests of prototype fuel capsules is under way for which facilities in the LITR, ORR, ETR, and GETR are being utilized. The results of these tests will be correlated with the results of out-of-pile heat transfer and flow tests to evaluate the seven-rod-cluster fuel element design The irradiation experiments are designed to test the mechanical stability of the capsule and of the UO_2 pellets and to examine the integrity of end closures. Pellet geometry, irradiation temperature, UO_2 density,fuel burnup, and thermal cycling are the variables to be investigated. Equipment required for irradiation of full diameter and reduced-size prototype capsules is being constructed.

Irradiations of miniature capsules were initiated early in 1958. The purpose of these tests is to determine the extent to which fission gases are released from the UO_2 crystal lattice into the fuel capsule, the effect of UO_2 density on the release, and the effect of high thermal stress on the stability of the pellets. Measurements and analyses of the fission gases released during irradiation of two miniature capsules were completed. The fission gases detected were Kr^{88}, I^{131}, Xe^{133}, and Xe^{135}.

An experimental facility designed for studying fuel materials, rather than fuel elements, at high temperatures in a radiation field is being constructed at the ORR. Of immediate interest are graphite-clad UO_2 compacts, and various ceramic materials will be tested in future experiments.

A hot cell in ORNL Building 3025 is being modified as required for examination of irradiated specimens. The ORR hot cell will be used for other operations on specimens, and some examinations will be performed at the General Electric Vallecitos Atomic Laboratory.

In studies of advanced reactor materials, the effects of irradiation on the calibration of the noble-metal thermocouples that will be required at the temperatures that will be used in the studies of ceramic fuel elements are being tested. Experiments were initiated to evaluate the usefulness of SiC-Si clad high-density graphite as a moderator for use at high temperatures. Equipment is being assembled for studying the instantaneous fission-gas release of ceramic fuel materials.

7. OUT-OF-PILE TESTING OF MATERIALS AND COMPONENTS

The extent of the reactions between graphite and its impurities and the various other materials required in gas-cooled reactor systems is being investigated in out-of-pile materials compatibility tests. The experimental equipment being utilized consists of pots in which the materials can be heated in a controlled static environment and loops in which the gas is circulated by natural convection over the materials of interest. A forced-circulation loop for studying graphite erosion and the aerodynamic characteristics of fuel element bundles is being constructed.

The results obtained thus far indicated that rapid outgassing of graphite occurs at the temperatures of interest and that the impurity content of the coolant gas decreases with time from a maximum value. The maximum impurity concentration of the gas depends on the maximum temperature and the type of graphite. The metals tested thus far have been stainless and low-alloy steels, Fe-Al alloys, columbium, Inconel, molybdenum, zirconium, zirconium-base alloys, and beryllium. With the exception of zirconium and beryllium, the data indicate that these materials would be suitable as structural materials for helium-graphite systems.

Experimental studies of the quantity and composition of the gas evolved by different types of graphite at various temperatures has been started. Preliminary results of tests in the temperature range 200 to 1000°C indicate that there are differences in composition of gases evolved by different types of graphite and that the composition is affected by the temperature. The effect of specimen geometry is to be studied, and data are to be obtained at temperatures up to 2000°C.

8. DEVELOPMENT OF TEST LOOPS AND COMPONENTS

A facility is being designed for in-pile testing of the heat transfer characteristics of advanced fuel elements. The loop is being designed for a power generation of 40,000 Btu/hr·ft for a single rod at loop pressures from 300 to 400 psig and gas coolant temperatures of up to 1500°F. Work done previously on the design of similar facilities for the ORR is being utilized.

Special gas compressors are being developed for in-pile and out-of-pile forced-circulation loop tests. Low leakage requirements are being met by enclosing the centrifugal compressors, motors, and bearings in a housing containing the process gas for the loop. Both grease-lubricated and gas bearings are being considered. For use with the gas-bearing compressors, a motor is being developed that will be operable at temperatures of 600 to 1000°F. Facilities for testing compressors are being designed and constructed.

CONTENTS

INTRODUCTION AND SUMMARY iii

PART I. DESIGN INVESTIGATIONS

1. REACTOR SYSTEMS 3
   Graphite-Moderated Th-U^{233} Breeder Systems 3
   Contaminated Coolant System 6
   Nuclear Gas Engines 8

2. DESIGN STUDIES 10
   Thermal Analysis of Fuel Elements 10
   Steam Systems and Components 13
   Structural Investigations 15
      Stress Analysis of Grid Structure 15
      Tube-Buckling Experiments 17
   Release of Activity from Fuel Elements 18
   Steam Generators for a Helium-Cooled Reactor Operating with a Gas Outlet Temperature of 1500°F 23
   Cost and Equipment Surveys 24

3. EXPERIMENTAL INVESTIGATIONS OF HEAT TRANSFER AND FLUID FLOW 26
   Fluid Friction Characteristics 26
   Flow Modification Studies 36
   Resistance-Heated-Tube Heat Transfer Experiment 36
   Globar Heat Transfer Experiment 45
   Mass Transfer Analogy to Heat Transfer 47

4. ADVISORY SERVICE TO AEC ON PROTOTYPE EXPERIMENTAL GAS-COOLED POWER REACTOR 55
   Design Review 55
   Site Investigations 56
   Plant Control Studies 56
      Startup Accident 57
      Loss of Coolant 58
   Reactor Coolant Investigations 59

PART II. MATERIALS RESEARCH AND TESTING

5. METALLURGICAL DEVELOPMENTS 67
   Fabrication of Bulk UO_2 Fuel 67
      Minimized Fabrication Process 67
      Preparation of UO_2 Powder 71
      Quality Control and Evaluation of UO_2 Powder 73
      Fabrication and Evaluation of Fuel Pellets 73
      Extrusion of UO_2 76

Mechanical Properties of Fuel Capsule Material..... 77
Creep Buckling of Capsule Tubing..... 77
Tube-Burst Testing of Type 304 Stainless Steel..... 81
Reactions of Type 304 Stainless Steel with Gases..... 85
Manufacturing Developments..... 90
Inspection of Fuel Capsules..... 90
Fuel Capsule End Closures..... 93
Beryllium Investigations..... 97
Welding of Beryllium..... 97
Compatibility of Beryllium with Coolants..... 101

6. IN-PILE TESTING OF COMPONENTS AND MATERIALS..... 105

Fuel Element Irradiation Program..... 105
Full-Diameter Prototype Fuel Capsule Irradiations..... 106
Reduced-Size Prototype Fuel Capsule Irradiation..... 112
Miniature Capsule Fission-Gas-Release Experiments..... 113
Examinations of Irradiated Capsules..... 114
Prototype Capsules..... 114
Miniature Capsules..... 116
Closed-Cycle-Loop Irradiation Facility..... 120
Hot Cell Modifications..... 124
Thermocouple Irradiation Studies..... 127
SiC-Si Cladding for High-Density Graphite..... 132
Instantaneous Fission-Gas Study..... 135

7. OUT-OF-PILE TESTING OF MATERIALS AND COMPONENTS..... 138

Reactor Materials Compatibility Tests..... 138
Gas Evolution By Graphite..... 147

8. DEVELOPMENT OF TEST LOOPS AND COMPONENTS..... 160

Large ORR In-Pile Loop..... 160
Special Gas Compressors..... 161
Grease-Lubricated Compressors..... 161
Gas-Bearing Compressors..... 161
High-Temperature Electric Motors..... 163
Compressors for Argon Forced-Circulation Loop..... 163
Supporting Activities..... 163

PART I. DESIGN INVESTIGATIONS

1. REACTOR SYSTEMS

GRAPHITE-MODERATED Th-U^{233} BREEDER SYSTEMS

The possibility of breeding with a graphite-moderated gas-cooled reactor operating on the Th-U^{233} fuel cycle was investigated.[1] Primary importance was placed on the development of a system which could satisfy the demands of an expanding power economy. Since the doubling time of the demand for power in this country is approximately 5 to 10 years, systems were sought which could produce their entire inventory of fissionable material at least this rapidly. Many of the results of the study, however, are not restricted by this condition and apply quite generally to graphite-moderated-U^{233} systems.

Simple considerations showed that the short doubling time requirement could not be met by a reactor in which a significant fraction of the thorium was mixed with the U^{233}. This is due to the high neutron flux required in the fissionable material and the low flux necessary in the thorium to avoid excessive losses in the breeding cycle because of neutron absorption in Pa^{233}, the precursor of U^{233}. A two-region system is thus preferred in which all the fertile material is in a blanket surrounding the fissile core.

In order to study the neutron thermalization properties of such a system, a series of multigroup calculations was performed for homogeneous mixtures of graphite and U^{233} of essentially infinite size. The results of these calculations are presented in Fig. 1.1. For low values of the carbon-to-U^{233} ratio the system is not well thermalized, and the low value of η in the resonance region of U^{233} results in a low average η for the spectrum. The maximum attainable breeding ratio is thus quite low. On the other hand, dilute mixtures of U^{233} in graphite result in excessive absorptions in graphite, and, even though η is high, the attainable breeding ratio is again low. The maximum breeding ratio of 1.18 is reached with a carbon-to-U^{233} ratio of 7000. The product ηf has a maximum for a carbon-to-U^{233} ratio of 5000.

---

[1] A. M. Perry, C. A. Preskitt, and E. C. Halbert, A Study of Graphite-Moderated Th-U^{233} Breeder Systems, ORNL-2666 (to be published).

Detailed calculations were next performed for specific system configurations. A three-region cylindrical reactor was considered that consisted of a graphite-U^{233} core, a graphite-thorium blanket, and a region of pure graphite of variable density between core and blanket. The purpose of this buffer region of graphite was to flatten the core power distribution, to provide reactivity control by variable core leakage, and to allow some degree of reflector moderation and thus possibly to permit some of the neutrons to avoid the resonance region of U^{233} where η is low. The initial carbon-to-U^{233} ratio was chosen to be 4000, since the loss of U^{233} by burnup would then not seriously affect the multiplication factor and the breeding ratio would approach its maximum value.

An initial survey established that with a core radius of 51 cm, a buffer thickness of 16 cm, a blanket thickness of 90 cm, and a carbon-to-thorium ratio of 20, the desired low thermal flux would be produced in the fertile material and there would be adequate reactivity control by the buffer. Multigroup burnup calculations were performed for this system, and the isotopic composition of the blanket was obtained through six successive core loadings. The buffer density was increased as a core burned out so that k was kept at unity by shifting neutrons from the blanket to the core to make up for losses in fission products. The core lifetime was reached when full graphite density in the buffer could no longer maintain k at unity. A burnup of 35 to 45% was achieved. The blanket lifetime was reached when enough U^{233} had been built into the blanket that the lowest buffer density could not control a fresh core loading. About eight core cycles were possible. A typical core cycle is shown in Fig. 1.2.

The core and blanket reprocessing cycle has been analyzed and the inventory summary for the core and blanket through six core cycles (249 days) is shown below:

	Amount (kg)
Th^{232} burnup,	181.9
Pa^{233} loss,	2.2
U^{233} burnup (blanket),	3.0
Final blanket inventory of U^{233},	176.7
Blanket processing loss (0.8%),	1.4
Core processing loss (1.0%),	2.1

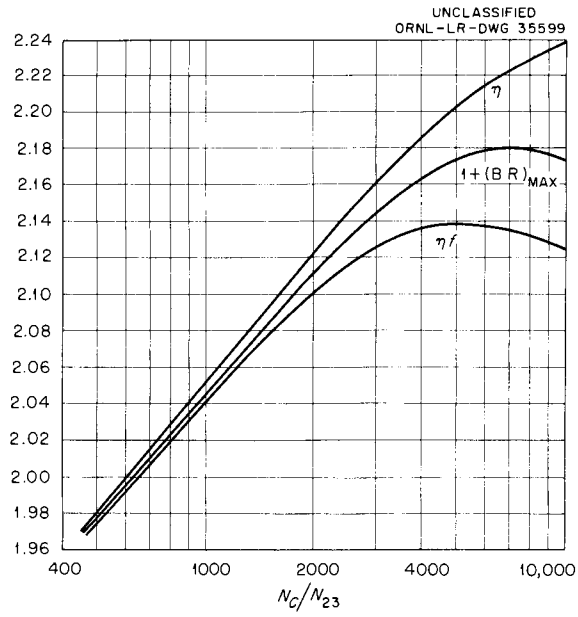

Fig. 1.1. Effect of the Carbon-to-U^{233} Ratio on Breeding in a Graphite-U^{233} System.

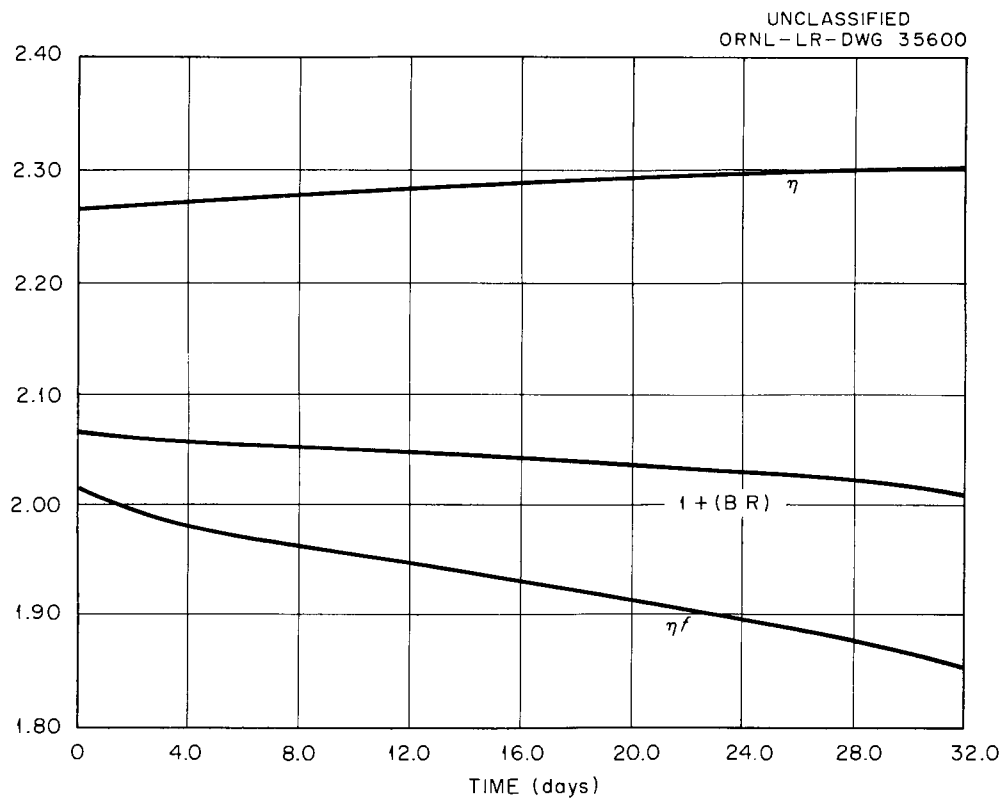

Fig. 1.2. Breeding Properties of First Core Loading.

	Amount (kg)
U^{233} burnup (core),	172.6
Net consumption and loss of U^{233},	176.1
Net amount of bred U^{233}.	0.6

It is concluded from these results that there is very little, if any, net breeding of U^{233}. This result is, in fact, independent of the requirement of a short doubling time and is the result of the poor thermalization of the most lightly loaded systems which can be tolerated from a parasitic absorption standpoint. It must be pointed out, however, that these results depend strongly on the normalization of η for U^{233}. Whereas the doubling time of the above system is essentially infinite with the normalization $\eta = 2.28$ at 2200 m/sec assumed here, if η is as high as 2.37 at 2200 m/sec, or if for any reason the average value of η in the reactor spectrum is actually 0.09 greater than it appears to be from these calculations, then a doubling time of 10 years would be obtained.

CONTAMINATED COOLANT SYSTEM

One possible way of reducing the cost of power from a gas-cooled reactor to below that estimated for the GCR-2 (ref 2 – 4), is to obtain a fuel element capable of operating at temperatures of 1800°F or above. Such a fuel element, with which both high heat fluxes and high power densities may be attained, seems to lead to low capital charges and low fuel costs. Metal fuel element capsules capable of operation at 1800°F are not available, however, and a refractory material would have to be employed. Such materials are not capable of complete retention of fission products, and therefore the primary coolant would contain appreciable activity. It is immediately obvious that such a system is penalized by the need for additional containment, additional shielding, and remote maintenance. The additional costs

---

[2] The ORNL Gas-Cooled Reactor, ORNL-2500 (April 1, 1958).

[3] The ORNL Gas-Cooled Reactor Materials and Hazards, ORNL-2505 (June 19, 1958).

[4] The ORNL Gas-Cooled Reactor Advanced Concepts, ORNL-2510 (Sept. 18, 1958).

imposed on the plant by these features must be evaluated against improved reactor and system performance, including better neutron economy and higher fuel and gas temperatures, and the lower fuel and capital costs which follow from these improvements.

A preliminary design of a 3095-Mw (thermal) helium-cooled graphite-moderated reactor (HGCR-1) employing graphite-UO_2 fuel elements has been prepared.[5] At design conditions, 1500°F reactor outlet gas would be circulated to eight steam generators to produce 1050°F, 1450-psi steam which would be converted to electrical power in eight 157-Mw (electrical) turbogenerators (see chap. 2). The over-all efficiency of this power station is 36.5%.

The fuel element plates consist of 25 vol % 200-μ UO_2 particles and graphite, and they operate with a maximum surface temperature of 2000°F. The heat flux of 245,000 Btu/hr·ft^2 in the 3/8-in. thick plates results in a core power density of 7.9 w/cm^3 and a specific power of 36.2 w/g.

The significant activity released from the unclad graphite-UO_2 fuel appears to be less than 0.2% of that produced and is equivalent to 0.002 curies/cm^3 in the primary helium circuit (see chap. 2). Although the disposition of the activity throughout the primary circuit is unknown, the cost of shielding and containment may be estimated. Maintenance of the plant would be performed by remote removal and replacement followed by remote maintenance work on the failed component in a hot cell. The following direct and indirect maintenance costs were included in the cost analyses: (1) spare components, (2) remote servicing equipment, (3) hot cells for component repair, and (4) an operating charge to maintenance of 0.75 mill/kwhr. Further the plant load factor was reduced to 0.75 to allow for the more time-consuming remote maintenance.

The capital cost of this nuclear power station per electrical kilowatt would be about $220, and the production cost of electrical power would be 7.8 mills/kwhr. Both of these cost figures must be considered in light of the plant size of 3095 Mw (thermal). These figures are based on

---

[5] W. B. Cottrell et al., The HGCR-1: A Nuclear Power Station Employing a High-Temperature Gas-Cooled Reactor with Graphite-UO_2 Fuel Elements, ORNL-2653 (Jan. 23, 1959).

those for the GCR-2, and because of the conservative approach used in the GCR-2 in the cost evaluation there is reason to believe that the relative cost position of the contaminated reactor plant will improve as a consequence of the development of equipment and additional studies of fuel fabrication, fuel lifetime, and fission-product release rates.

NUCLEAR GAS ENGINES

Experience in automotive, marine, and other fields has indicated that reciprocating engines are lighter, more compact, and more economical than steam turbines for many applications. The possibility of coupling a reciprocating engine to a gas-cooled nuclear reactor has been investigated and found to appear quite promising for power outputs up to 20,000 to 30,000 bhp.[6] The cost and weight of such a plant appear to be less than two-thirds of the corresponding values for a pressurized-water reactor plant. The savings are realized because the use of fuel elements made of UO_2 in stainless steel capsules cooled by nitrogen or helium makes it possible to use a single gas as both the reactor coolant and the working fluid of the thermodynamic cycle. This eliminates the complication and expense of high-temperature and high-pressure heat exchangers and pumps, together with much piping and instrumentation and control equipment.

The cycle is somewhat similar to that of a gas turbine. The principal difference is that the compression and expansion processes carried out with a piston and cylinder approach the ideal isentropic processes much more closely than is possible in a turbine type of machine, particularly for medium to high compression ratios. This, in turn, makes possible over-all thermal efficiencies for the plant of around 30% with a peak gas temperature of 1100°F. A gas turbine would require a peak gas temperature of about 1500°F to achieve the same thermal efficiency. In view of the great difficulty in getting satisfactory fuel elements for operation at greater than 1500 to 1600°F, and in view of heat transfer requirements and allowances for hot spots which make it very difficult to get a reactor gas outlet temperature much closer than 400°F to the maximum fuel element surface temperature, there appears to be a vital difference between the nuclear gas

[6] A. P. Fraas, Nuclear Gas Engine, ORNL CF-58-9-12 (Nov. 28, 1958).

engine and the nuclear gas turbine; the former appears achievable with known materials, while the latter does not unless severe contamination of the gas is accepted so that unclad ceramic fuel elements can be used.

The principal fields of application of the nuclear gas engine appear to include marine and stationary power plants up to about 20,000 to 30,000 bhp. For these applications the reactor could be graphite-moderated with a core perhaps 10 ft high and 8 ft in diameter. The fuel elements could be essentially similar to those proposed in ORNL-2500 (ref 2) with a fuel enrichment of about 3%. For portable or mobile power plants in which fuel costs are less important, a much smaller reactor core with highly enriched fuel could be employed to effect a drastic reduction in reactor and shield weight. The weight of the rest of the power plant would be essentially the same as for a conventional reciprocating engine of the same output.

2. DESIGN STUDIES

THERMAL ANALYSIS OF FUEL ELEMENTS

In the ORNL GCR-2 study[1] and in the subsequent designs of Kaiser Engineers-ACF Industries the proposed fuel assembly is a seven-rod cluster of stainless-steel-clad UO_2 pellets in a triangular array. From the heat transfer point of view, such an element provides both a large ratio of surface area to volume without the use of fins and an internal thermal path sufficiently short to keep the central temperature down.

In order to determine the thermal performance of the seven-rod cluster in a circular passage, an analytical investigation[2] of the temperatures throughout the fuel rods and coolant passages was made. For the calculations the following assumptions were made: (1) The eddy diffusivities for momentum and heat transfer were equal. (2) The flow was fully established, that is, the axial temperature gradient was constant in directions perpendicular to flow. (3) The total thermal conductivity, that is, the sum of the gas thermal conductivity and that due to the eddy diffusivity, was constant and isotropic. (4) The heat generation rate in the fuel was identical for all seven rods. (5) There was no heat transferred to or from the wall of the channel. (6) The velocity of the gas in the channel was a function of the distance to the nearest surface and was defined by the "universal velocity distribution."[3]

The calculations were made numerically on the IBM 704 digital computer for three different channel diameters: 3.05, 3.25, and 3.45 in. In all cases the rods were assumed to be 0.75 in. in diameter with the six outer rods centered on a 2.17-in.-dia circle. The results are presented in Fig. 2.1.

It is interesting to compare the local rod surface temperature in the hottest region of the reactor, as obtained from the above-described

---

[1] The ORNL Gas-Cooled Reactor, ORNL-2500 (April 1, 1958).

[2] L. G. Epel and W. T. Furgerson, Temperature Structure in Gas-Cooled Reactor Fuel Elements and Coolant Channel, ORNL CF-58-5-97 (May 27, 1958).

[3] R. C. Martinelli, Trans. ASME 69, 947 – 959 (1947).

calculations, with the corresponding value of 1200°F obtained from the conventional Dittus-Boelter equation ($Nu = 0.023\ Re^{0.8}\ Pr^{0.4}$). Examination of the results presented in Fig. 2.1 shows a marked circumferential variation. This arises from channeling of the coolant stream into heated and relatively unheated filaments. The magnitude of this temperature variation depends, of course, on the values used for the eddy diffusivities in the machine calculations. Recent experimental data suggest that the values used in the calculations were too low and that the actual temperature variation is about one-sixth as great as that calculated.

The results of the machine calculations give a good qualitative picture of the heat transfer process in fuel elements composed of bundles of rods, even though the data may not be quantitatively useful. For example, channeling, or stratification, of the fluid stream leads not only to local hot zones, but to a mean wall temperature higher than the average indicated by the Dittus-Boelter equation.

The analysis also revealed the possibility of thermal instability of fuel rod clusters, as shown in Fig. 2.2, which gives the temperature difference across the outer fuel rods. The data presented in Fig. 2.2 predict a 4°F temperature difference across the outer rods for each 0.001-in. variation in the channel diameter. Although no calculations were made to determine the effect of shifting the location of the rods, it is probable that thermal performance would be at least as sensitive to location as to variations in the channel diameter. Unless the rods are extremely short the temperature difference will lead to a shift in position as a result of bowing, which, in turn, will increase the temperature difference across the rods and eventually result in excessive temperatures in the capsule wall. (Experimental investigations of heat transfer and fluid flow in fuel channels are described in chap. 3).

The temperature structure analysis is also being applied to a seven-rod-cluster arrangement in which the channel wall is scalloped, as shown in Fig. 2.3. The calculations have been completed for only one case. For the spacing chosen the temperature variation on the surface of the element was found to be about 200°F, which was the best attainable in a circular channel if the spacing were optimized. Since the rod spacing chosen for

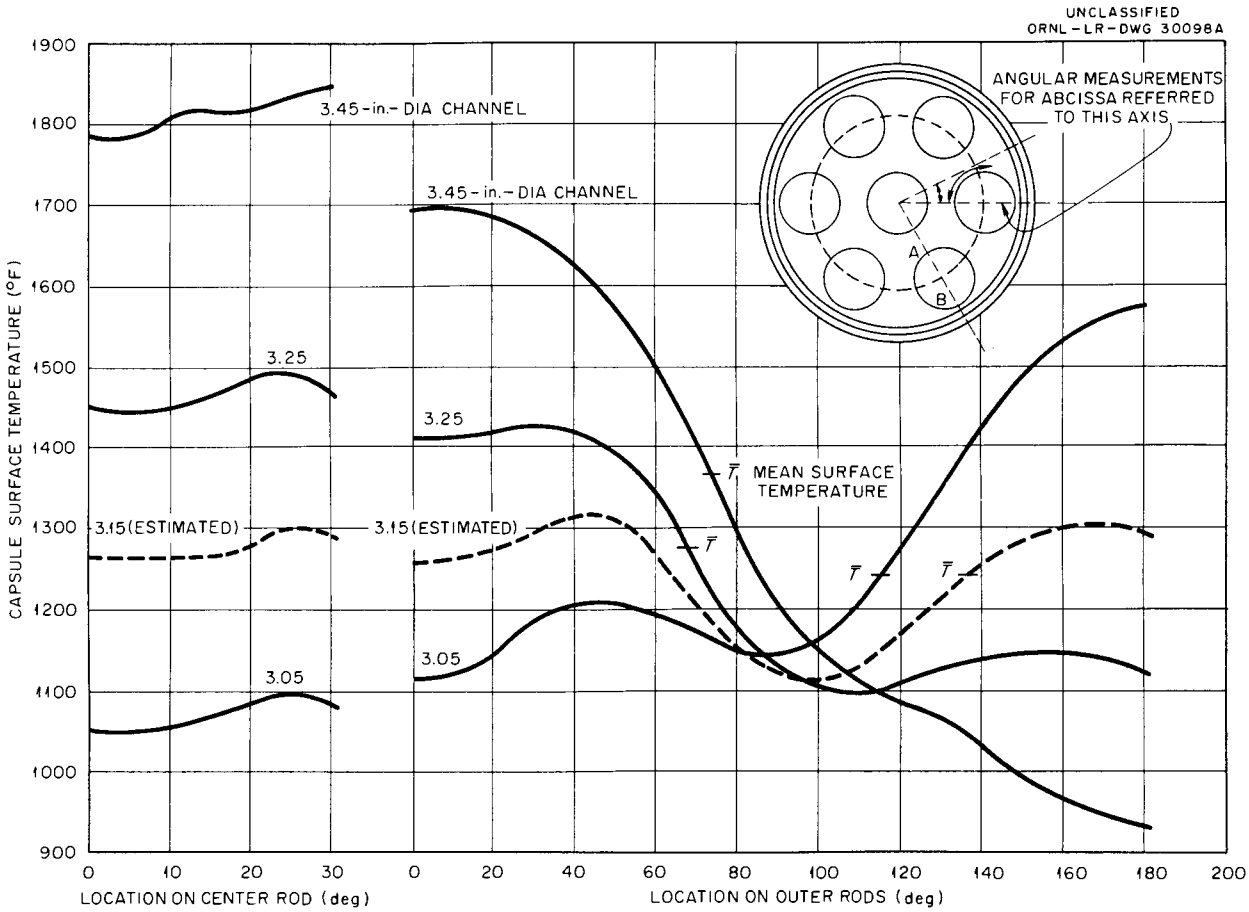

Fig. 2.1. Angular Variation of Capsule Surface Temperature.

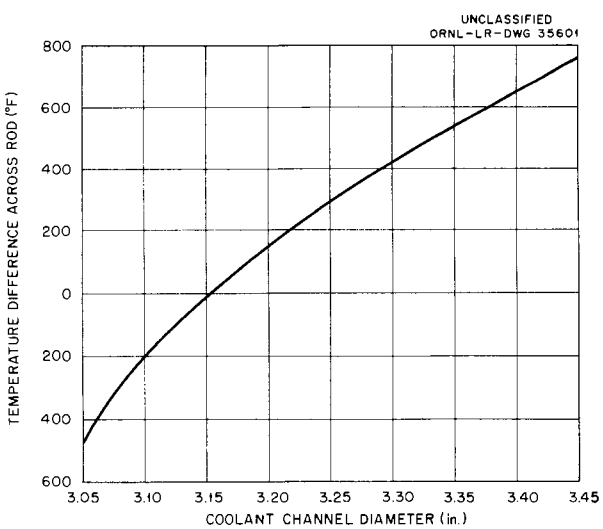

Fig. 2.2. Temperature Difference Across Outer Fuel Rods as a Function of the Coolant Channel Diameter.

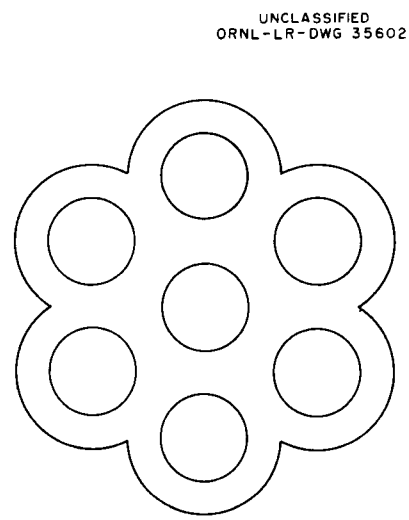

Fig. 2.3. Seven Rod Fuel Element in Scalloped Channel.

this first case was somewhat arbitrary, it is hoped that the optimum spacing will give a temperature variation well below 200°F. A minimum of two additional calculations will be required to evaluate the arrangement.

STEAM SYSTEMS AND COMPONENTS

In carrying out detailed design work on GCR-2 systems, it became evident that the unique characteristics of the steam generators should be studied more thoroughly in order to obtain the information needed for plant optimization. The cost of power is strongly influenced by the steam generator costs, which were found to represent approximately 10% of the total plant equipment cost.

The design conditions differ radically from those for steam generators in fossil-fueled steam plants in that there is no radiant transfer of heat in the steam generators and the heat transfer surfaces remain very clean over the entire life of the plant. An attempt is being made to develop methods for coding the heat transfer and pressure drop characteristics of the steam generator for numerical solution.[4] A partial review of the literature was made[5] and studies are under way to obtain the best heat transfer and pressure drop correlations available for use in calculations of the steam generator performance and in the solution to optimization problems, and a mechanical design study of the GCR-2 steam generator was undertaken to identify and solve specific problems related to costs and optimization.

A complete solution of the heat transfer and pressure drop equations for a steam generator of the type proposed for GCR-2 involves a very lengthy set of calculations. In the optimization of the over-all plant for minimum power cost, these calculations must be repeated many times to determine the effects of the significant variables. The calculations are

---

[4] R. I. Gray, An Outline for a Machine Calculation of a Gas-System Steam Generator, ORNL-2663 (to be published).

[5] R. I. Gray, Literature Pertinent to a Steam Generator Design for a Gas-Cooled Reactor System, ORNL CF-58-10-87 (Oct. 24, 1958).

complicated because on the steam side the problem includes heat transfer and pressure drop solutions for water in the economizer, for two-phase, mixed, steam and water flow in the boiler, and for dry steam in the superheater.

The complexities of the problem may be illustrated by observing that the temperature at which boiling occurs is dependent upon the pressure, that the pressures are functions of velocities and geometry, and that the heat transfer is a function of the temperature driving force which, in turn, is a function of the temperature at which boiling occurs. Obviously a mathematical steam generator model set up for machine solution is needed both for making rapid calculations with enough iterations to converge on a precise solution and for evaluating the optimization effects of a much larger number of parameters than could be evaluated by hand calculation. The method of approach to the coding problem is to define a set of input or independent variables that will facilitate matching the steam generator parameters to reactor parameters for the purpose of integrating the steam generator optimization into an over-all plant optimization study.

A steam system optimized on the basis of heat transfer and pressure drop evaluations must also be shown to be fabricable according to good practices before it can be said to be the truly optimized unit for minimum cost power. Therefore the mechanical design of the GCR-2 steam generator was studied to identify fabrication problems which might appreciably affect a purely analytical optimization. Drawings were prepared to determine accurately the sizes and weights of components, to identify and eliminate interferences between closely spaced parts such as return bends in the tube matrix, to establish the detailed geometries upon which to base refinements in heat transfer and pressure drop calculations, and to work out erection sequences to assure accessibility for welding and inspection. The techniques developed in this specific study should be applicable to the mechanical design analysis of systems developed in the optimization studies.

STRUCTURAL INVESTIGATIONS

Stress Analysis of Grid Structure. The core of a gas-cooled reactor with vertical fuel channels must be supported by a structure which does not adversely affect the flow of coolant and which covers a minimum of the lower surface of the reactor. A grillage beam arrangement which is supported at its outer edge and covered by a plate for transmitting loads to the beams was used in the Calder Hall design and is being proposed by Kaiser Engineers-ACF Industries for the prototype enriched gas-cooled power reactor (GCPR). This type of structure offers the advantages of a low depth requirement and increased accessibility to the reactor face, as compared with a truss arrangement. These considerations are of great importance where the fuel is loaded and unloaded from the bottom of the reactor.

Equations for analyzing a grid structure such as that proposed (Fig. 2.4) have been derived. These equations include the effects of bending, shear, and torsion. The analysis applies to a rectangular arrangement of beams with the ends of the beams simply supported. All beams are assumed to have a uniformly distributed load of the same magnitude; however, this loading can be modified to include concentrated loads or to vary the magnitudes of the distributed loads for various beams. These modifications are restricted only by the requirement for symmetry about the two centerlines.

The rigidities (cross sections) of the beams can also vary from beam to beam so long as the symmetry requirement is not violated. Thus, through the use of the equations derived, the beam size can be optimized for a given configuration and loading.

The expression for the lateral deflection is given by

$$w = \sum_m \sum_n a_{mn} \sin \frac{n\pi x}{L_x} \sin \frac{m\pi y}{L_y} , \qquad (m,n = 1, 3, 5, - - -)$$

where, as shown in Fig. 2.4, x and y are coordinates and L_x and L_y are lengths in x and y directions, respectively. The coefficients, a_{mn}, are determined by considering the strain energy in the beams. To facilitate the analysis of any beam arrangement, a program is being prepared for the IBM 704 to solve each of the equations for displacements, slopes, and other factors. In addition, a code has been written for making these

UNCLASSIFIED
ORNL-LR-DWG 35603

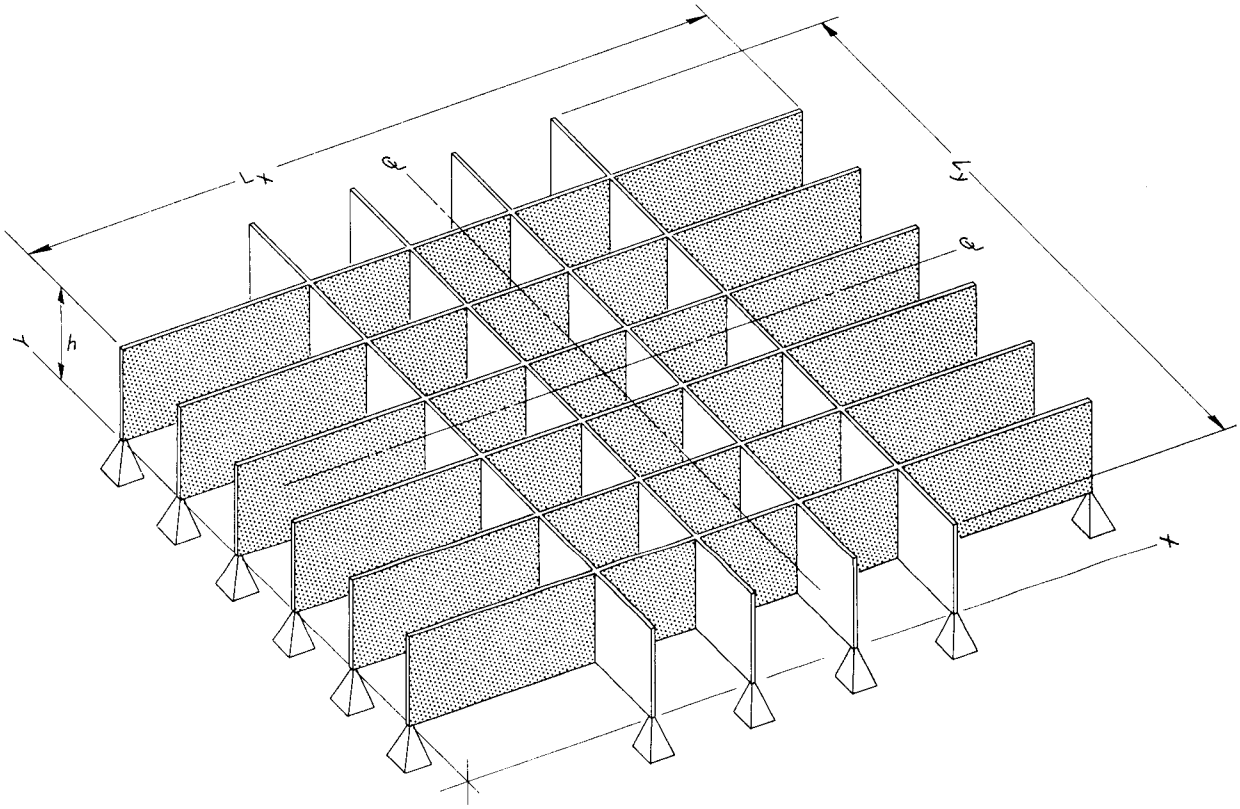

Fig. 2.4. Coordinate System of Grid Structure.

evaluations on the IBM 610; however, the analysis is limited to a square system of beams where only the bending rigidity is considered.

Tube-Buckling Experiments. Cylindrical shells are widely used as structural elements. Despite this usage, very little information is available regarding their creep-buckling behavior. Therefore, their use as fuel containers, such as those of the septafoil fuel element clusters proposed for the GCR-2 and the prototype enriched gas-cooled power reactor or as pressure vessels requires that creep-buckling data be obtained.

The variables related to the buckling of shells are primarily those of geometry and materials. The geometric variables are length, radius, wall thickness, diametral clearance between the tube and an element inside (such as a fuel element), ellipticity, eccentricity, and surface finish. Among the many material properties to be considered are tangent (or reduced) modulus,[6] secondary creep, and strength. Other important properties will become apparent as more information concerning creep buckling becomes available.

An experimental program has been set up to study the influence of the above factors upon the creep buckling of cylindrical shells. Since buckling without creep is not fully understood, the relationships between the geometric variables and the buckling modes and critical pressures will be established in room temperature (no creep) tests. When these correlations have been made, the effect of these variables on creep-buckling behavior can be more readily determined. Following a thorough investigation of the geometry effects, the influence of materials properties can be evaluated.

The University of Tennessee has established facilities for the room-temperature testing in which shells will be subjected to external pressure with and without axial loads. The creep-buckling tests for studying both geometric variables and materials properties are being done by the ORNL Metallurgy Division (see chap. 5).

The pressure chamber for the initial room-temperature tests at the University of Tennessee has been completed. This unit is suitable for testing tubes up to 1.25 in. in diameter and 12 in. long at pressures up

[6]This quantity replaces the modulus of elasticity in cases of plastic or creep buckling.

to 8000 psi. When the pressure is not more than 3000 psi, diametral measurements of the cylinder can be obtained to within ± 0.0002 in. These measurements are taken through the use of pairs of spindles which can be adjusted to contact the tube, as shown in Fig. 2.5. The spindles are located at three axial positions, 1 1/4 in. apart, and they are arranged for measuring the change in three diameters at 120-deg intervals for each axial station.

The dimensions of the tubes or cylinders must be closely controlled. Therefore, the final tube dimensions are obtained by honing the inside and grinding the outside of each tube. Instrumentation has been set up for measuring the wall thickness to ± 0.0001 in. at any position on a tube. Equipment is now available for fabricating tubing having inside diameters from 0.650 to 0.750 in. with a maximum variation of ± 0.00025 in., and equipment for extending the range to include diameters from 0.625 to 1.250 in. is being procured.

All the tubes tested thus far have buckled in the mode shown in Fig. 2.6. The tubes shown were made of aluminum and had an inside diameter of 0.700 in., a wall thickness of 0.020 in., and a length of 11 in. No fillers were used. The buckling pressure for all tubes was 1460 ± 50 psi; thus, good reproducibility of results was obtained. Variations in the rate of load application appeared to have no effect upon the critical pressure for these specimens.

RELEASE OF ACTIVITY FROM FUEL ELEMENTS

The release of activity from fuel elements is normally maintained at a very low level by using a capsule or cladding material which will retain the fission products. Reactors that have such fuel elements operate with a relatively low level of activity in the primary coolant. On the other hand, the use of unclad fuel elements of the type proposed for the system (HGCR-1) described in Chapter 1 would result in the release of large amounts of radioactivity into the coolant.

In order to estimate the level of activity in the primary gas system of a reactor operating with unclad fuel, the release of fission products from UO_2-graphite fuel elements was investigated.[7] A fuel element composed

[7] W. B. Cottrell et al., The HGCR-1: A Nuclear Power Station Employing A High-Temperature Gas-Cooled Reactor with Graphite-UO_2 Fuel Elements, ORNL-2653 (Jan. 23, 1959).

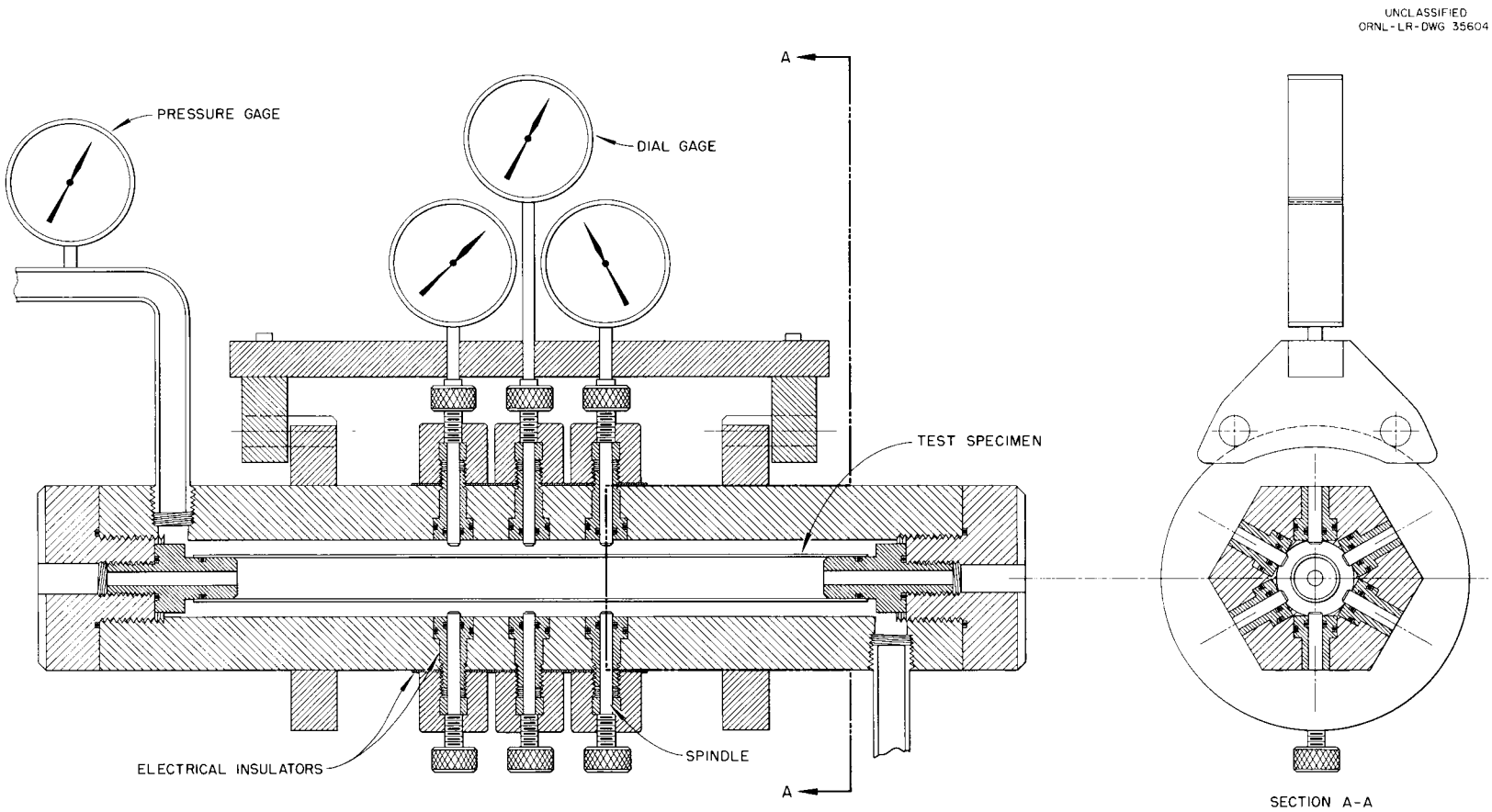

Fig. 2.5. Pressure Vessel Assembly for Tube-Buckling Tests.

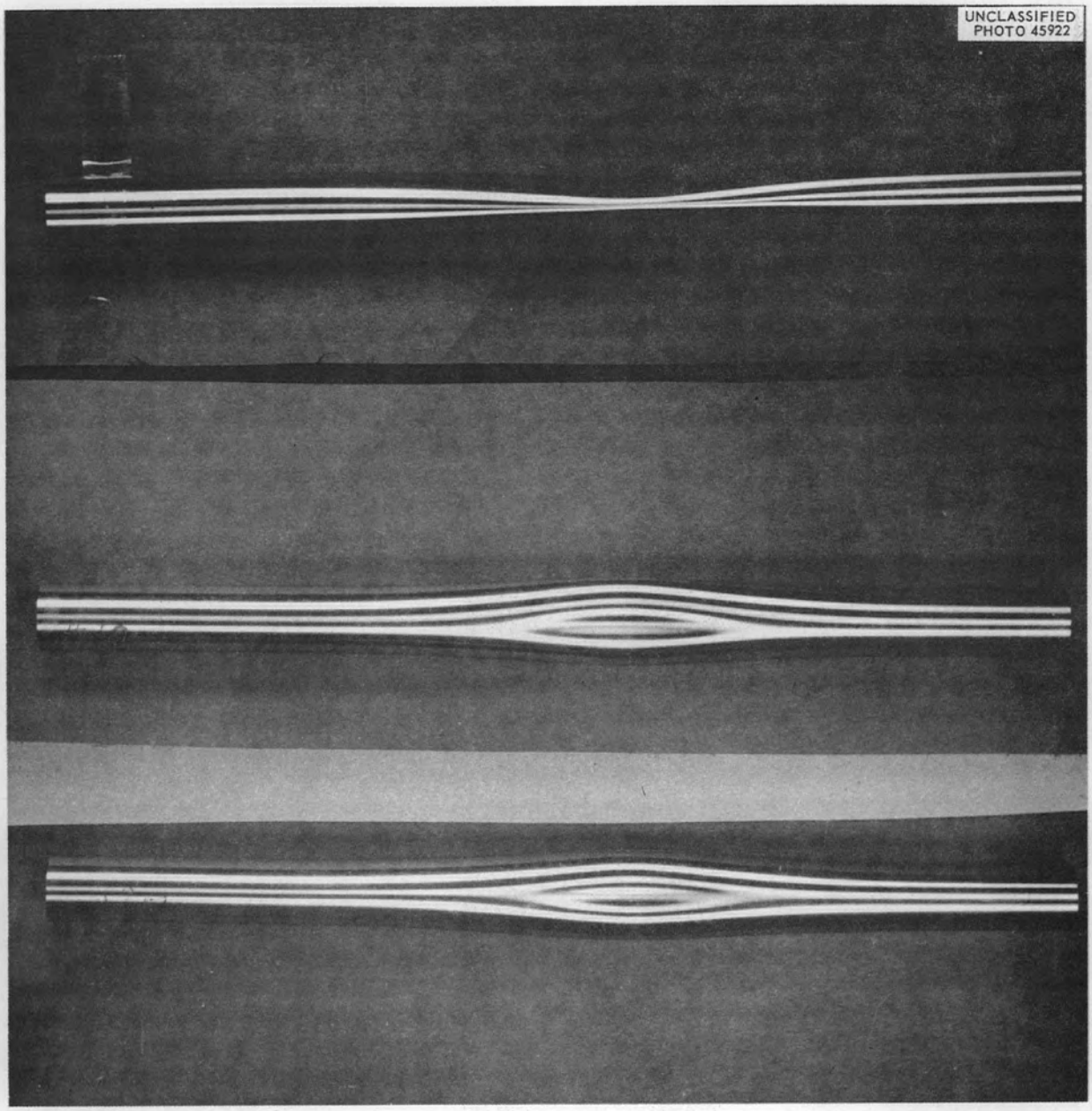

Fig. 2.6. Buckled Cylinders.

of UO_2 and graphite releases fission products by two processes: (1) diffusion of fission products directly from the UO_2 and (2) recoil of fission products from the UO_2 into the graphite followed by diffusion out of the graphite. The relative importance of the two processes in releasing fission products into the coolant depends primarily upon the choice of UO_2 particle size and the temperature at which the fuel operates during normal reactor operation.

The method used in predicting the release of the various fission products from UO_2 and from the graphite was based on the solid-state diffusion of a particular isotope in the fuel material. The equations used were developed at the Westinghouse Bettis Plant and at Chalk River.[8 – 11] For the study of the release of activity from the unclad fuel, the equations given by Eichenberg et al.[8] were used. Since the available experimental information concerning the diffusion coefficients of various elements in UO_2 is meager, the diffusion coefficients of Xe, Kr, Rb, Br, I, and Cs were assumed to be the same as the reported[8] diffusion coefficient of Kr. It would be expected that all the fission products would have the ability to diffuse from UO_2, but the study was limited to the six elements mentioned because the reported experiments[8] indicate that the release of other nuclides is small in comparison.

The release of activity from the graphite was investigated by the same method as that used for predicting the release of activity from the UO_2. However, in this case it was possible to determine the diffusion coefficients of the various fission-product elements in graphite. With the use of the same model for the release of a nuclide from the graphite as from UO_2, diffusion coefficients were calculated based on data obtained in

---

[8] J. D. Eichenberg et al., Effects of Irradiation on Bulk UO_2, WAPD-183 (Oct. 1951).

[9] A. H. Booth and G. T. Rymer, Determination of the Diffusion Constant of Fission Xenon in UO_2 Crystals and Sintered Compacts, CRDC-720 (Aug. 1958).

[10] A. H. Booth, A Suggested Method for Calculating the Diffusion of Radioactive Rare Gas Fission Products from UO_2 Fuel Elements, DCI-27 (Sept. 1957).

[11] A. H. Booth, A Method of Calculating Fission Gas Diffusion from UO_2 Fuel, CRDC-721 (Sept. 1957).

experiments performed by the North American Aviation Company.[12 – 15] The diffusion coefficients thus obtained were then used to calculate the release of activity from the graphite as a function of fuel temperature.

The relative proportion of the activity in the primary gas system from diffusion of fission products from the UO_2 and from the graphite depends primarily on the details of the temperature distribution in the fuel element, but it is also influenced by the mechanical design of the fuel element. The fuel element chosen for the contaminated-coolant system (HGCR-1)[7] consists of 200-μ particles of UO_2 dispersed in graphite. With this size of particle the fraction of fission products recoiling out of the UO_2 into the graphite is less than 5%. A smaller particle would result in a larger amount of fission products being introduced into the graphite by recoil. With impregnated graphite, about 65% of the fission products recoil from the UO_2 to the graphite.

As mentioned above, the diffusion of fission products from UO_2 and from graphite depends on the temperature of these materials. Experimental data indicate that at a given temperature the diffusion from graphite is significantly greater than from UO_2. With the graphite-UO_2 fuel configuration described, however, the fraction of the activity in the coolant is also dependent upon the UO_2 particle size, which determines both the UO_2 temperature and the recoil activity in the graphite.

The activity in the primary coolant of the HGCR-1 was estimated to be about 0.2% of the activity generated in the fuel.[7] This factor of 500 difference is primarily due to the ability of the fuel to hold up the release of the short-lived nuclides until they have decayed to daughters

---

[12] C. A. Smith et al., Diffusion of Fission Fragments from Uranium-Impregnated Graphite, NAA-SR-72 (May 1951).

[13] D. Cubicciotti, The Diffusion of Xe from Uranium Carbide-Impregnated Graphite at High Temperatures, NAA-SR-194 (Oct. 1952).

[14] C. T. Young et al., Preliminary Experiments on Fission Product Diffusion from Uranium-Impregnated Graphite in the Range 1800° – 2200°C, NAA-SR-232 (June 1953).

[15] L. B. Doyle, High-Temperature Diffusion of Individual Fission Elements from Uranium Carbide-Impregnated Graphite, NAA-SR-255 (Sept. 1953).

of longer life. For the case of the HGCR-1, the choice of a 200-μ UO_2 particle size resulted in about 64% of the activity being released by recoil and diffusion from the graphite. Larger particles of UO_2 could give a decrease of activity by another factor of 3 if the temperature structure remained constant, but the use of larger UO_2 particles or UO_2 rods clad with graphite would result in relatively large temperature rises in the UO_2 and therefore increase the fission-product release by diffusion from UO_2 because of the higher temperature.

STEAM GENERATORS FOR A HELIUM-COOLED REACTOR OPERATING WITH A GAS OUTLET TEMPERATURE OF 1500°F

One promising means of reducing costs in a gas-cooled power reactor system is that of increasing the gas outlet temperature. The higher temperature may be employed either in a direct power recovery cycle or to increase the steam generator power density and thus reduce the steam generator cost. As a part of the study of the HGCR-1,[7] a steam system to utilize the 1500°F reactor outlet gas was devised.

The steam generators proposed for the HGCR-1 are scaled-up versions of the GCR-2 straight-through design, but the much higher gas-to-steam temperature difference results in an appreciable improvement in performance. The HGCR-1 steam generator removes 2.25 times as much heat as the GCR-2 steam generator per boiler, and the total tube matrix height is actually 3 ft shorter.

It was found that the "pinch" temperature difference has a large effect on the required heat transfer surface in a system with a large gas temperature drop because of the comparatively low temperature drop in the economizer section. In the HGCR-1, for example, increasing the "pinch" from 50 to 80°F reduced the total matrix height by about 6.8 ft, but at the same time it decreased the allowable feedwater inlet temperature and the concurrent benefits of regenerative feedwater heating in the steam cycle. The optimization analysis showed 80°F to be about optimum for the case of a 1500°F reactor gas outlet temperature.

The main mechanical deviation from the GCR-2 design is that full coolant flow is returned in an annular duct to cool the pressure shell. This system is adaptable to the concentric piping arrangement used to

handle the 1500°F inlet gas to the steam generator. The temperature rise and the pressure drop of the gas as it cools the pressure shell are small.

The benefits of the high gas temperatures are illustrated in the following tabulation which compares the performance of the GCR-2 and HGCR-1 steam generators:

	GCR-2	HGCR-1
Steam generator gas inlet temperature, °F	1000	1500
Steam generator gas outlet temperature (to blower), °F	450	506
Steam outlet pressure, psia	950	1450
Steam outlet temperature, °F	950	1050
Feedwater inlet temperature, °F	325	440
Total matrix height, ft	34.8	28
Gas flow, lb/sec	243	300
Water flow, lb/sec	142	340

COST AND EQUIPMENT SURVEYS

In order to establish a yardstick for the cost evaluation of a gas-cooled power reactor design, it was considered important to become familiar with the status of capital cost estimates for competing reactor designs. A survey of the various capital cost estimates published in recent literature was completed,[16] and an attempt was made to correlate the data with reactor steam conditions and power output capacity. The survey showed that the most important factor affecting nuclear power plant capital costs is the net output capacity of the plant and that in the range of capacities above 125 Mw there is little difference between the many types of reactors on the basis of capital costs. The survey also showed that the steam conditions selected for the many reactor installations have relatively little bearing on the cost of the conventional turbine plant equipment in nuclear power stations.

---

[16] M. Bender and R. D. Stulting, Cost Comparisons of Capital Investment in Various Nuclear Power Plants for Central Station Application, ORNL CF-58-10-49 (Oct. 14, 1958).

A survey[17] of capabilities for fabrication of carbon steel vessels was carried out through contacts with the leading fabricators in this country, since, as indicated in the advanced reactor study,[18] the capabilities of the fabricators to manufacture the equipment required for advanced gas-cooled reactors will exercise a major influence on the direction in which the program moves. Very limited resources for field fabrication of reactor vessels larger than 14 ft in diameter in thicknesses exceeding 3 in. were found to exist. Extensive facilities are available for shop fabrication of smaller diameter (< 14 ft) heavy walled vessels up to 12 in. in wall thickness. Concurrently with the survey of manufacturers' facilities a compilation of reactor vessel costs was made that reconfirmed the fact that, when ferritic steel vessels of thicknesses greater than 1 in. are considered, the vessel cost in dollars per pound increases at a substantial rate as the vessel thickness increases.

---

[17] G. C. Robinson, Survey of US Pressure Vessel Fabrication Facilities and Cost Factors, ORNL CF-58-12-13 (Dec. 2, 1958).

[18] The ORNL Gas-Cooled Reactor Advanced Concepts, ORNL-2510 (Sept. 18, 1958).

3. EXPERIMENTAL INVESTIGATIONS OF HEAT TRANSFER AND FLUID FLOW

FLUID FRICTION CHARACTERISTICS

The optimization of the GCR-2 fuel element design for maximum heat transfer with minimum energy expenditure depends in part on knowledge of the fluid friction characteristics of the specific fuel element geometry. To obtain such information, a program was initiated for determining (1) the pressure drop through a full-scale model of a flow channel embodying the final design configuration and (2) the effects of such variables as fuel cluster misalignment, capsule bending, and ligament spacing on the flow distribution and over-all pressure drop.

In establishing the flow characteristics of the reference design fuel element, it is of value to separate the contributions of skin friction and form drag (principally from the hangers and spacers) to the over-all pressure drop. Accordingly, an initial experiment was performed in which only the skin friction component was evaluated. The experimental apparatus was a 24-ft-long by 3.25-in.-ID aluminum channel containing seven continuous (approximately 20 ft long) 0.75-in.-OD aluminum tubes (length-to-diameter ratio = 281). The model channel is shown before assembly in Fig. 3.1. The cluster tubes were supported at each end by the fixture shown. These end fixtures also allowed radial movement of the six peripheral rods so that the effect of cluster geometry on the pressure drop could be established. Central alignment was provided at 5-ft intervals by three sets of small-diameter rod spacers. The contribution from these spacers to the total pressure drop was small. The inlet support was located approximately 3 ft from the tube entrance to allow re-establishment of the velocity profile following the apparatus inlet. Pressure taps were located 18 in. downstream from the cluster entrance and 5 in. before the exit. Six circumferentially spaced static taps were installed at each position.

Air rather than helium was used as the working fluid. This enabled open-circuit operation at atmospheric pressure. The air flow was provided by a positive-displacement rotary blower capable of providing up to 1000 cfm of air at a pressure of 3 psig. A surge tank of approximately 30-ft^3

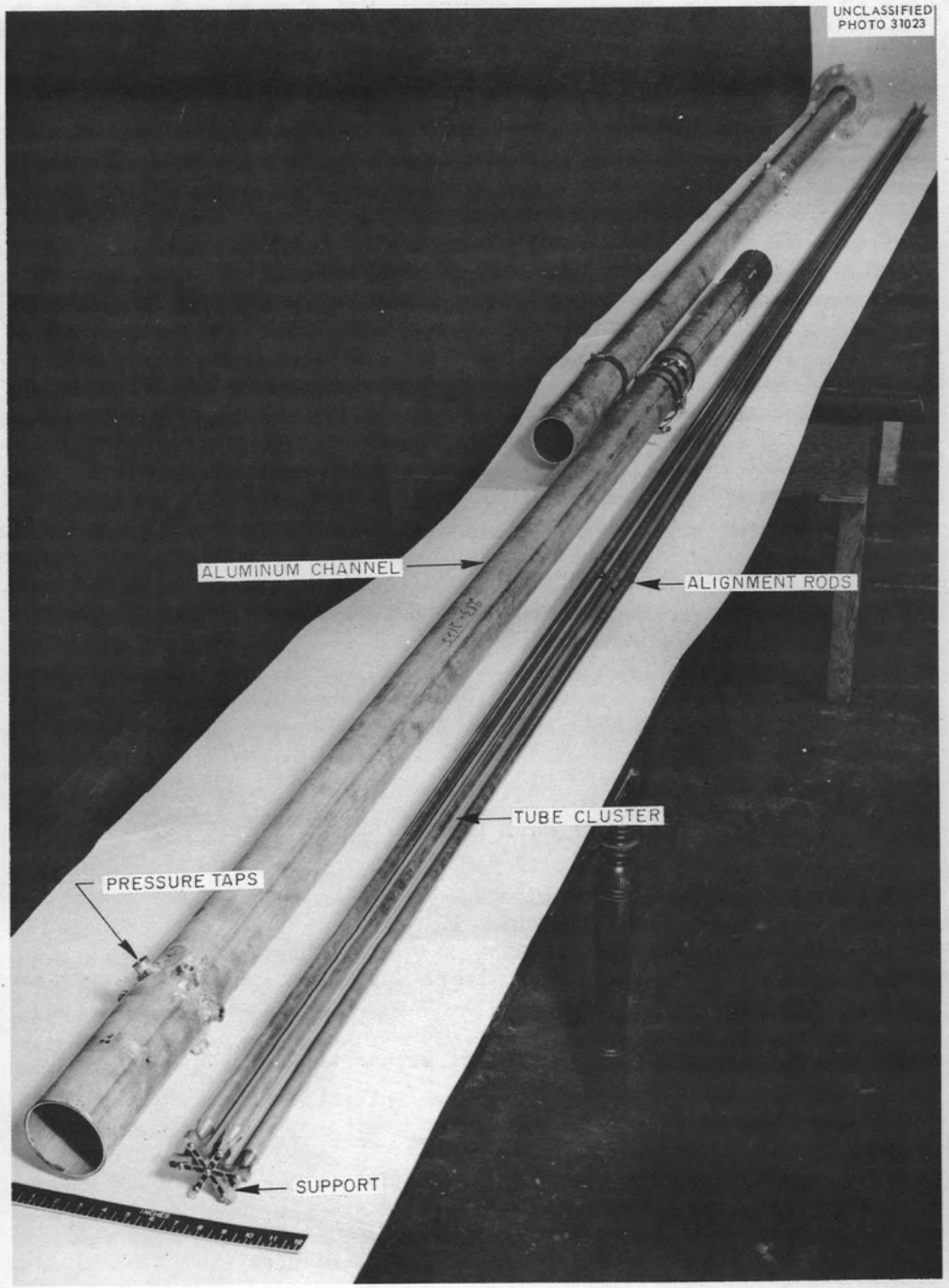

Fig. 3.1. Disassembled Seven Rod Cluster Test Section Used for Skin Friction Measurements.

capacity and an orifice run of 9 ft of 4-in. pipe were located between the blower and the test section. The test section was mounted vertically, and flow was upward through the unit. Details of the assembly are shown in the schematic diagram of Fig. 3.2 and the photograph of Fig. 3.3.

The results of the study are presented in Figs. 3.4 and 3.5 in which the Blasius friction factor, as defined by the equation

$$(1) \quad f = \frac{\Delta p}{\frac{L}{d_e} \frac{\rho \bar{u}^2}{2g_c}} ,$$

is presented as a function of the Reynolds modulus over the range 15,000 to 70,000 for center-to-center rod spacings of 1.152 in. and 0.852 in., respectively. In this equation Δp is the static pressure drop, L is the length of channel between the static pressure taps, d_e is the equivalent channel diameter, ρ is the mean fluid density, $\bar{u}$ is the mean fluid velocity, and g_c is the gravitational conversion factor. The experimental data of Figs. 3.4 and 3.5 can be represented by the following empirical equations:

$$(2) \quad f = 0.282 \, N_{Re}^{-0.232}$$

for the 1.152-in. spacing, and

$$(3) \quad f = 0.211 \, N_{Re}^{-0.205}$$

for the 0.852-in. spacing. The data lie approximately 10% above the Blasius equation

$$(4) \quad f = 0.316 \, N_{Re}^{-0.25} .$$

Within the precision of the results, there appears to be little dependence of the pressure drop on the rod spacing.

Having established the friction characteristics of the bare seven-rod-cluster arrangement, flow studies were initiated with a full-scale model of a single fuel channel based on the GCR-2 design, including hangers and spacers. A general view of the model is given in the photograph of Fig. 3.6. The channel was formed of Plexiglas in six sections with each section containing one complete fuel-rod cluster. Each cluster consisted of seven 0.842-in.-dia rods located on 1.094-in. centers and had

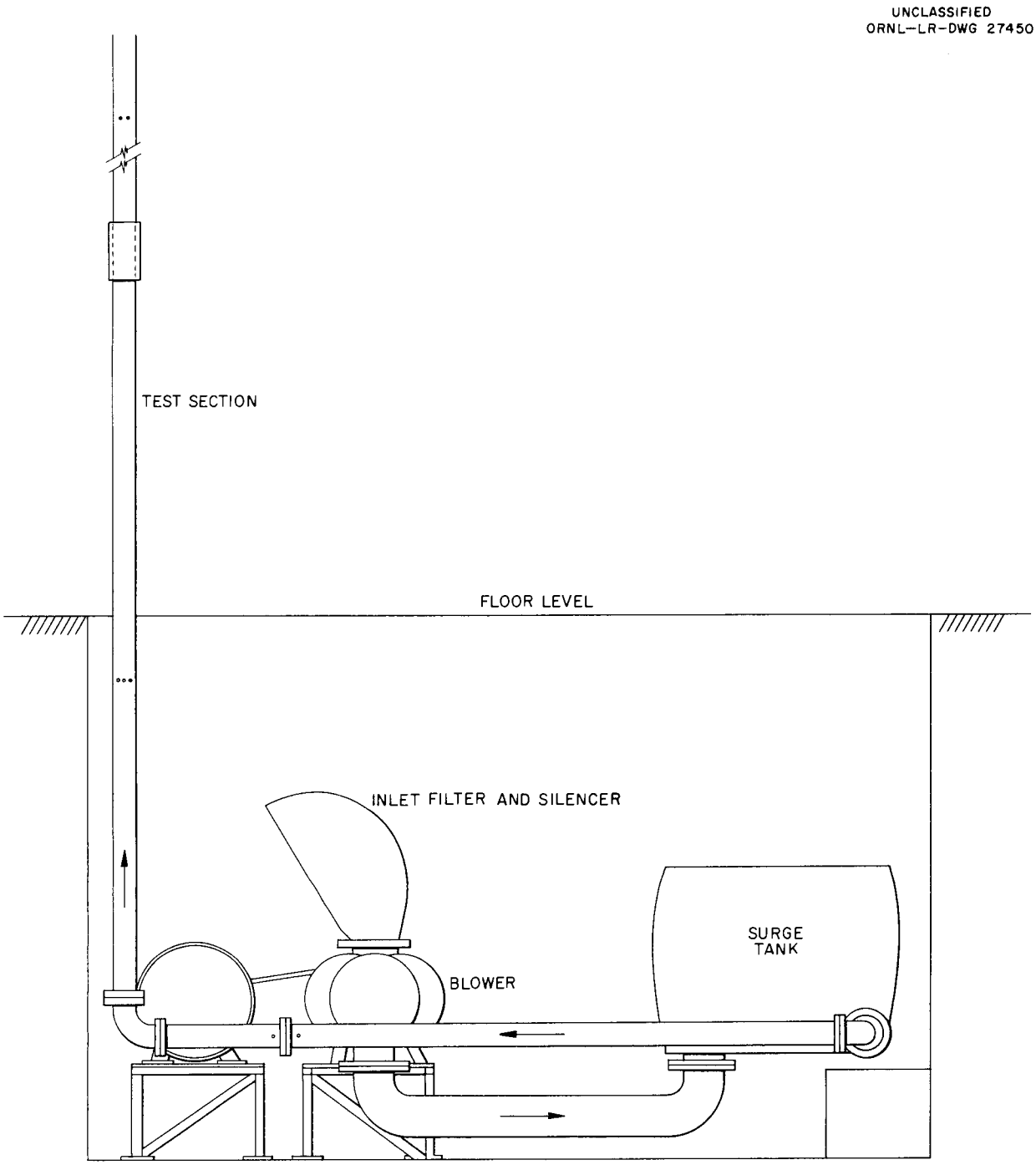

Fig. 3.2. Schematic Diagram of Experimental System for GCR Flow and Heat Transfer Studies.

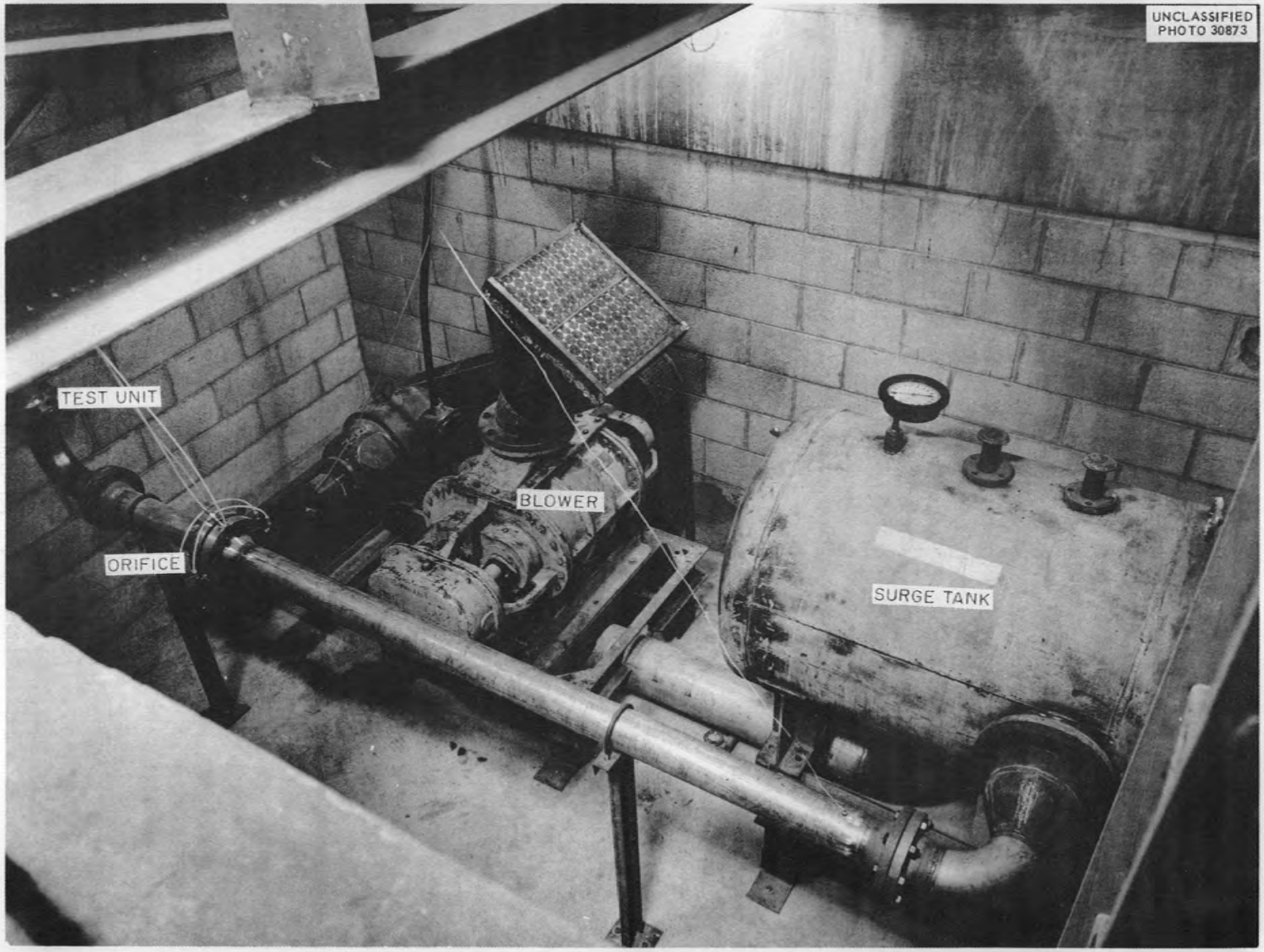

Fig. 3.3. Air Supply and Flow-Measuring System for GCR Flow and Heat Transfer Studies.

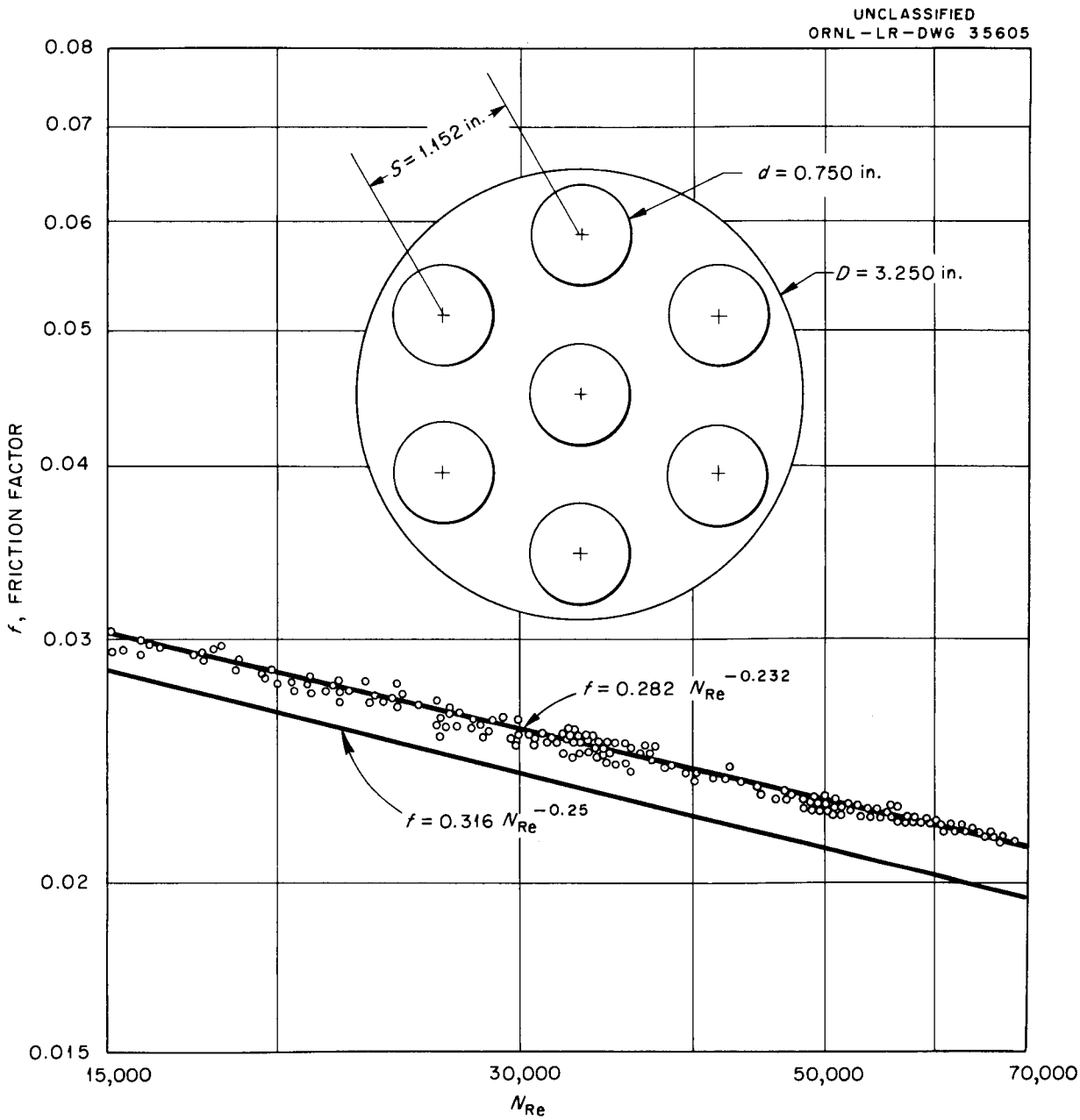

Fig. 3.4. Fluid Friction Characteristics of Bare Seven Rod Cluster Test Section with 1.152-in. Rod Spacing.

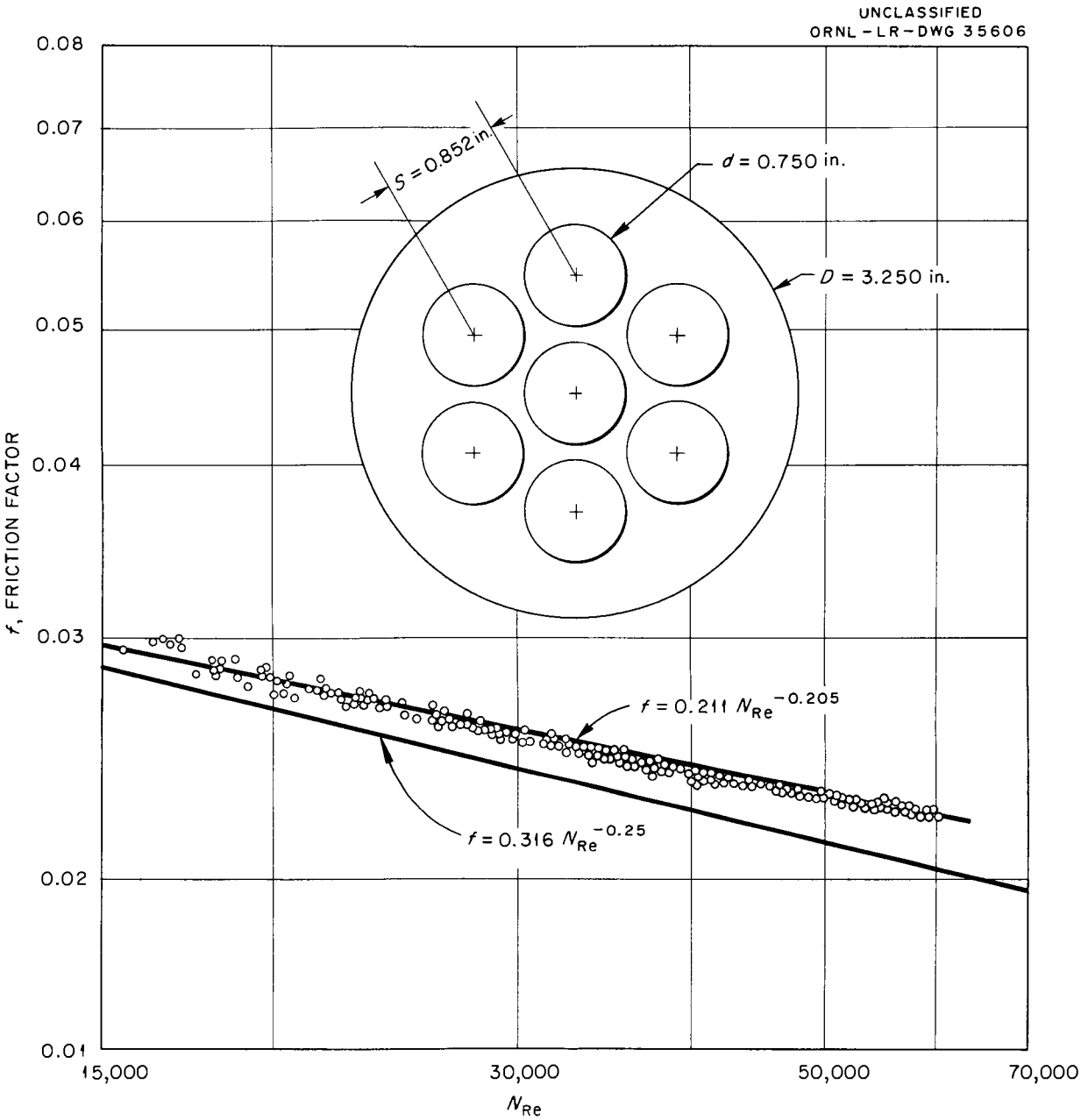

Fig. 3.5. Fluid Friction Characteristics of Bare Seven Rod Cluster Test Section with 0.852-in. Rod Spacing.

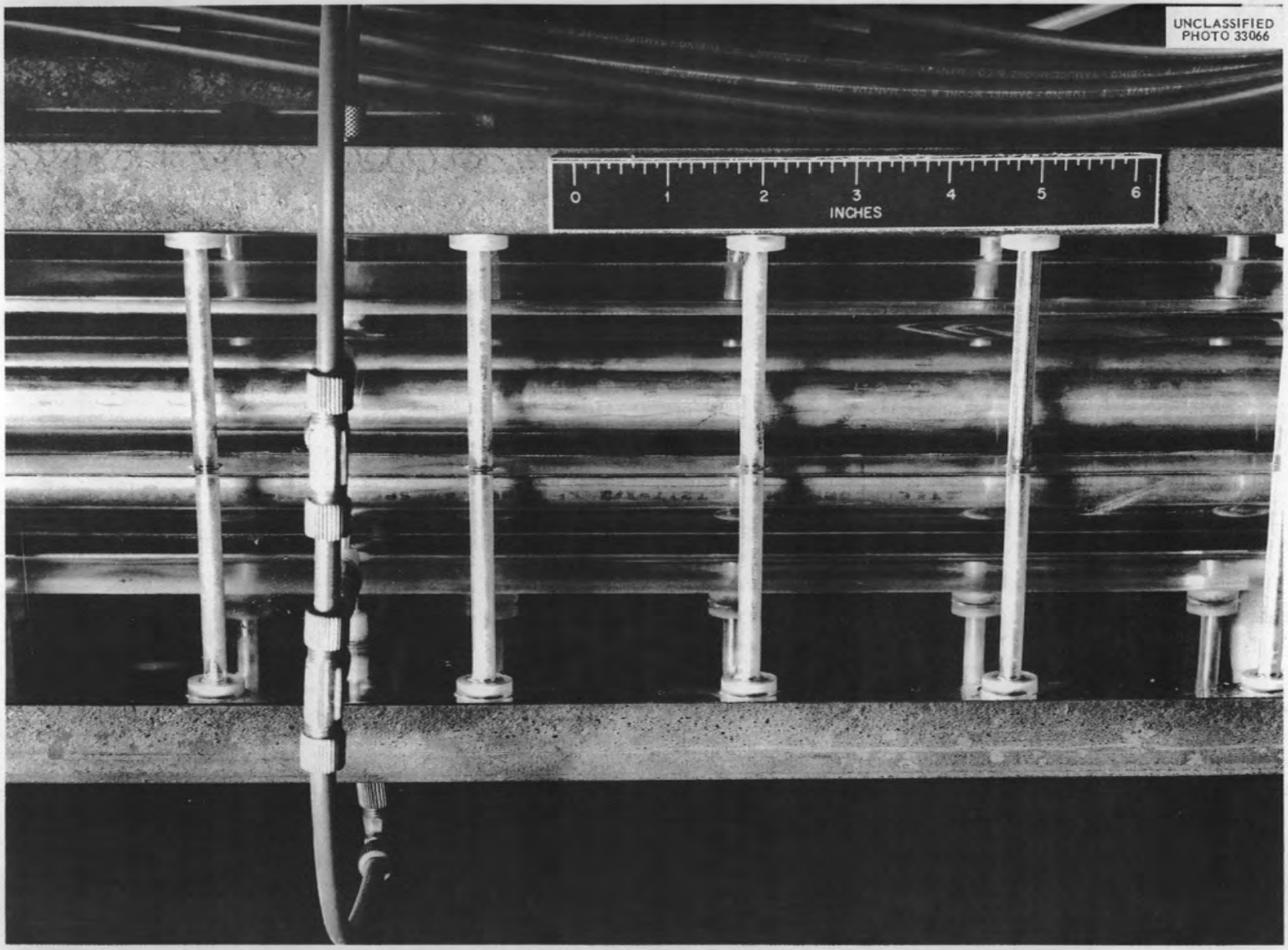

Fig. 3.6. Section of a Full-Scale Experimental Model for the Determination of the Flow Characteristics of the GCR-2 Fuel Channel.

an over-all length of 40 in. The channel inside diameter was 3.25 in., with two diametrically opposed guide slots 0.406 in. deep and 0.532 in. wide extending along the entire length. The assembly had an equivalent diameter of 0.053 ft and a length-to-diameter ratio of 377.5.

Preliminary results of over-all pressure drop measurements with this system are given in Fig. 3.7 in comparison with the Blasius equation. Over the Reynolds modulus range of 15,000 to 60,000 these data can be described by the empirical equation

$$(5) \quad f_T = 0.23\, N_{Re}^{-0.19} ,$$

where the friction factor f_T includes the effect of the hangers and spacers on the pressure drop.

If it is assumed that, in the turbulent range, flow bypassing through the guide slots does not significantly affect the friction characteristics of the system (the cross-sectional area of the slots is less than 10% of the total flow area of the channel), a hanger-spacer pressure loss coefficient can be derived from the data. The pressure drop in the system can be expressed as the sum of the skin-friction and form-drag factors, that is

$$(6) \quad \Delta p = f_T \frac{L}{d_e} \frac{\rho \bar{u}^2}{2g_c} = n \left(K_S + f \frac{\ell}{d_e}\right) \frac{\rho \bar{u}^2}{2g_c} ,$$

where n is the number of clusters in the channel or, equivalently, the number of hanger-spacer combinations, K_S is the hanger-spacer pressure loss coefficient, and ℓ is the length of the straight portion of the individual fuel rods. The friction factor f in Eq. 6 is evaluated from the bare-tube data (that is, no hangers or spacers) represented by Eq. 2, and f_T is determined from Eq. 5. For the specific geometry under consideration, Eq. 6 can be rewritten as

$$(7) \quad K_S = 59.21\, (1.063\, f_T - f) .$$

From this equation, $K_S = 0.53$ at $N_{Re} = 15{,}000$ and $K_S = 0.49$ at $N_{Re} = 60{,}000$. Since K_S evaluated in this manner results as a small difference between two sets of experimental data of the same magnitude, the accuracy of this calculation is low. Hence, a constant value of $K_S = 0.5$ between $N_{Re} = 15{,}000$

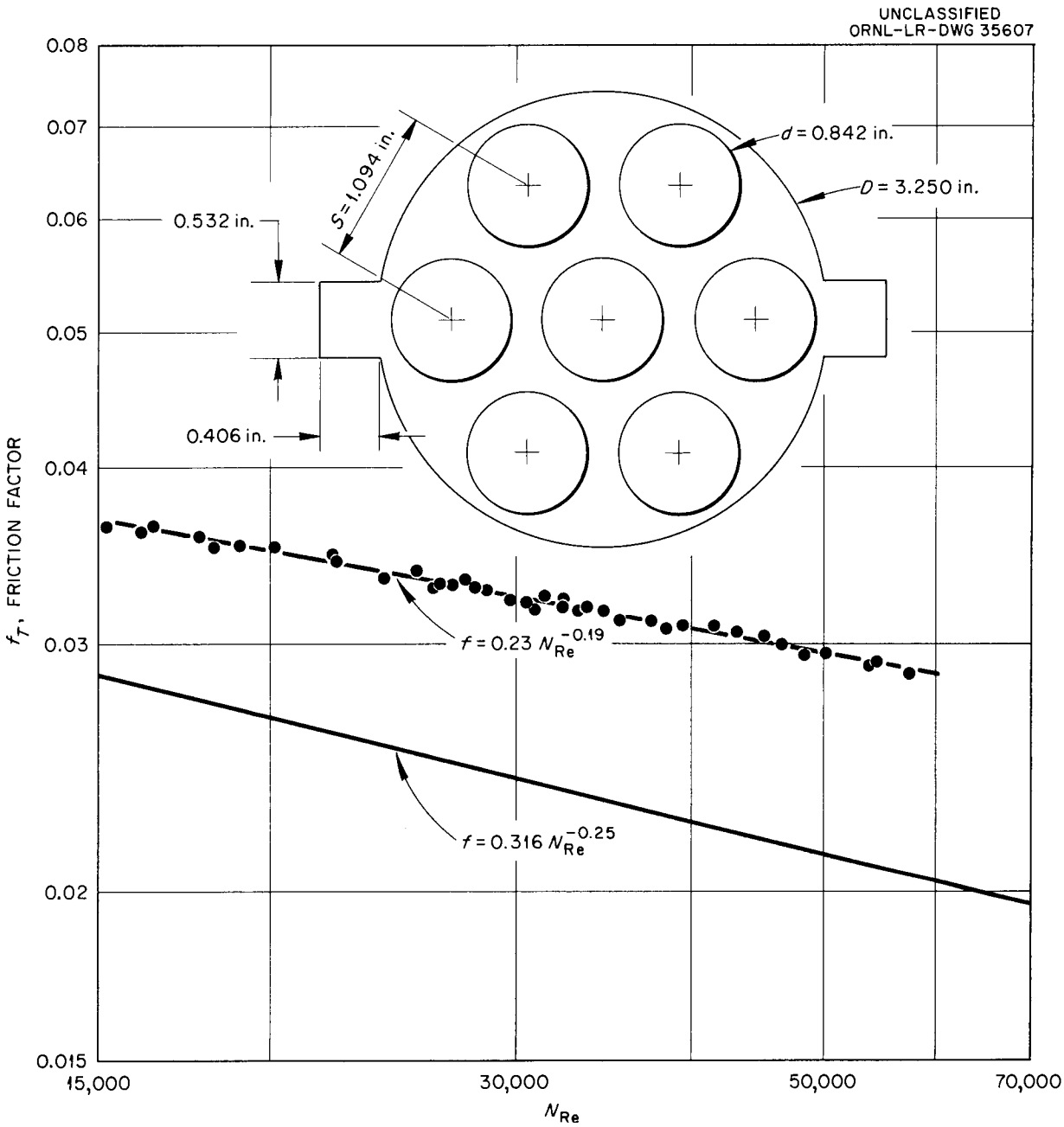

Fig. 3.7. Fluid Friction Characteristics of the GCR-2 3.25-in.-dia Fuel Channel Configuration, with Effect of Hangers and Spacers Included.

and N_{Re} = 60,000 can be taken as sufficient for use in design calculations. In future experiments, K_S will be determined by direct measurement of the pressure drops associated with the individual spacers and hangers.

FLOW MODIFICATION STUDIES

Analytical studies have indicated[1] and preliminary experiments have verified (see following sections of this chapter) that the flow distribution around the individual rods of the fuel-element cluster is not uniform. Since this leads to undesirable circumferential surface temperature asymmetries, a study of methods for redistributing the flow to establish optimum conditions has been started. The initial phase of this investigation will involve the visualization of the flow in a model channel both with and without entrance swirl generation. The apparatus currently under construction will consist of a 4-in.-ID clear plastic channel containing seven 1-in.-OD transparent tubes 45 in. long. Single cotton fibers will be attached to the surface of the tube being observed, and the fiber deflection patterns under varying conditions of flow will be photographically recorded. The effect of optical distortion will be reduced by observing simultaneously a rectilinear grid inserted within the tube being studied. Two entrance vane assemblies (as shown in Fig. 3.8) are being prepared. In the first of these, the vanes are located on the six peripheral rods to provide intermeshing helical flow around the tubes; in the second, vanes are located outside the peripheral rods to effect additional crossflow in the region between the tubes and the channel wall.

RESISTANCE-HEATED-TUBE HEAT TRANSFER EXPERIMENT

Two aspects of the thermal performance of the seven-rod-cluster channel are of primary interest: (1) the mean heat transfer coefficient associated with an individual fuel cluster and (2) the circumferential and axial fuel rod surface temperatures. The first of these two interrelated factors enables estimation of the mean temperature of the exit gas. Since the exit gas temperature is limited by the maximum allowable surface temperature in

[1] L. G. Epel and W. T. Furgerson, Temperature Structure in Gas-Cooled Reactor Fuel Elements and Coolant Channel, ORNL CF-58-5-97 (May 27, 1958); L. G. Epel, Supplementary Comments to ORNL CF-58-5-97, ORNL CF-58-8-37 (Aug. 12, 1958).

UNCLASSIFIED
ORNL-LR-DWG 35608

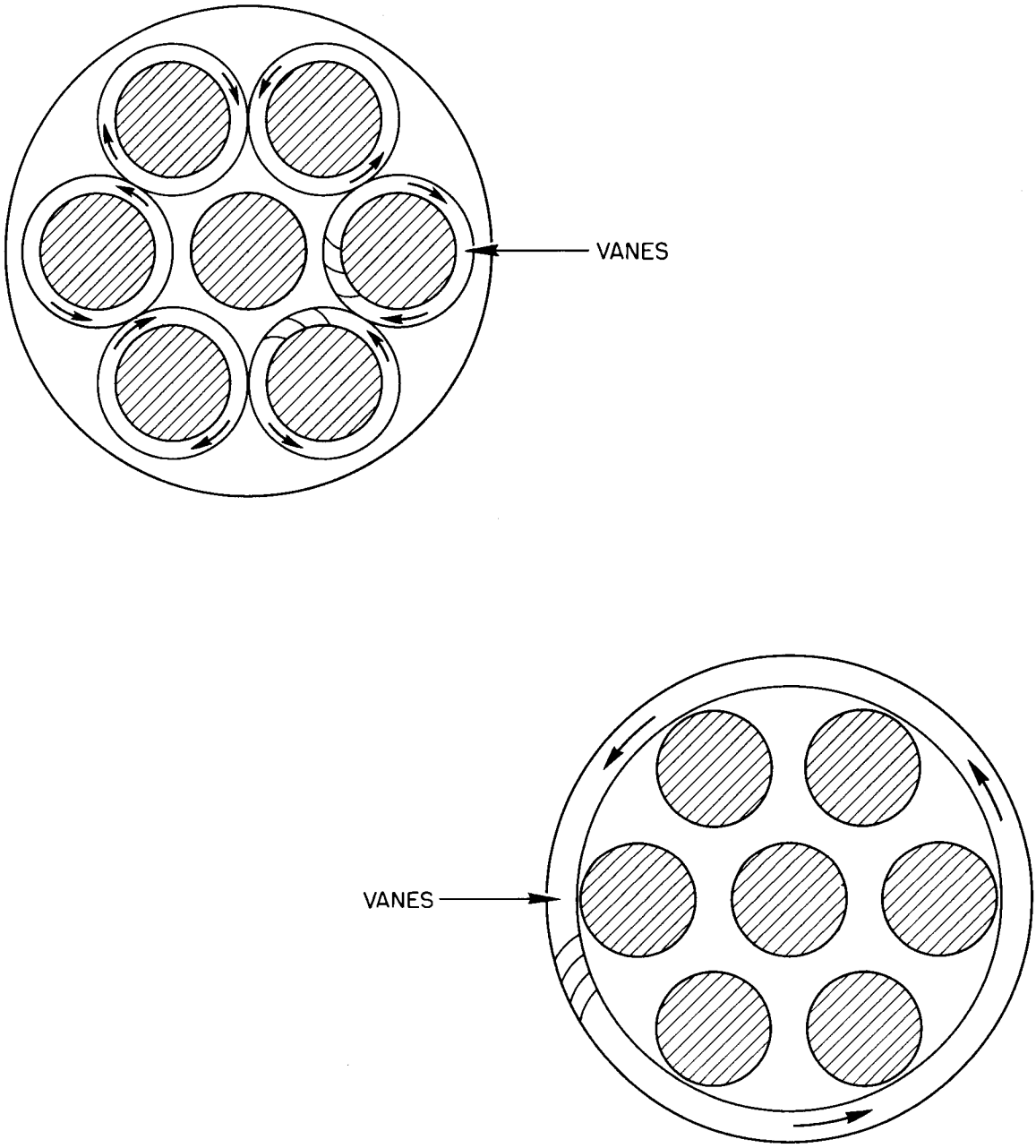

Fig. 3.8. Proposed Vane Arrangements for Modifying the Flow in a Seven-Rod Cluster Channel.

the system, knowledge of the fuel rod circumferential temperature asymmetry is also of importance. From consideration of the flow distribution in the channel, it can be expected that "hot-streaking" will occur on the tube surface; that is, the circumferential surface temperature profile will be similar at all axial positions so that the locus of maximum surface temperature will be a line running roughly parallel to the tube axis. Measurement of this circumferential temperature profile will also enable estimation of the magnitude and direction of other adverse phenomena such as tube bowing.

The experimental apparatus devised for these measurements is shown in Fig. 3.9. It consists of seven 0.800-in.-OD, 0.020-in.-wall type 347 stainless steel tubes contained within a 3.25-in.-ID, 40-in.-long graphite channel. The tubes are a-c resistance heated by using a series-connected electrical path. The power electrodes at the tube ends are designed to allow insertion of thermocouples into the tubes so that inside tube surface temperatures can be measured. Three of the seven tubes (tubes 3, 5, and 7) are so instrumented. Movable contact thermocouple probes are used in the central tube and one of the peripheral tubes.

Two slightly different thermocouples were developed for this usage: (1) a small bead thermocouple held against the tube surface by a spring and (2) two spring-loaded thermocouple wires which contact the surface in such a way that the wall becomes part of the thermocouple junction. Calibration studies with both types of thermocouples indicated readings within 1% of the true surface temperature at a level of approximately 500°F when subjected to a linear temperature gradient of approximately 500°F/in.

The probe head is positioned and rotated within the tube by means of a rigid extension rod; the angular position of the thermocouple is determined from the displacement of an index mark on the extension rod with respect to a fixed external scale. The other instrumented peripheral tube contains seven thermocouples resistance-welded to the inside tube wall and arranged to measure the surface temperature at four axial levels. This tube and its thermocouple assembly are calibrated for temperatures up to 625°F and serve as an additional check on the results obtained with the movable probes.

UNCLASSIFIED
ORNL-LR-DWG 35609

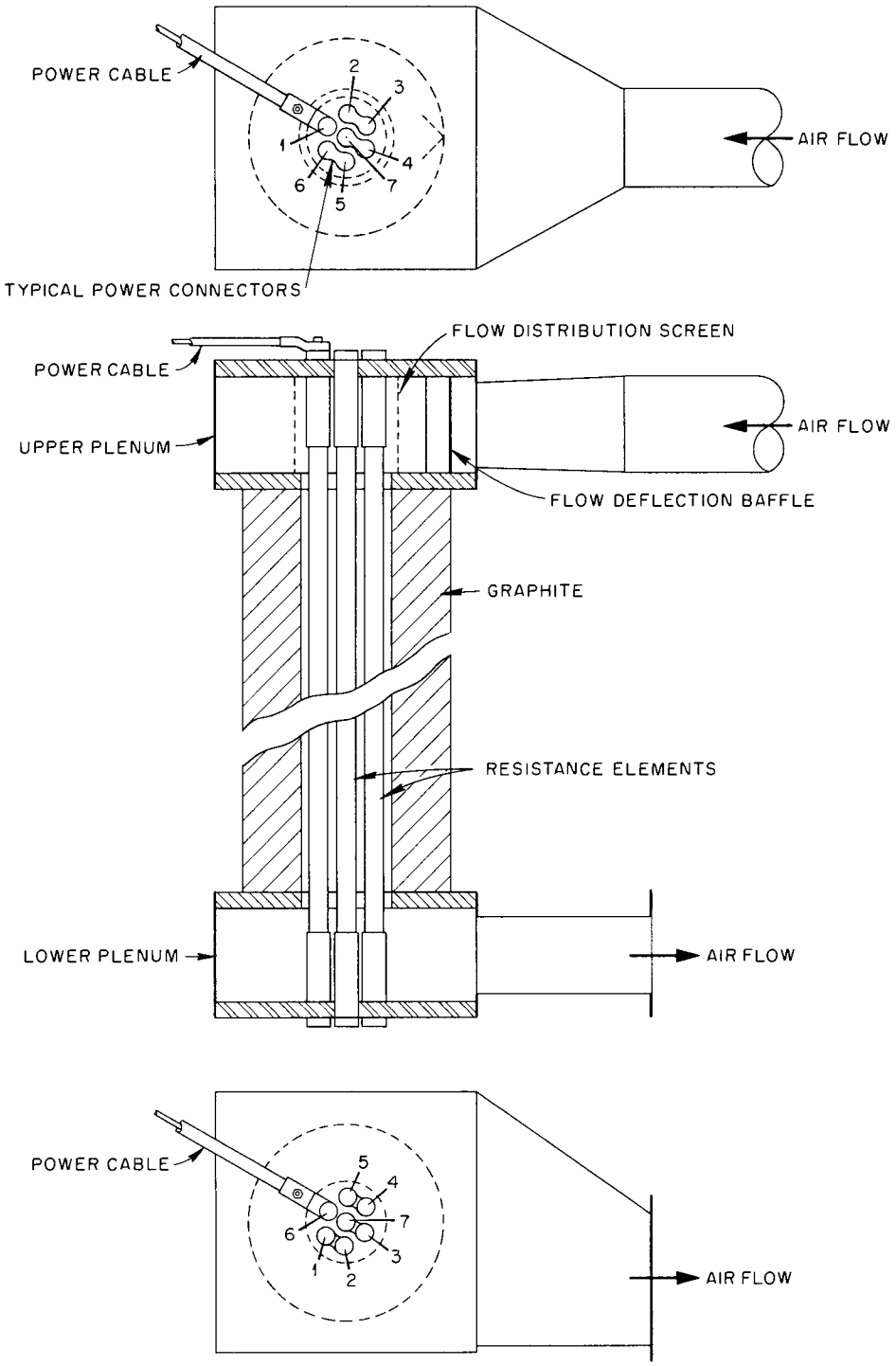

Fig. 3.9. Experimental Apparatus for GCR-2 Fuel Element Heat Transfer Experiments.

All tubes are filled with a high-temperature granular insulation in order to minimize flattening of the circumferential temperature profile by internal radiative and conductive mechanisms. Pressure taps are located at approximately every 4 in. along the length of the graphite channel. A screen and baffle plate are installed in the inlet plenum chamber to provide an initially uniform distribution of the flow into the channel. Air at near atmospheric pressure is used as the heat transfer medium, with the entire assembly being connected to the air supply system previously described for the fluid friction studies.

The air flow rates are determined by the dynamic similarity criterion that the Reynolds modulus be the same in the model as in the high-pressure helium flow of the reactor. Since geometrical identity also exists, it can be derived that the surface heat flux in the model need be only one-tenth of that in the reactor to achieve the same surface-to-gas temperature difference.[2] It also follows that the gas stream axial temperature rise per fuel cluster is equal in the two systems.

The results of preliminary measurements of the circumferential temperature profiles are given in Table 3.1. Tube position numbers are as indicated in Fig. 3.9; the thermocouple positions are given in terms of the L/d_e as measured from the channel entrance (total channel $L/d_e = 59.9$). Typical temperature distributions are given for tubes 5 and 7 in Figs. 3.10 through 3.15. With respect to the coordinate system used in these figures, the flow enters the upper plenum from the 270-deg direction for tube 5 and from the 90-deg direction for tube 7. The surface temperature is given as the temperature increment at any point above the minimum surface temperature.

The similarity of the temperature profiles for tube 5 at all axial positions (Figs. 3.10 and 3.12 are typical) indicates the stability of the flow in the vicinity of this peripheral tube. The asymmetrical nature of the profile may result from the specific entrance conditions employed (screen plus baffle). This will be checked in future experiments by removing

---

[2]This analysis is based on mean conditions of 900°F and 300 psia for the reactor and 140°F and 14.7 psia for the air-cooled model. Further, for simplicity the helium-air Prandtl modulus ratio is taken as 1; it actually differs from this by only about 5%.

Table 3.1. Preliminary Results of Resistance-Heated-Tube Experiment

Run	Reynolds No.	Heat Flux (Btu/hr•ft^2)	Air Temperature		Tube No.	Thermocouple Position, L/d_e	Tube Surface			
							Minimum		Maximum	
			Inlet (°F)	Outlet (°F)			Position* (deg)	Temperature (°F)	Position (deg)	Temperature (°F)
A-31	69,300	7720	107	184	5	44.5	120	334.0	235	363.5
A-32	69,200	7720	113	189	5	58.6	130	357.0	230	385.5
A-33	68,100	7720	115	193	7	58.6	220	372.0	340	380.0
A-34	67,800	7720	116	193	7	44.4	120–240	351.0	300–340	359.5
A-81	71,200	7850	99.5	178	5	44.5	120–130	372.0	240	358.5
A-91	71,900	7720	99	175	5	30.4	120	300.0	235	332.0
A-92	71,100	7770	104	180	5	37.7	120	315.0	235	348.3
A-93	70,600	7770	106	182	5	52.2	120	338.0	235–255	367.0
A-94	70,000	7770	107.5	183	7	52.2	220	350.0	330	358.5
A-95	70,400	7770	108	184	7	37.7	160–220	328.0	320	334.0
A-102	70,500	7720	106	183	5	30.4	120	309.0	235	338.5
A-181	69,100	7670	101	180	7	30.3	140–160	310.0	300	316.2

*The angular position is measured from a 90-deg line which is taken to be the line joining the centers of tubes 5 and 7 (see Figs. 3.10 through 3.15).

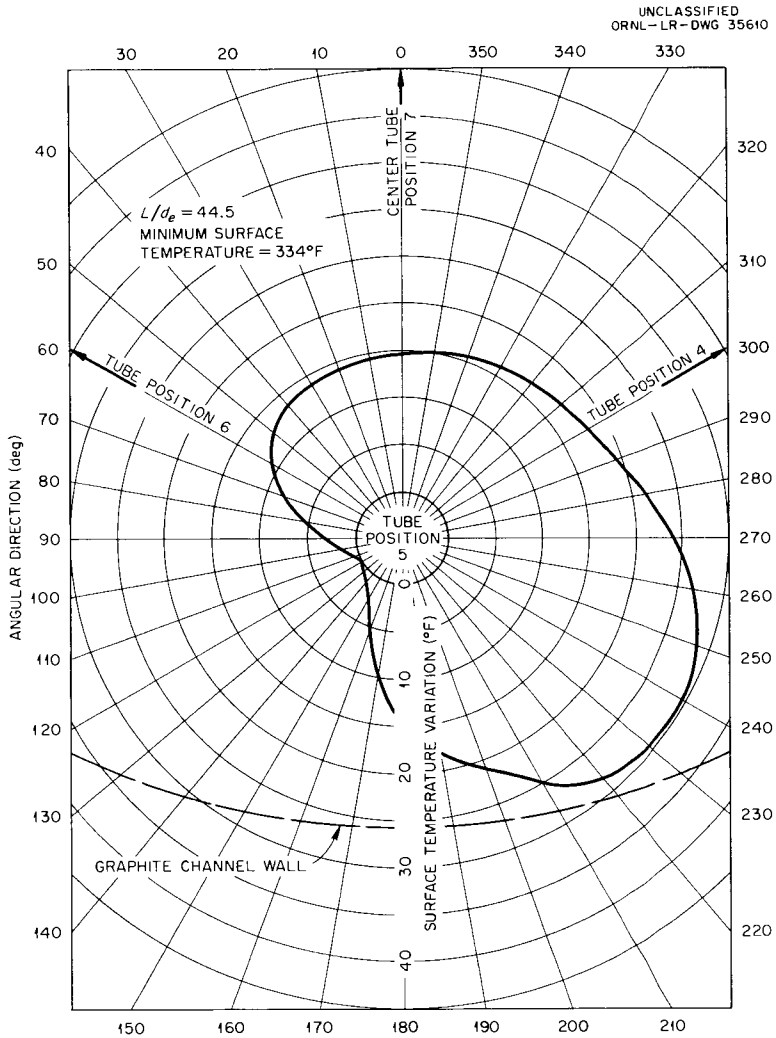

Fig. 3.10. Temperature Profile Obtained in Run A-31 of Resistance-Heated-Tube Experiments.

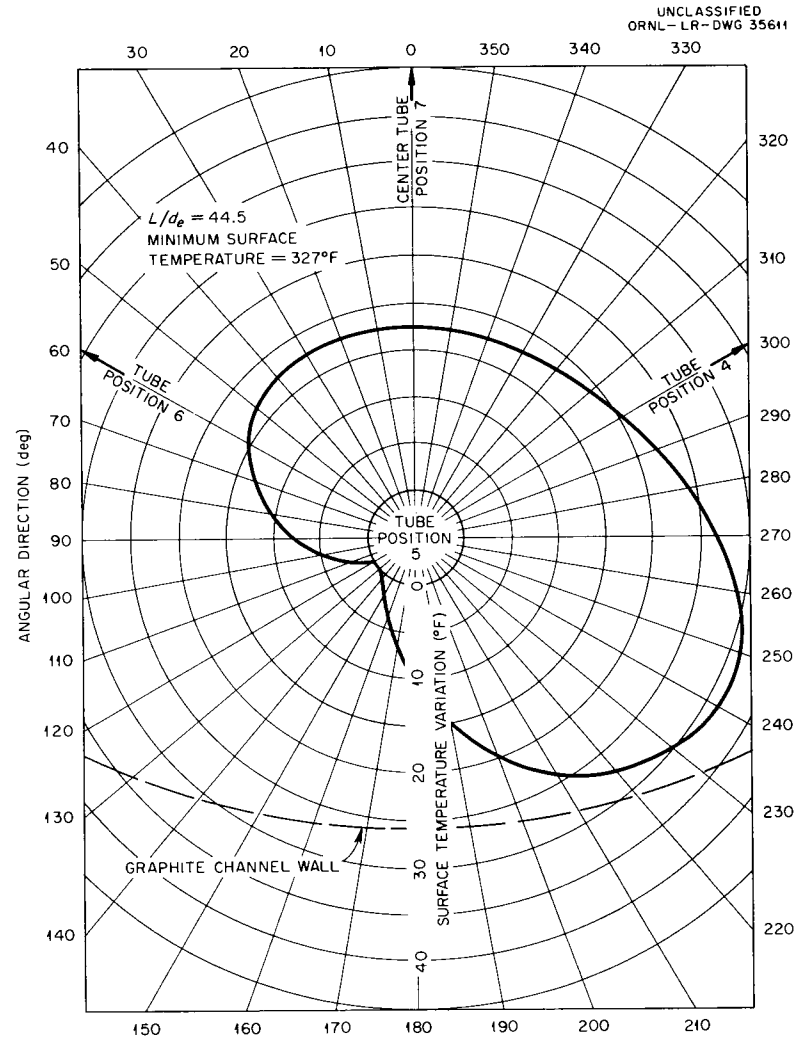

Fig. 3.11. Temperature Profile Obtained in Run A-81 of Resistance-Heated-Tube Experiments.

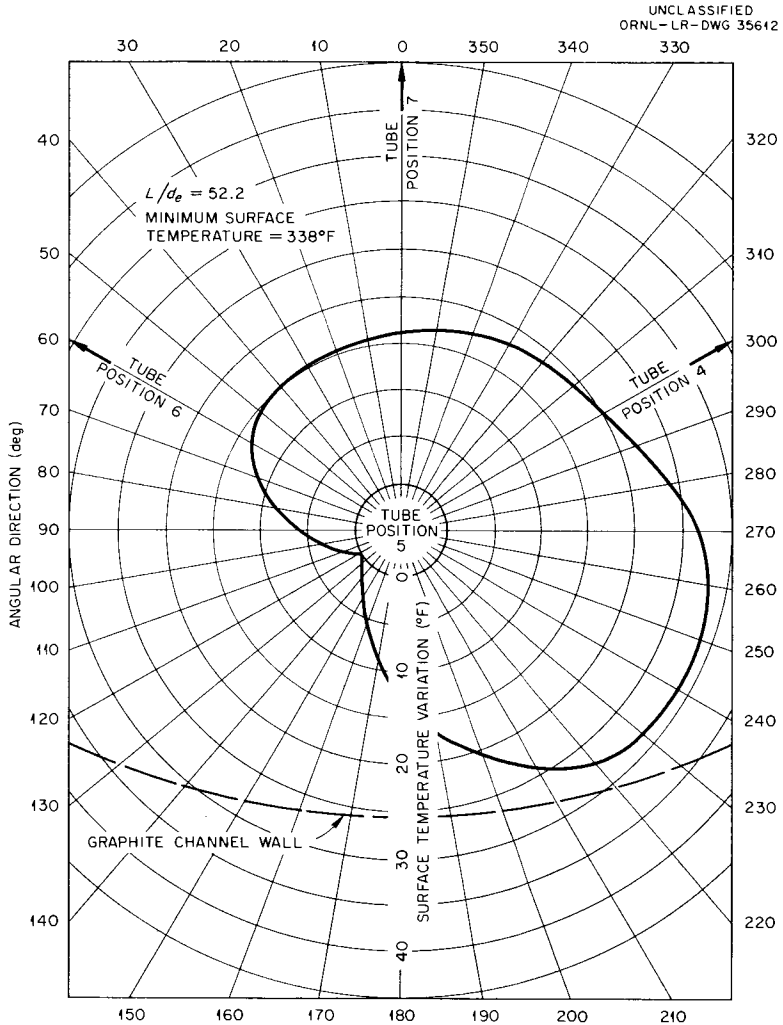

Fig. 3.12. Temperature Profile Obtained in Run A-93 of Resistance-Heated-Tube Experiments.

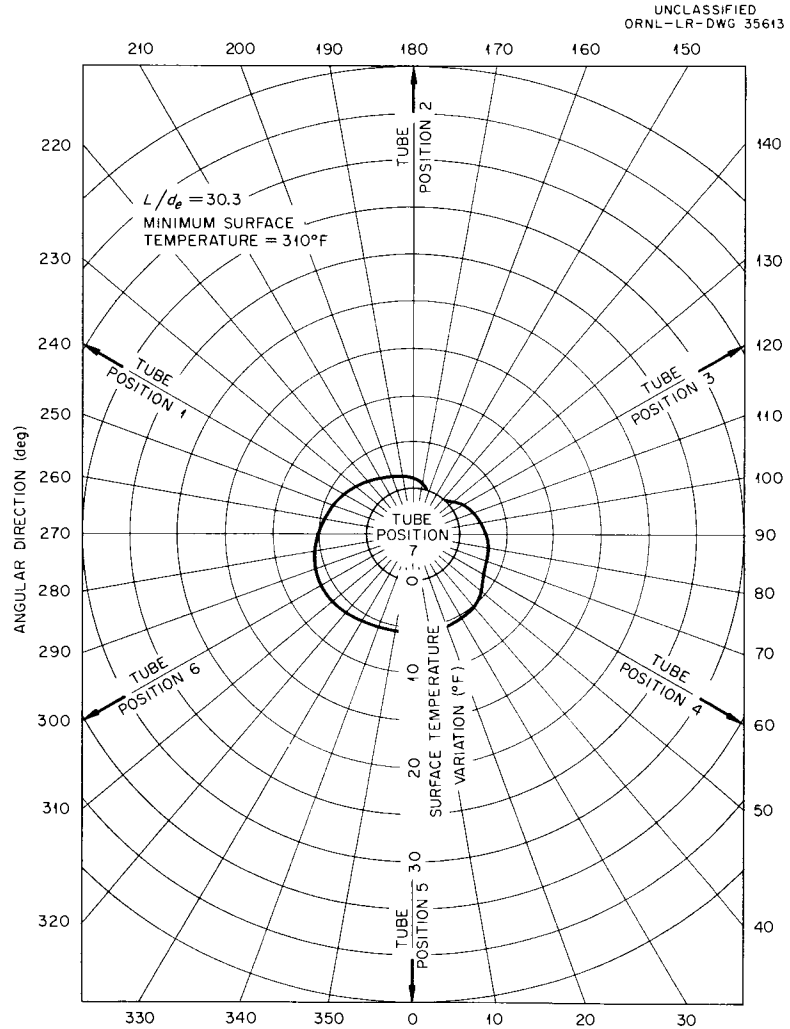

Fig. 3.13. Temperature Profile Obtained in Run A-181 of Resistance-Heated-Tube Experiments.

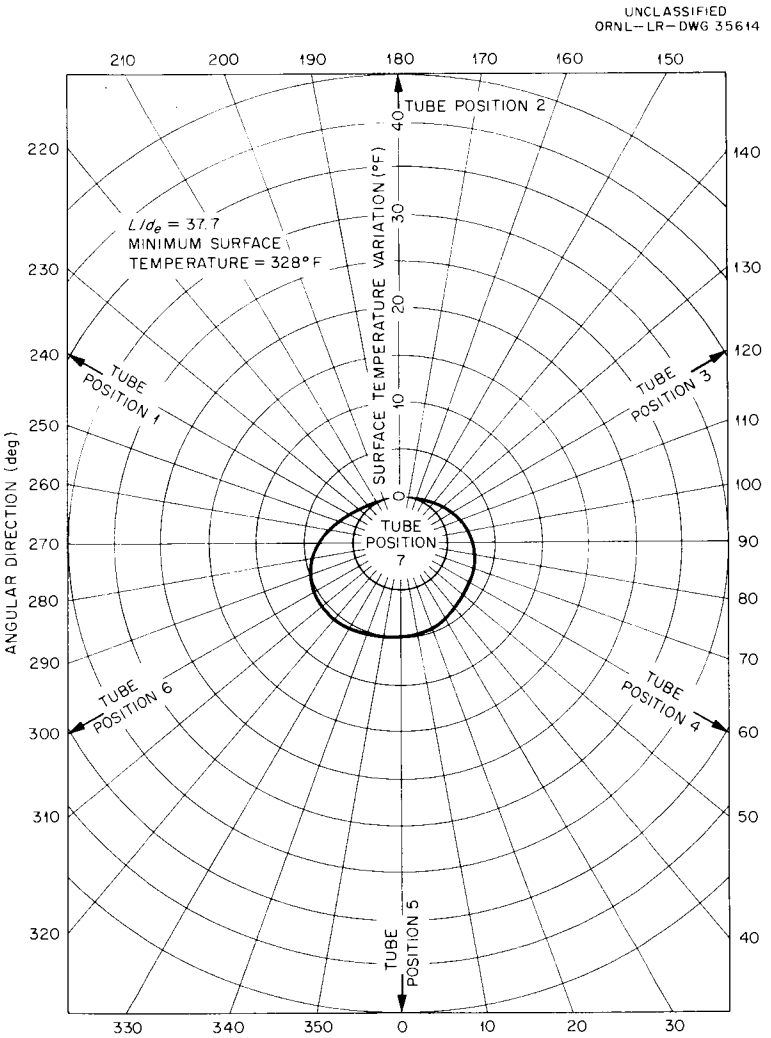

Fig. 3.14. Temperature Profile Obtained in Run 95 of Resistance-Heated-Tube Experiments.

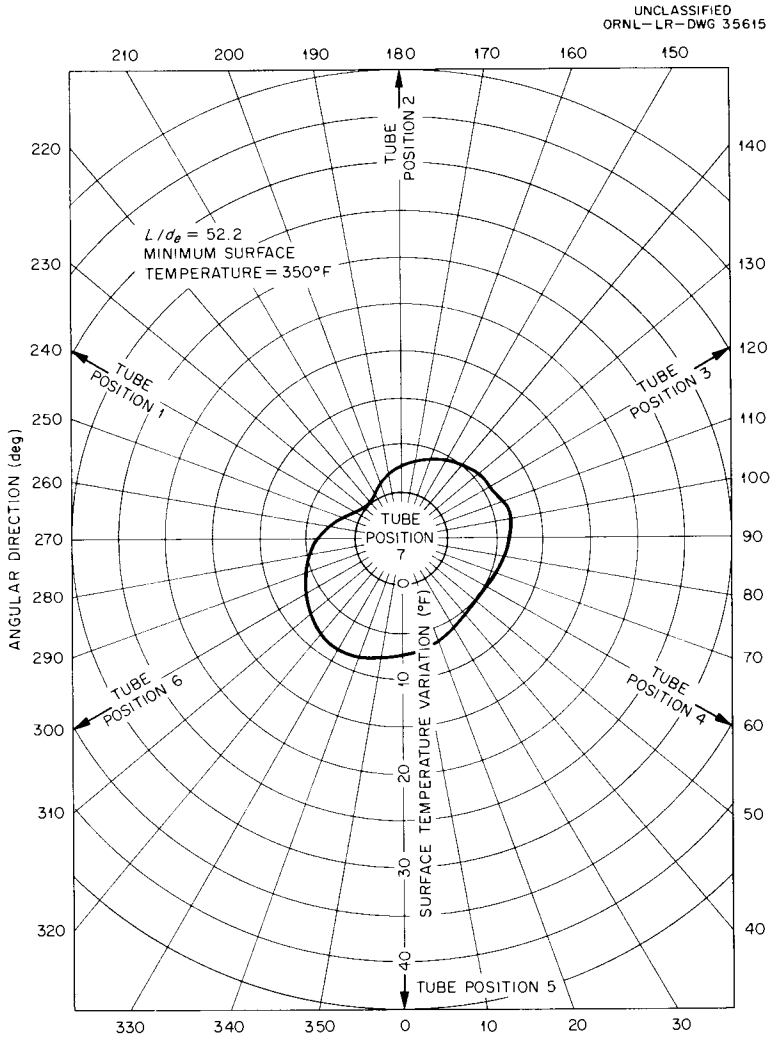

Fig. 3.15. Temperature Profile Obtained in Run 94 of Resistance-Heated-Tube Experiments.

the baffle and by rotating the rod assembly in 60-deg steps so that measurements can be made in tubes 1, 2, 3, 4, and 6. The results given in Fig. 3.11 (a duplicate of Run A-31, Fig. 3.10) are representative of the excellent reproducibility obtainable with this apparatus.

The temperature profiles at three different axial positions along the central tube (tube 7) are given in Figs. 3.13, 3.14, and 3.15. Two differences between the temperature distributions around the central tube and the peripheral tube are immediately obvious: (1) the lower circumferential temperature variation for the central tube and (2) the angular displacement of the central tube temperature pattern between the several measuring positions. From this, it may be concluded that the velocity distribution is more nearly uniform in the vicinity of the central tube and that there exists a slight swirl in the flow around the central tube (1/3 to 1/2 complete turn) as the gas passes the length of the channel.

The maximum and minimum surface temperatures for tube 5 can be plotted (Fig. 3.16) as a function of tube length so that an initial estimate can be made of a heat transfer coefficient for the cluster geometry. Thus, by using the mean inlet and outlet air temperatures to establish the axial gas temperature variation and the minimum curve of Fig. 3.16, a maximum heat-transfer coefficient of 47 $Btu/hr \cdot ft^2 \cdot {}^\circ F$ is obtained that corresponds to a Nusselt modulus of 219. This may be compared with $N_{Nu} = 160$ for the flow of air through a circular tube at $N_{Re} = 70{,}000$. Since the air temperature in the vicinity of the minimum surface will be less than the mean (the gas flow is higher than the mean), this initial estimate of the maximum heat-transfer coefficient is probably too high.

GLOBAR HEAT TRANSFER EXPERIMENT

A single fuel-element model of the GCR-2 fuel cluster was constructed from seven 0.75-in.-OD, 0.020-in.-wall stainless steel tubes arranged on 1.09-in. centers. This cluster was then contained within a 3.18-in.-ID Vycor glass tube to enable use of optical techniques for obtaining the surface temperatures and to allow visual observation of rod bending. The tubes were heated internally by 0.5-in. silicon carbide (Globar) resistance elements. Air at near atmospheric pressures was used as the heat transfer medium.

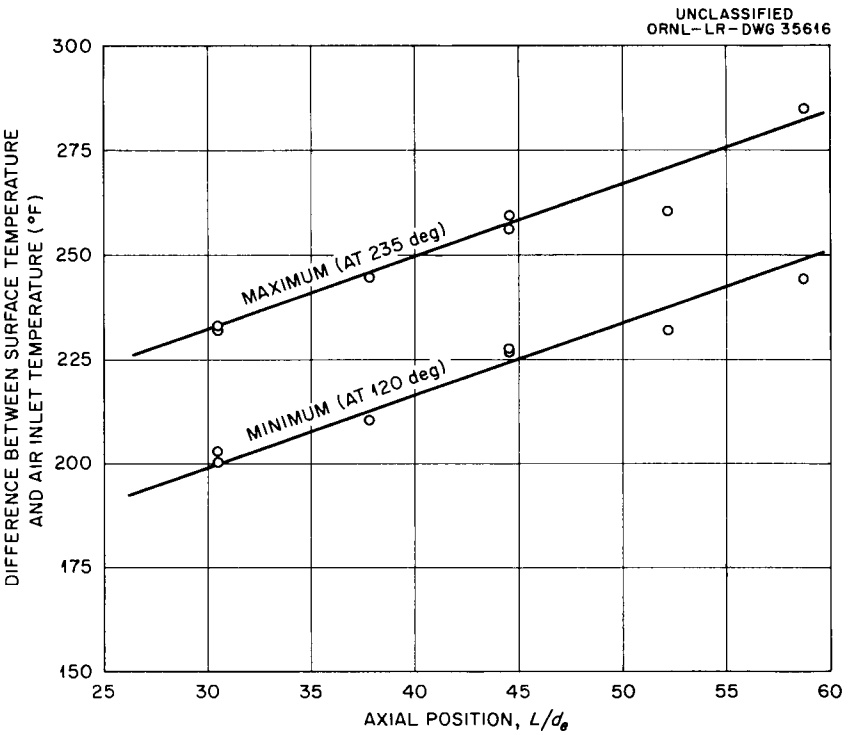

Fig. 3.16. Variation of Maximum and Minimum Surface Temperatures Along the Length of Tube 5.

Attempts to obtain quantitative surface temperature data were unsuccessful because of instabilities in the infrared pyrometer used. The instabilities were manifested primarily in an inability to maintain a consistent calibration both as to position and temperature; the pyrometer was strongly sensitive to variations in the tube surface emissivity. Further, at the relatively low temperatures of this experiment, variations in the electrical and physical properties of the Globar units resulted in nonuniform heating. An additional complication arose from the unexpectedly large optical distortion of the Vycor channel. For these reasons, this approach to the heat transfer study of the GCR fuel cluster has been discontinued.

In preliminary operation of the apparatus, evidence of the bowing of the fuel rods was obtained. Outward bowing of the tubes is clearly visible at the arrows in the photograph of Fig. 3.17 in which the cluster was observed from a fixed camera position both with and without heating. The Reynolds modulus for the air flow was 75,000.

MASS TRANSFER ANALOGY TO HEAT TRANSFER

Preliminary results were obtained for the circumferential variation in the heat transfer coefficient of rods arranged in the GCR cluster geometry by means of the analogy between mass transfer and heat transfer. The data can be combined with the circumferential surface temperature profiles obtained in the heat transfer experiment (see preceding section of this chapter) to estimate the distribution of the mean air temperature in the channel.

If it is postulated[3] that the laws governing heat and mass transfer are the same, there results the expression

$$(8) \qquad j_D = j_H \quad ,$$

where

$$(9) \qquad j_D = \left(\frac{k_L \rho}{G}\right)\left(\frac{\mu}{\rho k_D}\right)^{2/3} \quad ,$$

$$(10) \qquad j_H = \left(\frac{h}{c_p G}\right)\left(\frac{c_p \mu}{k}\right)^{2/3} \quad .$$

[3]In a manner analogous to that used by Reynolds for relating fluid friction and heat transfer, Lewis derived the relationship between heat and mass transfer. Equation 8 represents an empirical extension of this analogy according to the method of Colburn.

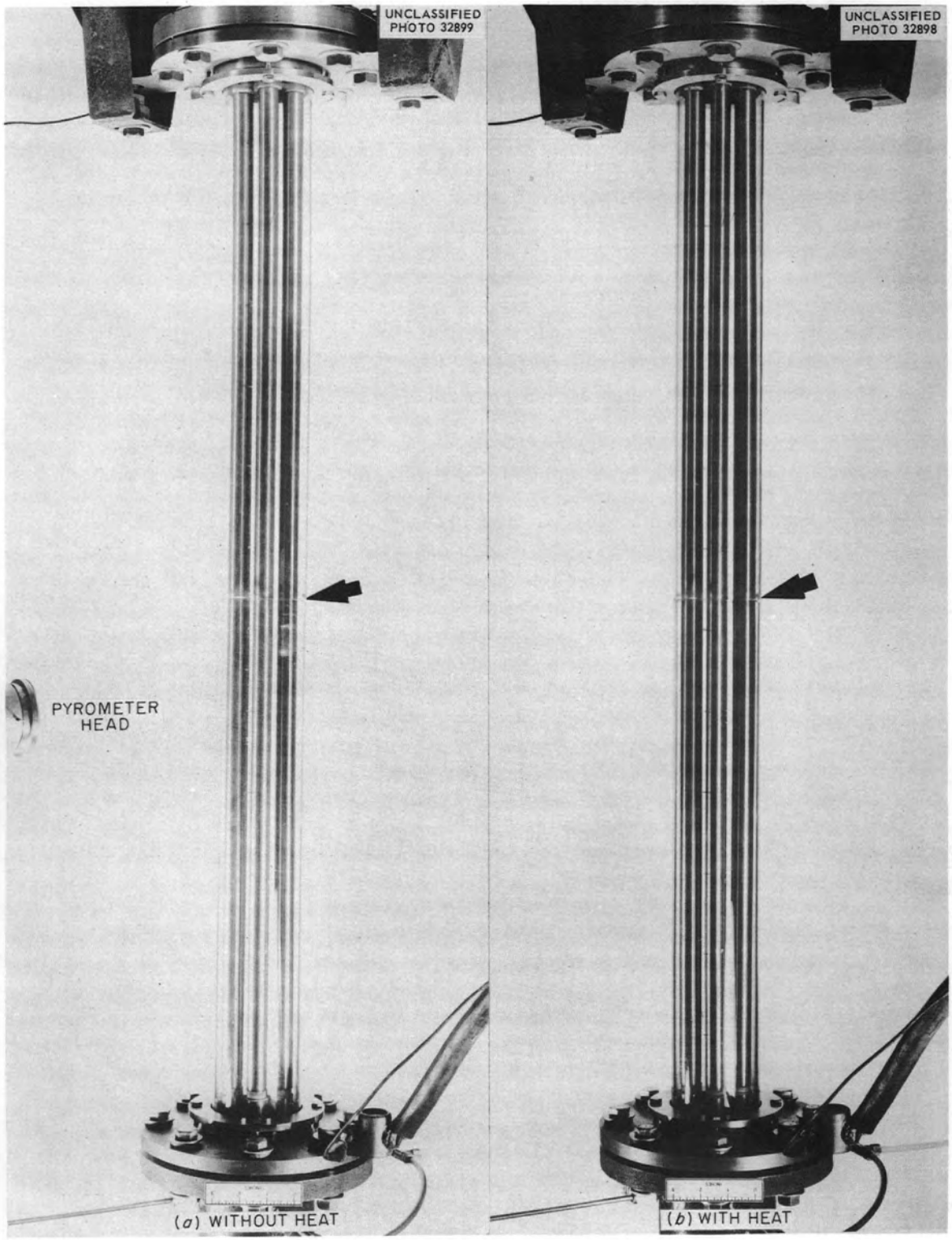

Fig. 3.17. Photographs of Tube Bending in Glo-bar Experiment.

In Eqs. 9 and 10, k_L is the mass transfer coefficient (ft/hr), h is the heat transfer coefficient (Btu/hr·ft^2·°F), G is the mass velocity of the gas (lb/hr·ft^2) in the channel, k_D is the molecular diffusivity of the component diffusing into the gas stream (ft^2/hr), k is the thermal conductivity of the gas (Btu/hr·ft·°F), μ is the viscosity of the gas (lb/hr·ft), and c_p is the heat capacity of the gas (Btu/lb·°F). The mass transfer coefficient can be defined by the equation

$$W_D = k_L \Delta c \quad , \tag{11}$$

where W_D is the mass flux of the diffusing component at the diffusion interface (lb/hr·ft^2) and Δc is the concentration difference of the diffusing component between the interface and the mean fluid (lb/ft^3). This concentration difference can be related to the partial pressure of the diffusing gas in the mixture.

An experiment was performed in which naphthalene, which had been cast into rod geometry, was used as the mass transfer medium, with diffusion into air flowing past the surface. The apparatus, shown in Fig. 3.18, consisted of a cluster of 1-in.-OD rods approximately 9 in. long contained within a 4-in.-ID glass channel. To simplify initial studies, a single naphthalene rod was used in each experiment; the remaining six rods were fabricated from glass tubing. The end supports allowed variation of the rod center-to-center spacings. Air was supplied to the channel from the source used for the fluid friction studies. The mass of naphthalene transferred was determined from local measurements of the depth of material removed by using the apparatus pictured in Fig. 3.19. Dial gage readings were recorded for both the unexposed and exposed rods at 15-deg intervals.

Data were obtained for rod center-to-center spacings of 1.40, 1.31, and 1.26 in. (equivalent γ's[4] of 6, 2.1, and 1.33, respectively) at a Reynolds modulus of approximately 60,000. All measurements were taken at $L/d_e = 10$ (approximately 8 in. from the test-section inlet; data further

---

[4] γ, which is defined as the ratio of the length of the inner ligament (distance between the surfaces of the central and peripheral rods) to the length of the outer ligament (distance between the surfaces of the peripheral rod and the channel), is a useful criterion for comparing cluster geometries.

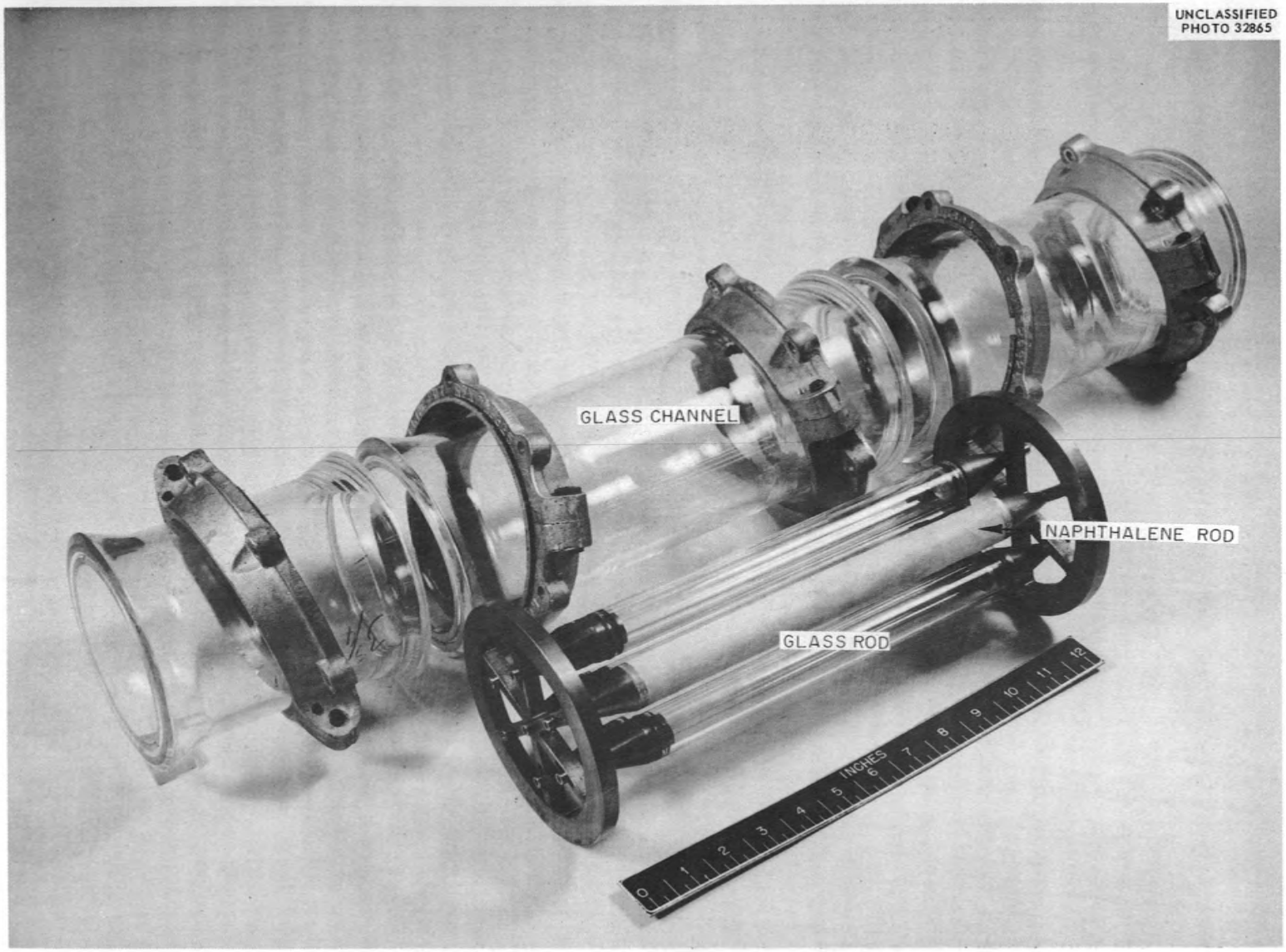

Fig. 3.18. Mass Transfer Study Experimental Apparatus.

UNCLASSIFIED
PHOTO 32864

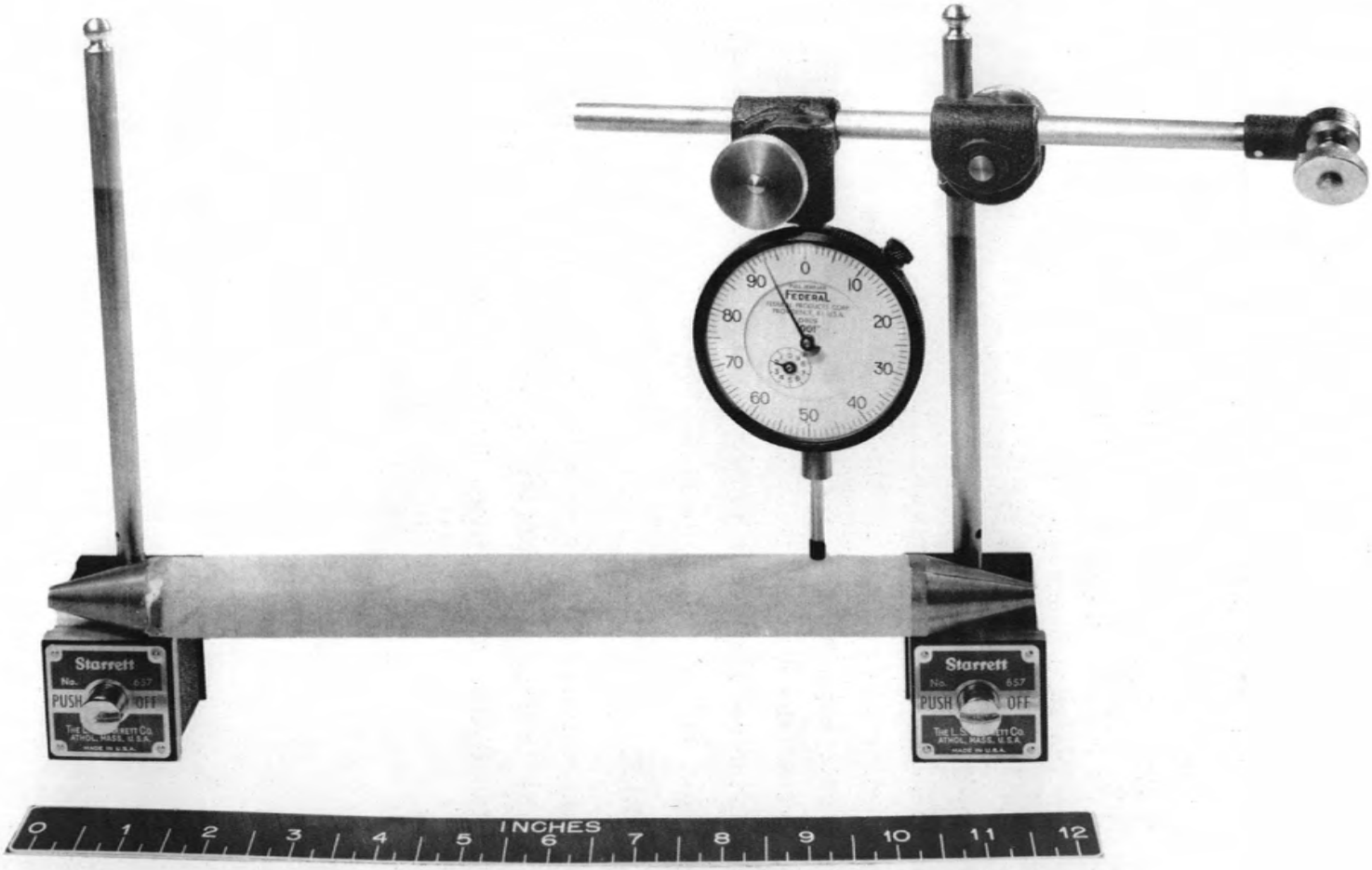

Fig. 3.19. Apparatus for Measuring Amount of Surface Material Removed.

upstream indicated that conditions were essentially established at $L/d_e = 10$). A typical naphthalene rod after exposure is shown in Fig. 3.20. The deep undercutting at the inlet end resulted from (1) the high rate of mass transfer associated with entrance regions and (2) the presence of an eddying wake behind the entrance piece after initial mass transfer had reduced the naphthalene diameter.

The circumferential variation of the calculated heat transfer coefficient is given in Fig. 3.21 for several typical runs. It is to be noted that the variation in h decreases with decreasing γ, with a maximum variation of h of 30% occurring for $\gamma = 6$. The results have not been satisfactorily reproducible because of variations in the surface condition of the cast naphthalene (primarily variations in grain size) and because of difficulty in determining exactly the angular orientation of the naphthalene rods in duplicate experiments. A new apparatus now being fabricated should eliminate most of the difficulties. It is of interest to observe that the mean value of the mass transfer factor as calculated from the experimental data lies within 25% of the value predicted by the equation

$$(12) \qquad j_D = 0.023\, N_{Re}^{-0.2} \quad .$$

In general, these mass transfer results exhibit the same pattern as that observed in the temperature profiles of the resistance-heated-tube experiment and in the bowing of the tubes in the Globar experiment.

UNCLASSIFIED
PHOTO 32863

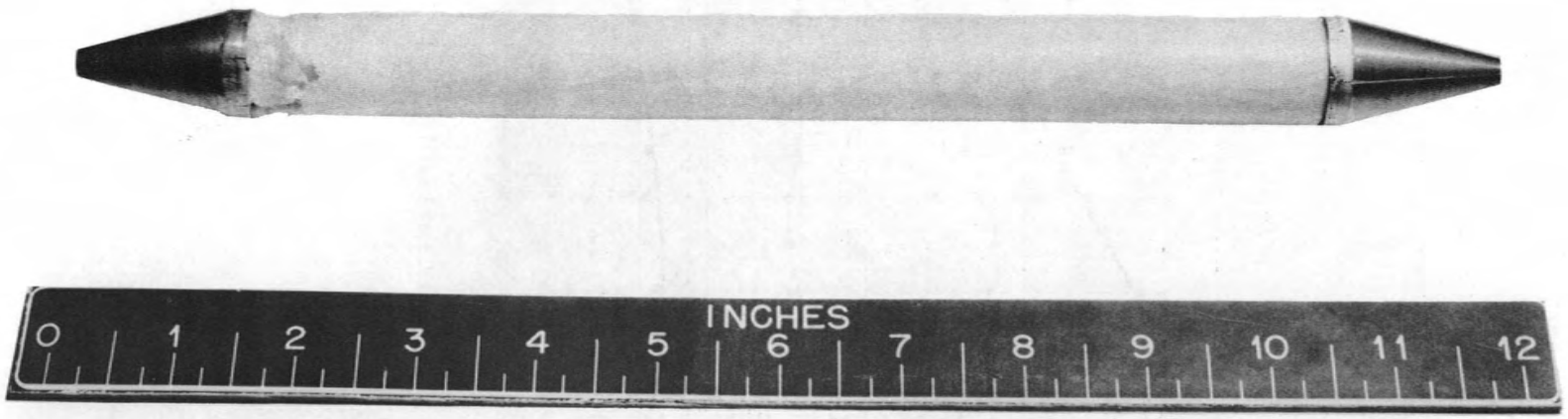

Fig. 3.20. Naphthalene Rod After Test.

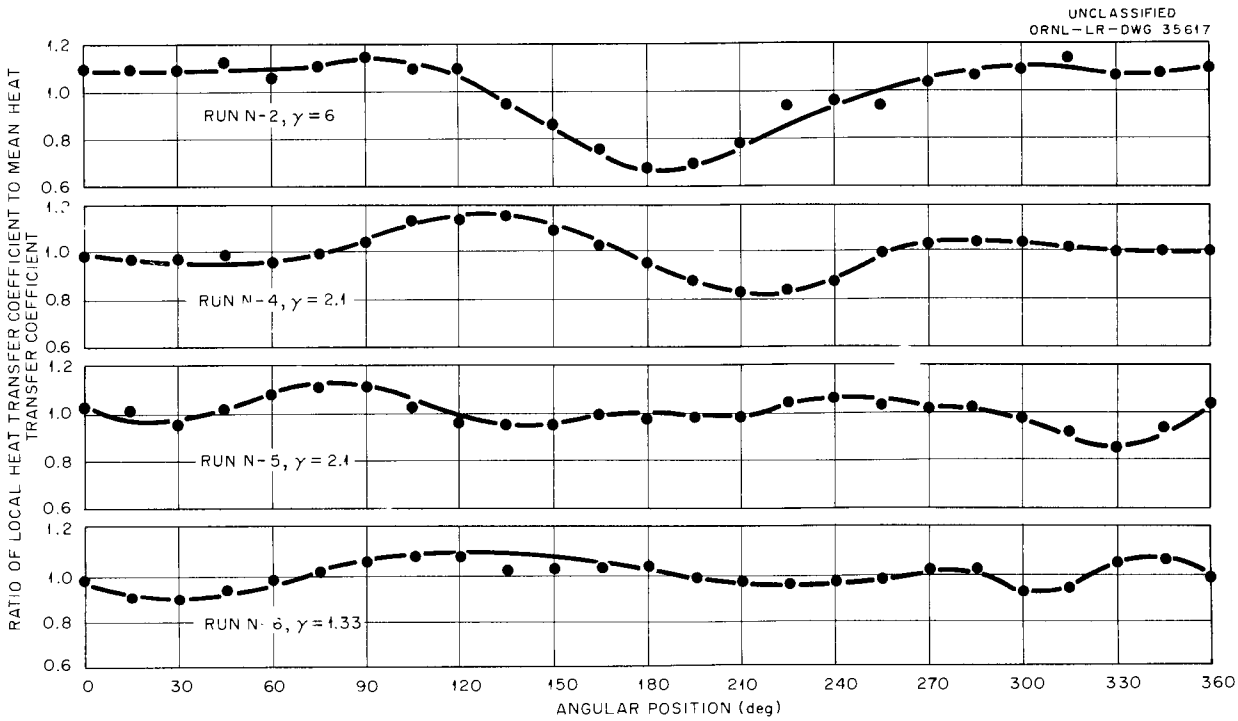

Fig. 3.21. Circumferential Variation of Local Heat Transfer Coefficient as Determined from Naphthalene Mass Transfer Experiment.

4. ADVISORY SERVICE TO AEC ON PROTOTYPE EXPERIMENTAL GAS-COOLED POWER REACTOR

DESIGN REVIEW

At the request of the AEC, the Laboratory established an advisory group to review the detailed plans for the construction of the prototype experimental gas-cooled power reactor (GCPR) being designed by Kaiser Engineers-ACF Industries. The advisory group consists of an average of ten to twelve men experienced in the fields of nuclear physics, instrumentation and controls, stress design, and nuclear power plant engineering. In their review of the reactor design, emphasis was placed on the following aspects: fuel elements, gas system fabrication and stress analysis, reactor physics and core design, instrumentation and controls, fuel handling and core servicing, steam system and power production, and hazards evaluation.

Specific recommendations developed in the course of the review were transmitted to the AEC. Independent checks of some calculations, some analog simulator studies of the controls problem, and careful examinations of equipment performance requirements were carried out in connection with the review.

At the request of the AEC, ORNL also conducted and reported[1] on an evaluation review report, S & P 1963, The Pebble Bed Reactor, which was written by Alco Products Company and Sanderson & Porter personnel. The pebble bed reactor is a two-region thermal breeder in which all the core structural materials are graphite. The fuel is in the form of unclad spherical elements of graphite containing fissile and fertile material (uranium and thorium), and the blanket elements are graphite spheres containing fertile thorium material only. The reactor coolant is helium. It was concluded in the review that the pebble bed reactor shows promise of being competitive with other gas-cooled reactors in the nuclear power market if it can be established that the fuel will have an adequate lifetime under the irradiation conditions specified and that coolant contamination can be controlled in a manner which will permit economical

---

[1] Review of S & P 1963, The Pebble Bed Reactor, ORNL CF-58-7-65 (July 17, 1958).

maintenance of the system by either direct or remote methods. The review also indicated a need for further examination of contaminated coolant systems and a re-examination of the nuclear properties of the system with the use of recently reported nuclear constants in order to determine whether breeding can be realized for this type of reactor. The report showed a conversion ratio of 0.863 with U^{233} fuel. It was noted in the review that unless the reactor can be designed as a breeder, its potential use with U^{233} fuel will be greatly dependent upon economic coupling with some efficient U^{233} breeder having relatively high fuel costs compared with those of the pebble bed reactor.

SITE INVESTIGATIONS

A general survey was made of the Oak Ridge area to identify possible sites for construction of a reactor of the type being designed by Kaiser Engineers-ACF Industries for the AEC. A site evaluation committee from AEC, Washington, visited Hanford, NRTS, Oak Ridge, and Savannah River to inspect and gather information on possible sites at each of these locations. Specific site data were compiled for two Oak Ridge locations. These sites, both on AEC land, were presented as generally typical of a number of other sites in Oak Ridge which would also be suitable. In a joint effort between the Oak Ridge Operations Office, and K-25 and ORNL personnel, site evaluation reports were prepared on each of the two sites. Both reports were submitted to the Oak Ridge AEC and were consolidated with other information into an AEC-ORO report entitled "Site for Gas-Cooled Prototype Reactor." These reports contain information on site topography and geology, construction resources, operational facilities, power utilization, and waste disposal, as well as evaluations of reactor hazards and their relationship to wind and topography.

PLANT CONTROL STUDIES

Studies of plant control were made, as described here, to facilitate the design review work.

The probability of fuel element failures will be increased sharply by excessive temperature variations in the stainless steel fuel capsules. The temperature conditions produced by a severe drop in heat removal from the fuel or by a startup accident are therefore of major concern. Analog

computer studies were performed on a simplified concept of the GCR-2 to examine the variation in temperatures and nuclear power resulting from such accidents. These studies provide the basis for specifying the operational requirements of the reactor safety system. The following general assumptions were made in the analyses: (1) the temperature of the graphite remained constant; (2) all the fuel was at the fuel mean temperature at every instant; (3) all the stainless steel in the fuel capsules was at the capsule mean temperature at every instant.

Startup Accident. The reactor was assumed to be initially at source power level[2] with no mechanism available to remove heat from the fuel. Failures of certain portions of the control system were then assumed to provide continuous withdrawal of the control rods. The results of this simulation are described by the curves in Fig. 4.1.

The initial conditions set into the simulator were taken at the time the reactor multiplication had reached 1.005, which corresponded to a nuclear power level of 3.94 Mw. Numerical integration of the subpower transient[3] indicated that, at this power level, the temperature rise in the fuel from the beginning of rod withdrawal was less than 3°F. The simulator initial conditions and reactor data are listed below and in Table 4.1:

Assumed source power level at start of rod withdrawal = 7 w

Reactor multiplication at start of rod withdrawal = 0.90

Rod withdrawal rate = 10^{-4} $\Delta k/sec$

Reactor multiplication at simulator initial conditions = 1.005

Reactor power level at simulator initial conditions = 3.94 Mw

Fuel heat capacity (UO_2) = 2.685×10^4 kw·sec/°F

Fuel capsule heat capacity (stainless steel) = 0.315×10^4 kw·sec/°F

Fuel temperature coefficient = -2.61×10^{-5} $(\Delta k/k)/°F$

Neutron lifetime = 10^{-4} sec

Fissionable material = U^{235}

---

[2]For definition of source power level see The ORNL Gas-Cooled Reactor, ORNL-2500, Part 3, p 7.2 (April 1, 1958).

[3]E. G. Good, Subpower Range Start-Up Transients, WAPD-TM-1 (March 1956), Curve 541508.

Table 4.1. Delayed Neutron Data at Simulator Initial Conditions

Group	λ_i (sec^{-1})	β_i	Fraction of Steady-State Value
		x 10^{-5}	
1	14.0	25	1.00
2	1.61	84	0.74
3	0.453	240	0.45
4	0.154	210	0.24
5	0.0314	170	0.07
6	0.0125	26	0.04

As may be seen in Fig. 4.1, the sudden increase in fuel temperature limited the initial power rise to a maximum of approximately 700 Mw, which was the design power. Thus a neutron flux level safety system set to initiate an emergency shutdown of the reactor at 150% of design power would be of no value under these conditions.

If the rod withdrawal continued, the asymptotic fuel temperature rise would be 3.8°F/sec, which is the rate of rise necessary to cancel the rate of increase in Δk being introduced by the rods. The nuclear power would become constant at approximately 115 Mw to produce this rate of temperature rise.

The temperatures of the fuel and capsule were essentially the same because no heat was being removed from the can; consequently a very small temperature difference between the fuel and can was sufficient to heat the can. Safety action would be required to reverse the temperature transient and prevent melting of the fuel elements.

Loss of Coolant. Under steady-state design power conditions, the fuel capsule temperature was assumed to be 1200°F. In the loss-of-coolant studies, the steady-state mean fuel temperature was taken as 1450°F in the first case examined, and as 1900°F in the second case. The severity of the temperature transients in the fuel capsule are directly related to the initial steady-state difference between the temperatures of the fuel and capsule.

The curves in Fig. 4.2 were obtained for a step decrease in the rate of heat removal from the fuel capsules from a steady-state value of 700 Mw to a new constant value of 70 Mw. The mechanism to accomplish this change in the actual plant was not specified.

The fuel temperature coefficient would be of considerable value in turning back the temperature rise of the fuel cans; however, it appears that rod insertion would also be necessary. A large rod acceleration together with a fast insertion speed might be required in case there was a large temperature difference between the fuel pellets and the fuel capsule.

REACTOR COOLANT INVESTIGATIONS

A study of possible coolants for the prototype experimental gas-cooled power reactor was completed.[4] In the selection of a coolant for use in a gas-cooled reactor the following factors are significant: materials compatibility, the relationship between the heat transfer rate and the pumping power, and the induced radioactivity in the gas stream. The study showed that, at the design conditions of interest for the proposed reactor, CO_2 and helium were possible coolant choices. In the case of CO_2 there was insufficient information to establish its compatibility with graphite at temperatures above 500°C. For helium the important considerations were found to be availability and cost. It was concluded that an adequate helium supply would be available for a reactor power complex of substantial size if the proposed helium conservation program[5] of the Bureau of Mines is implemented.

A more general investigation[6] of the application of coolants to gas-cooled reactors showed that, since the coolant properties, the fuel element configuration, and the reactor power density are all significant in the evaluation of performance for various coolant gases, an evaluation can be considered to be valid only when it has included a complete thermal

---

[4] Gas-Cooled Reactor Coolant Choice, ORNL-2667 (to be published).

[5] Bureau of Mines, Helium Symposium (Oct. 14 – 15, 1958).

[6] G. Samuels, Comparison of Gases for Use as the Coolant in a Gas-Reactor, ORNL CF-58-4-108 (April 28, 1958).

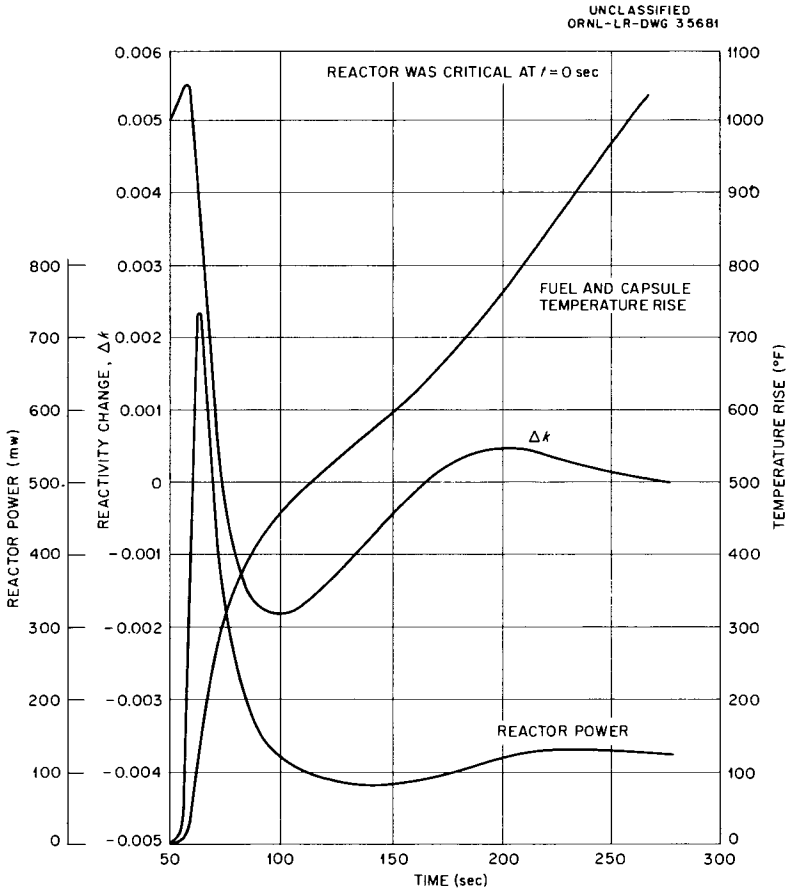

Fig. 4.1. Startup Accident with No Heat Removal. See text Table 4.1 for initial conditions and data.

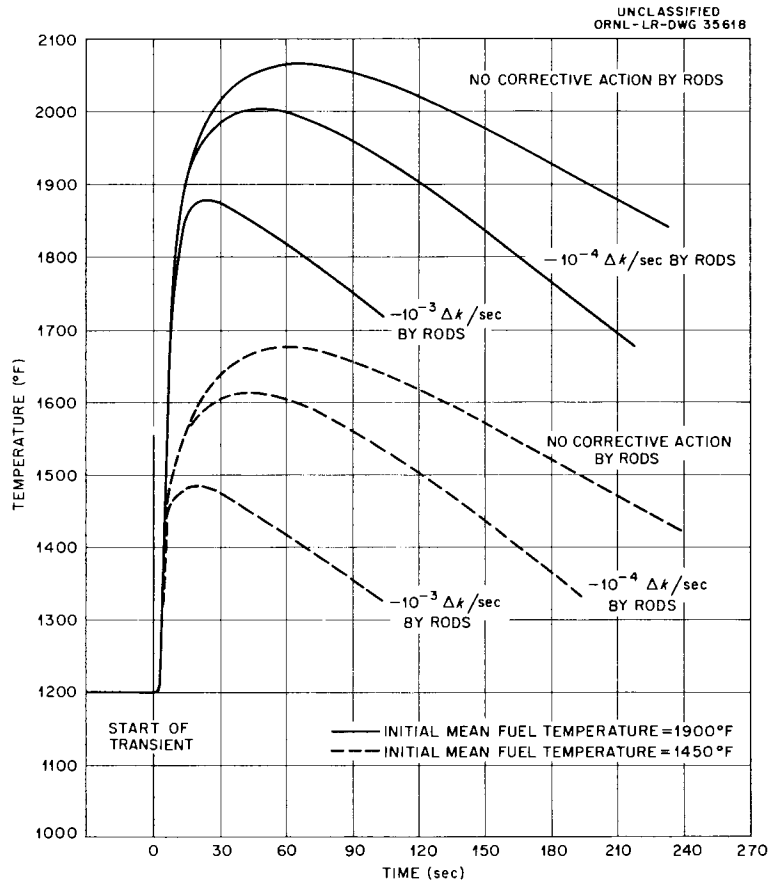

Fig. 4.2. Fuel Capsule Temperature Variations Following a Change in Heat Removal from 100% to 10% of Design Value.

analysis of the reactor system under consideration. In this connection some preliminary studies were carried out for the seven-rod cluster fuel element configuration by using coolant channel diameter and reactor coolant gas as variables. The preliminary results are presented in Table 4.2, which shows the effect of the coolant choice on the power cost increment of coolant-dependent features. For this investigation a plant layout similar to that of the GCR-2 was assumed. Although carbon monoxide and air were not included in this study, it is assumed that the results would be identical with those for nitrogen because of similar thermodynamic properties, if chemical compatibility considerations are ignored. The accuracy of the reported data is subject to the usual reservations concerning the capital cost estimates used in the calculations.

The effects of impurities on induced activity in the gases were also examined. The most undesirable impurity is argon, because A^{41}, which has a 1.8-hr half-life and emits 1.7-mev gamma radiation, is produced from A^{40} by an (n,γ) reaction. Commercial high-purity nitrogen containing about 50 ppm argon would have low activity, but air, which contains 1% argon, would have equilibrium activity sufficiently high to make routine servicing difficult. The activities that would be induced in various gases in a GCR-2 type of reactor relative to the activity induced in CO_2 are listed in Table 4.3.

Some preliminary studies were completed which show that steam has many advantages for use as a coolant in small high-pressure systems. The heat transfer properties of steam are not good at low pressures, but at pressures above 1000 psia they are comparable with those of helium. Aside from its inexpensiveness and availability, the principal advantage of steam would be the possibility of using a Loeffler boiler of similar cycle in which the reactor serves as a steam superheater. This would allow steam to enter the turbine at the full reactor discharge temperature and would also eliminate the multitube steam generator. Material compatibility considerations have not been fully examined, but the reaction of steam with graphite is known to be a serious drawback to the system. The

Table 4.2. Effect of Coolant Choice on Power Cost Increment*

Gas Outlet Temperature (°F)	Maximum Capsule Temperature (°F)	Power per Channel (Mw)	Channel Diameter (in.)				Ratio of Pumping Power to Total Output (%)				Cost** (mills/kwhr)			
			H_2	He	CO_2	N_2	H_2	He	CO_2	N_2	H_2	He	CO_2	N_2
900	1200	0.82		3.85	3.42			3.72	5.76			1.09	1.15	
		1.00	3.88	3.80	3.38	3.39	1.00	5.78	9.09	22.2	0.82	1.04	1.21	2.93
		1.44		3.71	3.31			13.40	19.50			1.52	3.15	
1000	1200	0.82		3.41	3.10			4.17	6.94			1.10	1.20	
		1.00	3.45	3.38	3.05	3.05	1.10	6.65	11.10	27.4	0.81	1.07	1.37	4.00
		1.44		3.30	3.00			15.64	26.50			2.05	4.69	
1000	1300	0.80		3.74	3.35			2.40	3.72			1.04	1.07	
		0.97		3.69	3.30			3.75	5.93			0.94	1.01	
		1.40		3.60	3.23			8.69	14.00			1.09	1.68	

*Calculations were made on the basis of 700 channels 20 ft long with seven 0.8-in.-OD fuel rods. The coolant gas pressure was taken as 485 psia and the inlet temperature as 450°F.

**Reflects effect of coolant choice on coolant-dependent features, such as the pumping power, pressure vessel, reactor, shield, graphite moderator and reflector, coolant blowers and drives, and containment vessels for the blowers and drives.

reaction rate of steam with graphite is more rapid than that of carbon dioxide, perhaps by a factor of 2, and it would be necessary to provide a suitable coating on the graphite that would prevent the reaction or to use a different moderator material.

Table 4.3. Induced Activities in Gases as Coolants in a GCR-2 Type of Reactor Relative to the Induced Activity in CO_2

Gas	Relative Activity	
	Gamma	Total
CO_2	1.0	1.0
H_2	0	4.5×10^{-4}
He	0	18.5
N_2	4.6×10^{-2}	9290
Air	1280	7230
CO	0.50	0.51
A	137,000	1390

PART II. MATERIALS RESEARCH AND TESTING

5. METALLURGICAL DEVELOPMENTS

FABRICATION OF BULK UO_2 FUEL

The initial design studies on the GCR-2 specified pelletized UO_2 as the fuel because of the need for stability at extremely high operating temperatures and high burnup of fissionable material. The fabrication of bulk UO_2 rods or pellets has been studied for some time at various sites, and the successful manufacture of reactor loadings has been demonstrated. The emphasis on economy in the gas-cooled reactor concept, however, provided sufficient motivation for further development of the fabrication processes used in manufacturing UO_2 fuel pellets. Other sites have used extensive operations for milling the as-received powder, adding binders, and sizing sintered pellets, and it was thought that if a fabrication process could be developed that involved only the minimum number of operations, such a process would contribute greatly toward minimizing the fuel costs for the gas-cooled power reactor. The progress in the development of such a process is described here.

Minimized Fabrication Process. Existing knowledge of fabrication techniques and of the types of UO_2 available indicated that it would be quite possible to sinter UO_2 to the required size and density, provided the specified tolerances were not too severe. A type of UO_2 prepared from ammonium diuranate precipitated from a nitrate solution has been used successfully in the ORNL Ceramic Laboratory for fabricating high-density bulk shapes. This material is characterized by high green strength when formed at moderate pressures and by its uniform shrinkage to high densities after sintering. This type of oxide was selected as most suitable for use in developing a minimized fabrication process.

The fabrication of ceramic shapes involves three basic steps: powder preparation, forming, and sintering. Assuming that UO_2 powder of the above-described type could be made available, a simplified process involving the fewest operations possible was selected for development. This process, as outlined in Fig. 5.1, includes only a granulation process, forming by dry pressing, and sintering in an induction-heated furnace.

Granulation Process - For a cold-pressing operation, the powder-preparation step consists of granulating the material to obtain free-

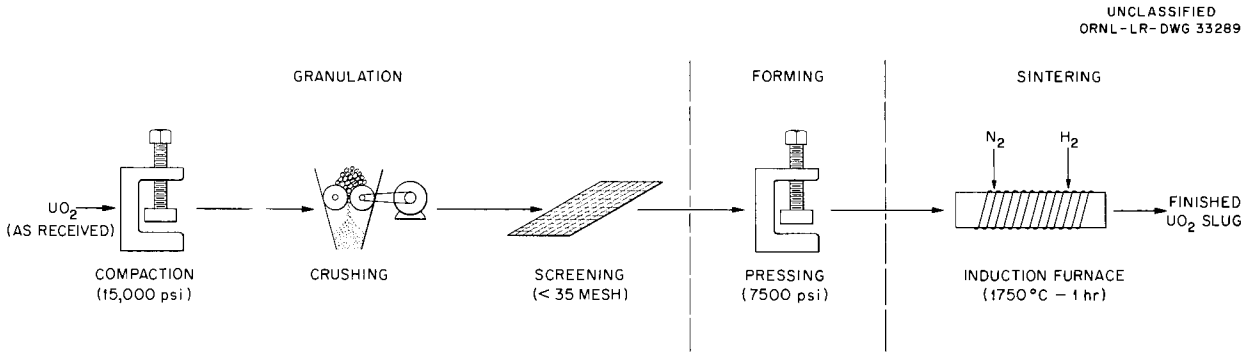

Fig. 5.1. Minimized Fabrication Process Proposed for GCPR Fuel.

flowing powder which will charge a die uniformly. The techniques employed in the granulation process can vary widely, depending on the material and the forming and sintering operations. The usual granulation procedure for UO_2 is to blend moisture and a soluble binder into the material and to follow this with drying, breaking up, screening, and the blending in of a lubricant. The binder and lubricant must then be removed by a preheating or presintering operation. Since the type of UO_2 chosen compacts readily into a piece of moderately high green strength without the use of organic additives, this portion of the granulation procedure was eliminated. In addition, the procedure was further modified to compact as-received UO_2 at a low pressure (15,000 psi), followed by breaking of the compact through a 35-mesh screen. The screened material, including the fines, is a fairly free-flowing powder that contains no additives. Therefore the granulation process eliminates blending, drying, and baking, or presintering operations while adding only a compacting operation.

Pressing - The dry-pressing operation is merely one of compacting powder in a die. To achieve high sintered densities, it is ordinarily necessary to compact UO_2 to a fairly high green density, approximately 60 to 75% of theoretical density. Also, depending on the particular type of UO_2, the pressure required for compacting to a high green density ordinarily ranges between 20 and 125 tsi. At these pressures it becomes necessary to add a lubricant or binder to the oxide to aid in the compacting. In addition, the green compact must have sufficient strength to withstand a moderate amount of handling.

In compacting pieces of any appreciable length, the length-to-diameter ratio can become very important. An increasing hourglass effect is noted in the sintered piece as the length-to-diameter ratio increases and as forming pressures increase. This effect is caused by a density differential between the ends and center of the pressed piece. If the sintered piece is to be machined to its finished diameter, this hourglass effect is relatively unimportant, but if the piece is to be sintered to its final dimensions, the effect becomes very important and must be minimized.

After considering these problems, the conditions for pressing fuel pellets were selected. The forming pressure was set at a maximum of

10 tsi, and the maximum length-to-diameter ratio was set at one. Within these limits, the selected UO_2 forms a low-density body that has sufficient green strength for easy handling. At near the required size, experience has established that a pressure of 7500 psi and a length-to-diameter ratio of approximately 0.65 yield a piece with a density ranging between 40 and 50% of theoretical, and the better grades of oxide yield density values close to 48% of theoretical. Formed in this manner, the better oxides give sintered densities ranging from 93.5 to 95% of theoretical density. In general, the hourglass effect does not exceed 2 mils on the diameter of a piece which sinters to approximately 3/4 in. in diameter. The low compacting pressure also permits the use of light and relatively inexpensive presses and dies.

Sintering - The sintering temperature chosen for the fuel pellets is 1750°C, with a soak time of 1 hr at temperature. These conditions are sufficient to sinter the oxide selected for the fabrication process. In general, 1750°C is a fairly standard temperature for sintering UO_2, but, depending on the type of UO_2 being sintered, the soaking time usually ranges between 2 and 10 hr.

Sintering is done in an induction-heated controlled-atmosphere furnace with graphite as the susceptor. This type of furnace was chosen rather than the usual molybdenum-wound alumina-refractory furnace for several reasons. With the short one-day heating cycle of this furnace, the results from firing of experimental batches are made available quickly. In addition, the furnace allows experimentation at different temperatures with suitable control, and it is a small inexpensive unit which may be easily replaced.

In general, it has not been considered good practice to sinter UO_2 in the presence of carbon; but experience has shown that it can be done successfully, with very minor, if any, carbon pickup. The only requirements are that the furnace be kept scrupulously clean and that the atmosphere be carefully controlled. The atmosphere consists of a mixture of nitrogen and hydrogen in the ratio of 7:3, although a better atmosphere would consist of a mixture of hydrogen and argon. The disadvantage of using nitrogen is that, if a carbide is formed, it will decompose to form the

more stable nitride, and the consequent changes in density and volume can be catastrophic to the piece being sintered.

Preparation of UO_2 Powder. The fabrication process selected, as stated above, is entirely dependent upon the availability of a particular type of oxide. Some generalized specifications for the oxide state that (1) a material is needed which can be granulated for flowability of the powder and compacted in steel dies at pressures of 20,000 psi or less without the use of either an organic binder or lubricant, (2) the compacted piece should have sufficient green strength for easy handling, and (3) the material should have a high surface activity and be sinterable to achieve the required high density (95% of theoretical) and uniform shrinkage which are needed for the material to be sintered to within tolerances.

The type of powder desired has been available for several years, but a method had to be devised to produce powder of the same quality and characteristics from partially enriched UF_6. Making UO_2 from UF_6 is a straight-forward and well-established process, but the product does not meet the requirements. With the close cooperation of the Y-12 Production Group, a double precipitation process was developed, as shown in Fig. 5.2, which yielded several good powder batches. This is a batch process, however, and the reproducibility is not as good as is needed; the best oxide made by this process was never reproduced.

When it became obvious that much tighter control would have to be maintained over the various chemical and calcining conditions, a continuous process, illustrated in Fig. 5.3, was tested. This process, which was established by the Y-12 Development Group, is proving to be much the better from the standpoints of control and reproducibility and will be the preferred process on the basis of cost, quantity, and time. This process should lend itself well to the concept of a production facility which starts with UF_6 and ends with a sintered, finished UO_2 shape.

Recently, powder produced by this process has reached the high quality needed, and the process is now being refined. Small variations in chemical and calcining conditions are being investigated for quality control. Oxide powder from this process apparently has the forming and sintering characteristics needed to produce UO_2 shapes at 95% of theoretical density by the fabrication process described above.

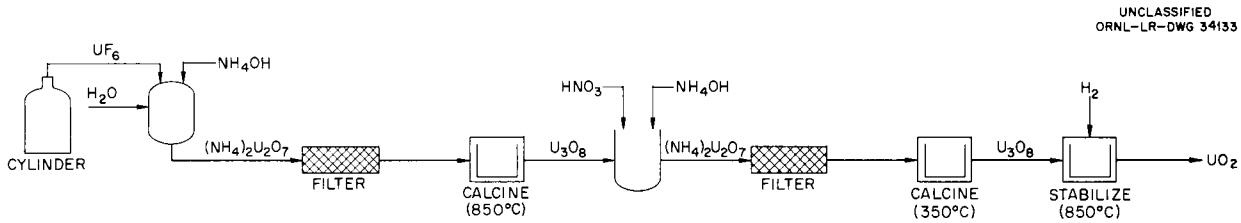

Fig. 5.2. Batch Process for Producing Highly Sinterable UO_2 from UF_6.

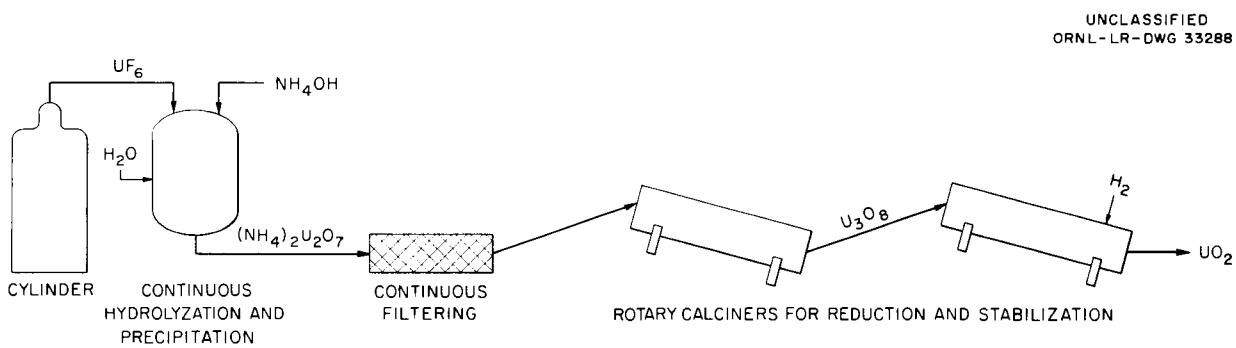

Fig. 5.3. Continuous Process for Producing Highly Sinterable UO_2 from UF_6.

Quality Control and Evaluation of UO_2 Powder. Testing of the powder consists of combined thermogravimetric and differential thermal analyses, followed by forming and sintering under the stated conditions. The thermogravimetric analysis which records weight changes as a function of thermally induced reactions or changes in the material gives information on the stoichiometry of the oxide. The differential thermal analysis records the temperature at which thermally induced reactions or changes occur and gives information on reactivity and changes in reactivity caused by changes in the processing history of the material.

These analyses are a valuable tool when employed collectively, for they give a rapid check on the effect of changes in the processing history of the material and the reproducibility of the oxide. The analytical data for an oxide made under very poor reducing conditions in the calciner are presented in Fig. 5.4a. The poorly defined peaks and extremely low over-all weight gain through the oxidation steps from UO_2 to U_3O_8, coupled with the continual depression of the weight-change pattern, which indicates that the weight gain through the oxidation steps is continually offset by a weight loss, show that the reduction in the calciner was incomplete. The sample was composed of a mixture of UO_3, U_3O_8, and UO_2. The material was recalcined under good reducing conditions and the analysis patterns shown in Figs. 5.4b and 5.4c were obtained. The effect of the reduction process on the shape and position of the peaks and on the over-all weight gain of the sample may be easily seen. The effect of a change in the atmosphere used during the reduction is shown in Fig. 5.5; all other conditions remained constant. The results of a reproducibility check on two batches prepared at different times are presented in Fig. 5.6. In this case the reproducibility was rather good.

Forming and sintering of the oxides complete the testing. Note is made of the relative strength of the formed piece, and the length to which a given amount will compact. After sintering, checks are made on density, dimensional variation (hourglass effect), and the uniformity of shrinkage.

Fabrication and Evaluation of Fuel Pellets. Fabrication of specimens for use in the capsule irradiation program (see chap. 6) is in process;

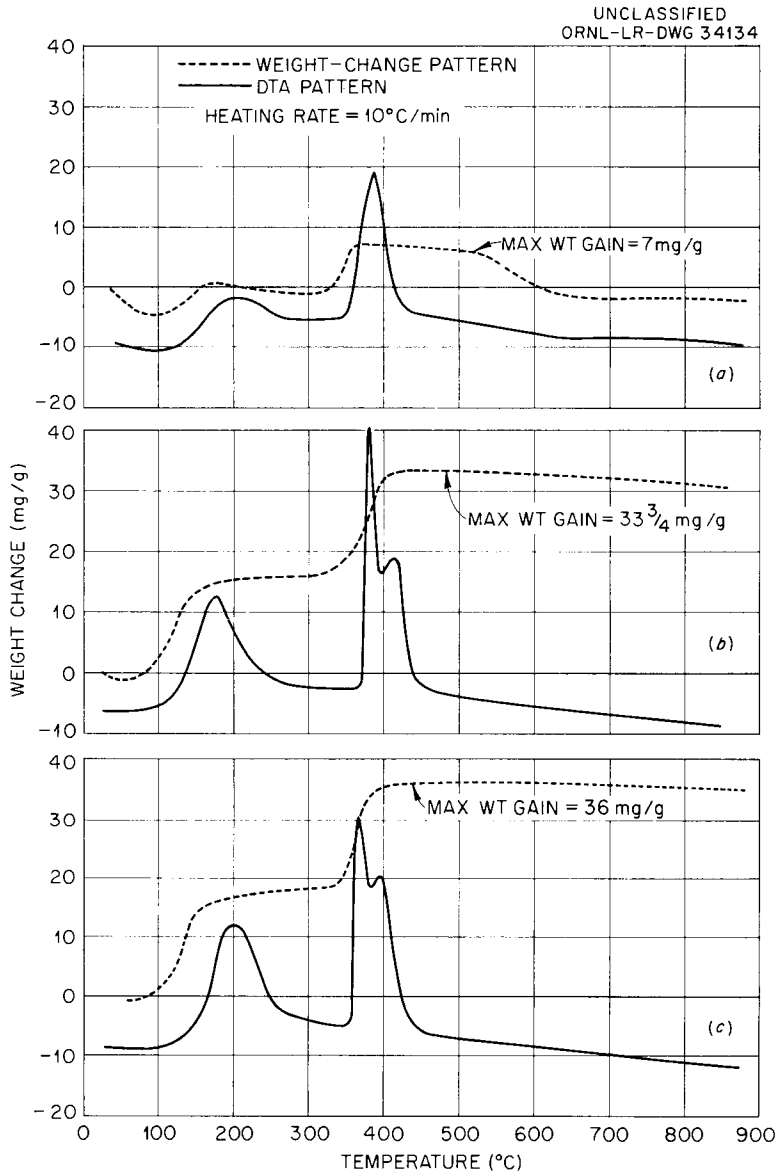

Fig. 5.4. Thermogravimetric and Differential Thermal Analyses of Samples of UO_2 Prepared Under Various Reducing Conditions.

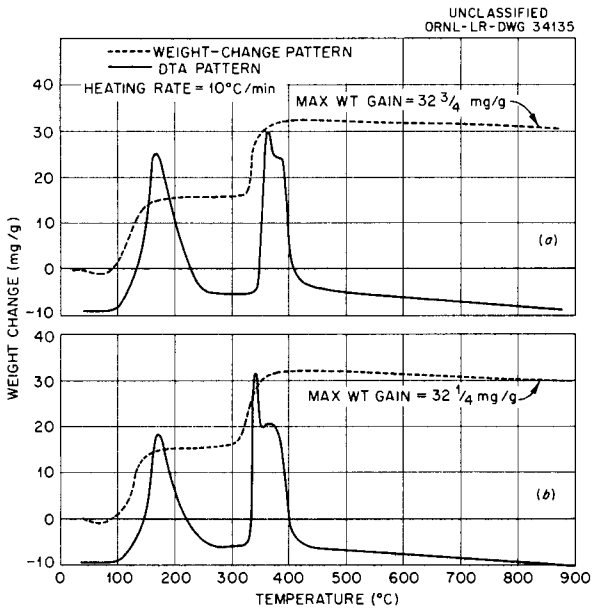

Fig. 5.5. Thermogravimetric and Differential Thermal Analyses of Samples of UO_2 Calcined in Different Atmospheres. (*a*) Reduced in H_2; (*b*) reduced in 1:1 N_2-H_2.

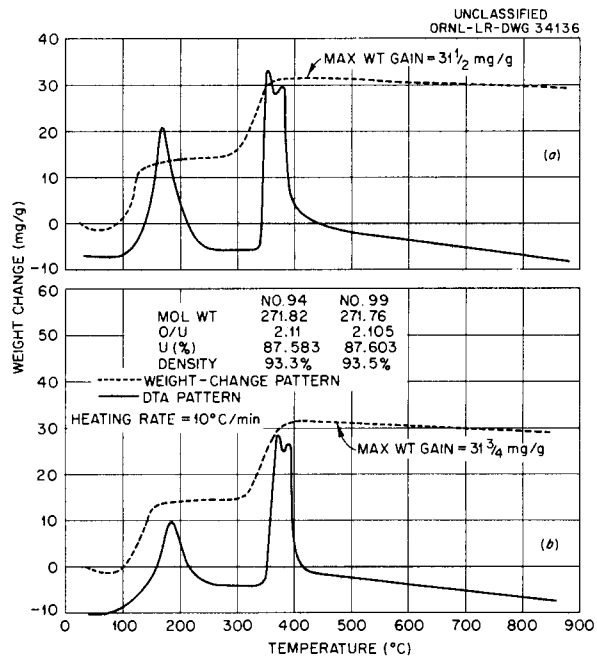

Fig. 5.6. Reproducibility Check on Two Batches of Oxide.

the miniature prototype specimens (0.156 in. OD, 0.078 in. ID, 0.25 in. long) are being fabricated; and oxide powder is being prepared for the prototype specimens (0.705 in. OD, 0.323 in. ID, 0.5 in. length). The powder is prepared by the continuous process outlined above.

Finished pellets for use in the irradiation program are evaluated by a series of physical measurements. The diameter and length tolerances are determined and noted, the concentricity of cored pellets is checked and maintained to within 0.005 in., and the bulk density of pellets is determined from the calculated volume and the weight in air. In addition, the apparent density of the pellets is determined by weighing them in CCl_4 after vacuum infiltration with CCl_4.

The immersion density determination gives a good check on the bulk density and a direct measure of the closed porosity. It is interesting that the closed porosities of specimens of 75 and 95% density are nearly identical, as may be seen in Table 5.1. In addition, the immersion density

Table 5.1. Results of Density Measurements of Miniature Pellets

Pellet Density (% of theoretical)	Calculated Density (g/cm^3)	Immersed Density (g/cm^3)
95	10.31	10.60
75	8.18	10.49

determination also quickly detected the presence of other compounds of uranium in a few pellets as a result of the anomalous densities of these compounds.

Extrusion of UO_2. Extrusion as a forming technique for UO_2 was not considered for the minimized fabrication process because of the difficulty in achieving high sintered densities from extruded parts. Long ceramic shapes are, however, produced to close dimensions by the extrusion process; therefore, some work to determine the feasibility of the process was initiated.

This work is being done by the Electric Auto-Lite Company, Fostoria, Ohio.[1] The initial stage of the investigation consists of finding the binders and plasticizers which can be used in the least quantity to yield the highest density. The investigation is being restricted to two types of UO_2, one low-calcined and the other dead-burned. It is felt that the optimum extrusion mixture may be a combination of these two types. The later stage of this work will be to investigate the possibility of fabricating larger and longer shapes than can readily be obtained by dry pressing and to note the possibility of sintering these shapes to specified tolerances, leaving only raw ends to be finished by machining.

MECHANICAL PROPERTIES OF FUEL CAPSULE MATERIAL

In order to utilize the advantages of UO_2 as fuel, it is necessary to provide a metallic capsule to contain the UO_2 and the gaseous fission products released during operation. As an aid in the selection of the metal for the capsule, a literature survey was conducted on the strength properties of several alloys in the temperature range of interest. The ultimate choice of type 304 stainless steel was based on such factors as cost, fabricability, compatibility with the coolant and fuel, and high-temperature strength.[2] Creep-buckling and tube-burst tests were then undertaken to evaluate type 304 stainless steel tubing experimentally.

Creep Buckling of Capsule Tubing. The fuel element assembly consists of pellets of UO_2 inserted into a closed-end cylindrical capsule sealed with a welded end cap. There is, of course, a clearance space between the outer surfaces of the pellets and the inner surface of the capsule. The extent of the clearance space must be a compromise between tolerances which are economically feasible in the production of large quantities of each item and those which are feasible from the standpoint of structural stability. This latter consideration is complicated because some capsules will have hot streaks along their lengths as a result of the configuration of the fuel element bundle.

---

[1] ORNL Subcontract No. 1217.

[2] The ORNL Gas-Cooled Reactor, ORNL-2500, Part 2, p 3.13 (April 1, 1958).

Results of preliminary investigations[3] indicated that the capsules would collapse because of creep buckling at all temperatures at which type 304 stainless steel undergoes plastic deformation by creep. This prediction has been confirmed by tests at 1300°F which showed that a 0.020-in.-wall tube would collapse by creep buckling in about 2000 hr with a pressure differential of 300 psi. Further tests at 1300 and 1500°F showed that the degree of distortion at a uniform temperature varies from slight wrinkles when there is a 0.020-in. diametral clearance to complete collapse if there are no fuel pellets to support the capsule wall. A summary of the data is presented in Table 5.2. Even with the gross distortion that occurs with

Table 5.2. Relationship of Diametral Clearance and Temperature to Buckling Behavior of Tubes with Inserts

Diametral Clearance (in.)	Mode of Collapse	
	At 1300°F	At 1500°F
0.002	Uniform	Uniform
0.005	Nonuniform	Uniform
0.010	Nonuniform	Nonuniform, one wrinkle
0.020	Nonuniform	Nonuniform, two wrinkles

complete collapse, cracks do not penetrate the metal wall; thus no fission gases would escape into the helium stream of an operating reactor fueled with elements of this type. Creep buckling of the fuel capsules will not be a serious problem therefore, except for the possibility that the wrinkles might become hot streaks or might produce hot spots in the UO_2 underneath the wrinkle where no metal contact occurs and poor heat removal results. Either of these factors might eventually lead to failure of the capsule. An example of the gap formed between the UO_2 and the capsule wall as a result of buckling is shown in Fig. 5.7.

[3] The ORNL Gas-Cooled Reactor Materials and Hazards, ORNL-2505 (rev), p 12.9 (June 19, 1958).

A solution to the hot-spot problem might be to specify tolerances so close that uniform collapse would be assured. It may be seen in Table 5.2 that the maximum tolerances allowable for uniform collapse are 0.005 in. at 1500°F and 0.002 in. at 1300°F. Such tolerances would be rather difficult and expensive to achieve. In addition, those fuel capsules in which hot streaks occurred because of the configuration of the fuel element bundle might wrinkle during collapse despite adherence to the tolerance, since the hot area would deform more readily than the remainder of the tube.

As a solution to these problems, an investigation was made of collapsing the capsule tubing under controlled conditions of pressure and temperature before inserting the fuel element into the reactor. A generous commercial tolerance of 0.012 in. was allowed as the diametral clearance between the capsule and the pellets in the initial tests. The satisfactory results of these tests are presented in Table 5.3, and the type of collapse

Table 5.3. Results of Creep Buckling Tests of Type 304 Stainless Steel Tubes with a Diametral Clearance of 0.012 in.

Temperature (°F)	External Pressure (psi)	Time in Test (hr)	Mode of Collapse
1900	300	8	Uniform
1800	300	25	Uniform
1700	500	18	Uniform

obtained is illustrated in Fig. 5.8. Other specimens are being tested to determine the limitations of this technique.

It is also possible that cracks might develop in the UO_2 and that large gaps might be left between the UO_2 and the end caps of the capsules. Experiments are therefore under way to determine how an area of unsupported wall will behave at reactor temperatures and pressures. For these tests a 1/16-in. gap is left between the top pellet and the end cap. Collapse of the capsule in this area has produced a small dished-out ring around the tube; but thus far no failures have occurred that would

UNCLASSIFIED
Y-27183

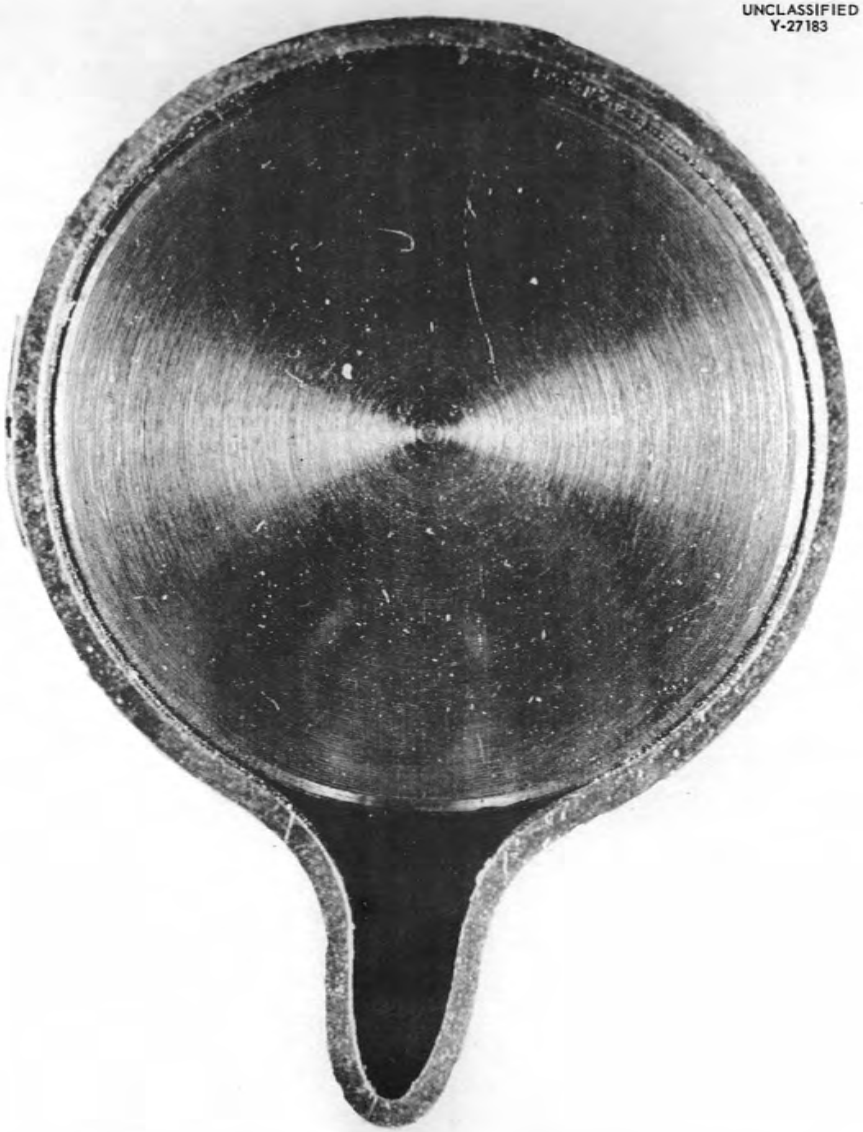

Fig. 5.7. Cross Section of a Buckled Type 304 Stainless Steel Tube.

UNCLASSIFIED
Y-27181

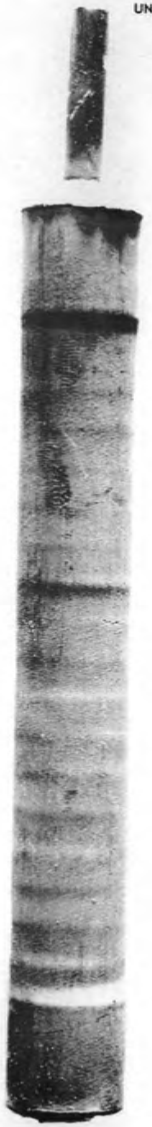

Fig. 5.8. Creep-Buckling Specimen with 0.012-in. Diametral Clearance Showing Uniform Collapse.

have released fission-product gases. Additional tests with cracked pellets are in progress to determine the behavior of the unsupported capsule in the vicinity of a crack. The testing arrangement shown in Fig. 5.9 is being used to investigate the effect of a hot streak along the length of a fuel capsule. In the initial test no observable deformation of the capsule wall was obtained in 500 hr at a uniform temperature of 1300°F with a hot streak of 1500°F and an external pressure of 300 psi. This test is being continued for an additional 1000 hr.

Tube-Burst Testing of Type 304 Stainless Steel. The most serious possibility for fuel element failure would be a large buildup of pressure inside the capsule. The pressure in the capsule will build up gradually as fission gases are released and will reach a maximum late in the life of the fuel element when the stainless steel has already absorbed considerable thermal and mechanical strain. The question of how high an internal pressure will be produced is unresolved, since estimates of the quantity of fission gases that will be released vary from 10 to 100%. Any appreciable pressure differential between the inside and the outside of the capsule will eventually lead to the formation of intergranular cracks that will propagate through the wall of the capsule and allow escape of the fission gases. The most critical situation will be present in those elements which have hot streaks at a temperature of about 1500°F along their length. Even as small a differential pressure as 100 psi will cause failure in these areas in a relatively short time.

In addition to the concern with failure under normal operating conditions, it is recognized that in case of an accident which resulted in the loss of coolant pressure there would be a real possibility of failure of a large majority of the fuel elements. The loss of the coolant would cause a rise in temperature of the fuel element which, in turn, would increase the internal pressure. Therefore, an extensive investigation of the time to rupture of type 304 stainless steel capsules in terms of pressure and temperature is being conducted.

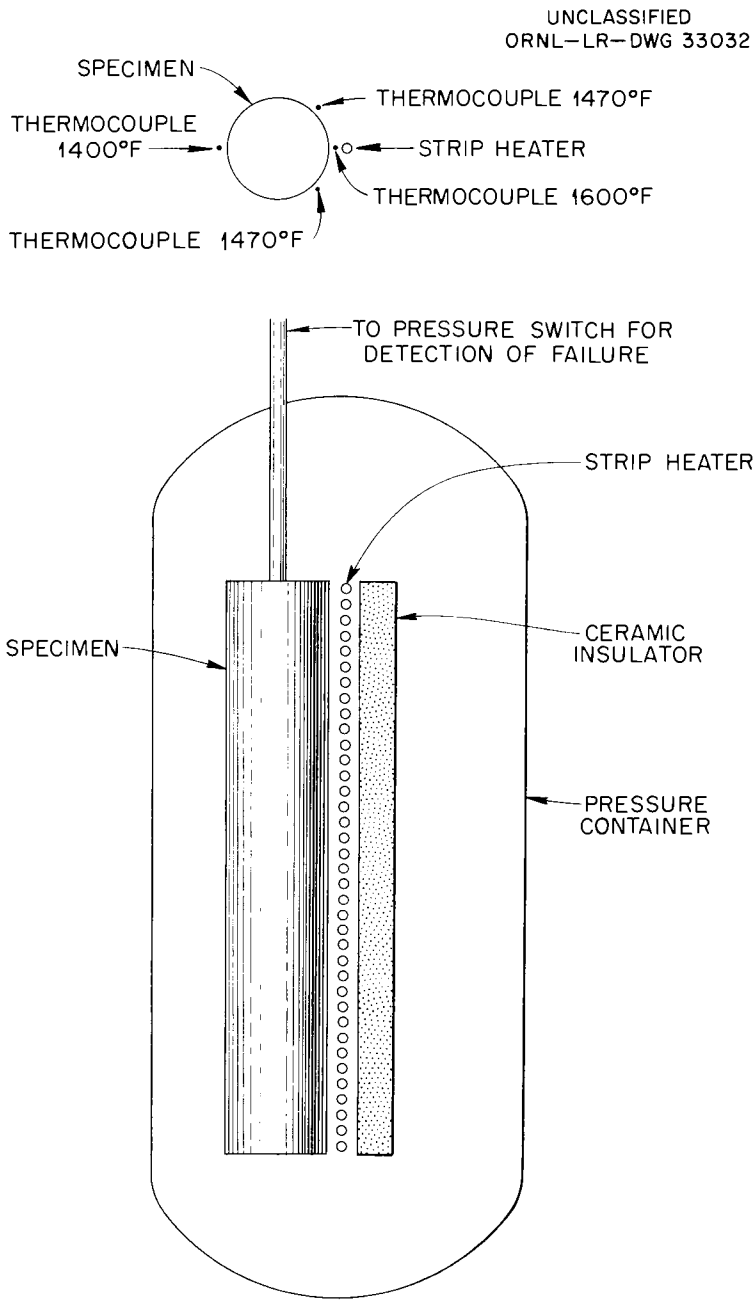

Fig. 5.9. Testing Arrangement for Investigating the Effect of a Hot Streak Along the Length of a Fuel Capsule.

At the beginning of this investigation the end plugs of the specimens were welded with edge-fusion welds of the type used in the preparation of specimens for the creep-buckling tests. In all tube-burst tests, failure occurred in the fusion zone of the weld, as illustrated in Fig. 5.10, which shows an example of the type of failure obtained at 1500°F with an internal pressure of 300 psi. The time to failure was 500 hr. In an attempt to improve the welds, specimens were prepared with closer tolerances maintained on the end plugs. These specimens are currently being evaluated. Specimens fabricated by using a butt-fusion end-closure design were also subjected to tube-burst tests. Satisfactory welding conditions appear to have been established for this type of design, inasmuch as all failures occurred in the tube area. A summary of the tube-burst data obtained thus far is presented in Table 5.4.

Table 5.4. Results of Burst Tests of 0.020-in.-Wall Type 304 Stainless Steel Tubing

Temperature (°F)	Internal Pressure (psig)	Time to Rupture (hr)	Tangential Stress (psi)	Average Tangential Strain* (%)	Maximum Tangential Strain (%)
1500	400	375	7,140	6.36	7.29
1500	200	1184	3,750	2.64	5.04
1300	700	306	12,495	1.86	3.18

*Tangential strain obtained by averaging six diameter measurements along length of specimen.

Other possible means by which the fuel capsule might fail are strain fatigue failure as a result of thermal cycling and a stress-accelerated corrosion reaction between the impurities in the coolant and the stainless steel. It is possible that there will be a variety of oxidizing and reducing conditions present at various stages of reactor operation, and some of the conditions might produce grain-boundary attack which

UNCLASSIFIED
PHOTO-45319

Fig. 5.10. Type 304 Stainless Steel Capsule with an Edge-Fusion Welded End Cap That was Burst Tested at 1500°F and with an Internal Pressure of 300 psi. Time to failure: 500 hr.

could contribute to failure. The possible modes of failure are presently being explored to determine how significant they may be in restricting the mechanical life of the fuel element.

REACTIONS OF TYPE 304 STAINLESS STEEL WITH GASES

The reactions of type 304 stainless steel with pressurized impure helium at elevated temperatures have been studied on the basis that the principal trace impurities will be O_2, N_2, and H_2O. It was assumed that the contaminants would react with, or be evolved from, the graphite moderator to various degrees, depending on the pressure and temperature, and would therefore give rise to various other gas species which also could react with the capsule material. The impurities of concern would be CO, CO_2, CH_4, H_2O, H_2, and other metastable gases derived from radiation effects.

Since it would be possible for several of these gases to react simultaneously with the stainless steel, the determination of detrimental gas compositions or the interpretation of corrosion data can be approached best through a study of the effects of individual gases or selected mixtures. Having determined the effect of the individual gases, it will then be possible to determine the effect of more complex mixtures and to ascertain the degree to which purification of the reactor gases is necessary.

Any reaction of stainless steel with gases could be detrimental to the properties of the steel because of the embrittling effects of oxidation, carburization, or decarburization of the metal. Embrittlement by oxidation would occur if the mode of oxide penetration was nonuniform; for example, grain-boundary penetration. Stresses superimposed by the corrosive effect of the gas would aggravate this tendency and have a serious effect in thin-walled tubing. Carburization would result in a loss of ductility because of the precipitation of chromium carbide. In moderate quantities (less than 0.20% C), carbon would improve the creep strength. Embrittlement by decarburization, which is a special case peculiar to an unbalanced composition of the stainless steel, could also occur. For example, in those heats in which chromium is on the high end

and nickel on the low end of the specified composition range, removal of carbon would favor the precipitation of a brittle iron-chromium (sigma) compound.

Free-energy calculations for the reactions of the various gases with stainless steels indicate that CO_2, CO, and H_2O will be predominantly oxidizing. Methane and CO, on the other hand, will be carburizing, and hydrogen will be reducing. Decarburization, if it occurs, will be due to CO_2, H_2, or H_2O. In the absence of significant amounts of H_2 and H_2O, however, the occurrence of the decarburizing reaction appears to be unlikely, since temperatures much greater than the proposed design temperatures are necessary to produce significant decarburization by reaction with CO_2. In addition, it has been demonstrated that oxide films prevent carburization,[4] although the protective action may be peculiar to certain types of oxide. Since the formation of oxide films appears to be a certainty, the occurrence of carburization or decarburization will indicate the permeability of the films.

The effect of CO_2 on type 304 stainless steel is assumed to be oxidizing according to the reaction

(1) $Fe + 2Cr + 4\ CO_2 \rightarrow FeO \cdot Cr_2O_3\ (\text{film}) + 4\ CO\uparrow$

and decarburizing according to the reaction

(2) $FeO \cdot Cr_2O_3 + 4\ C \rightarrow Fe + Cr + 4\ CO\uparrow$,

In a dynamic system containing only CO_2 plus an inert carrier gas, the occurrence of reaction 2 was calculated to be only a remote possibility, since the equilibrium CO pressure at 1500°F has been determined to be about 10^{-9} atmospheres.[5]

If reaction 1 is significant, the effect of CO_2 in a static system might be entirely different from that in a dynamic system, since the reversal of a reaction such as reaction 2 would promote the possibility of carburization or the deposition of soot on the metal.

---

[4] J. B. Giacobbe, Trans. ASM 45, 134 – 150 (1953).

[5] T. N. Rhodin, "Surface Reactions on Stainless Steels," J. Chem. Phys. 54, 72 – 89 (1957).

After considering the possible reactions and reaction products, the two experiments described below were performed. In one experiment specimens of hard-drawn type 304 stainless steel tubing, 0.500 in. OD, 0.002 in. wall, and 5 in. long, were exposed to flowing gas in an all-glass system that included suitable flowmeters and was constructed to provide gas mixtures ranging from 0.1 to 100% CO_2, with argon as the carrier gas. The results of tests run at one atmosphere total pressure, a temperature of 1500°F, and a flow rate of 300 cm^3/min are presented in Table 5.5. The film which formed on the metal

Table 5.5. Results of Tests of the Reaction of Type 304 Stainless Steel Tubing with Flowing CO_2 at 1500°F

CO_2 in Argon (%)	Test Time (hr)	Weight Gain of Tubing ($\mu g/cm^2$)
100	68	180
1	68	60
0.63	90	117
0.10	117	109

was greenish, adherent, and gave indications of being magnetic. Electron diffraction patterns of the film revealed the presence of two different compounds. The bulk of the surface oxide was identified as rhombohedral $3Cr_2O_3 \cdot Fe_2O_3$, and a very thin film between the outer bulk oxide and the metal substrate had structure that corresponded to an oriented cubic spinel. This film was identified as $MnO \cdot Fe_2O_3$. Spectrographic analysis of the stripped film indicated that Fe, Mn, and Cr were the strong constituents. Carbon analyses of the metal before and after testing were inconclusive with respect to carburization or decarburization.

In the second experiment, clippings of type 304 stainless steel foil from the same lot of tubing were sealed in a quartz capsule containing 20.75 mm of purified CO_2. The capsule was heated for 336 hr at 1500°F, after which time the residual gases were analyzed, and the results were compared with the initial gas composition. The analytical data are presented in Table 5.6.

Table 5.6. Results of Tests of the Reaction Between Static CO_2 and Type 304 Stainless Steel

Gas Constituents Analyzed for	Quantities Present in CO_2 (ppm)	
	Before Test	After Test
H_2O	33	9
HC	13	None
N_2 + CO	None	15.1
O_2	None	None
CO_2	25,300	1.3

Since pure CO is reducing to Fe at 1500°F, it was assumed that the reaction would involve only the chromium in the metal according to the following reaction:

$$(3)\quad 2\,Cr + 3CO \rightarrow Cr_2O_3 + 3C\ (soot)\ .$$

In a closed system, the reaction rate would be proportional to the decrease in pressure. If, however, the decomposition of CO were catalyzed by the oxide film according to the following reaction:

$$(4)\quad 2\,CO \overset{Cr_2O_3}{\rightleftarrows} CO_2 + C\ ,$$

a decrease in pressure would be meaningless with respect to determining the reaction rate. In order to test these hypotheses, stainless steel was exposed to pure CO at a pressure of 95 mm Hg under static conditions for 118 hr at 1500°F. As expected, the pressure in the system decreased as the reaction proceeded. Examination of the reaction vessel showed no carbon deposits. The metal was covered with a greenish, nonmagnetic film, and a weight increase of 1.3 $\mu g/cm^2 \cdot hr$ was noted. Oxide film identification tests and gas analyses are in progress. The results of carbon analyses of the metal before and after the test are presented in Table 5.7.

Table 5.7. Change in the Carbon Content of Type 304 Stainless Steel Exposed to Static CO for 118 hr at 1500°F

Sample No.	Condition	Carbon Content (%)
4	As received	0.098
4a	As tested	0.26
4b	As tested after oxide removal	0.29

The results of the tests described above indicate that the principal effect of CO and CO_2 on type 304 stainless steel is an oxidizing reaction involving the formation of apparently different oxides of chromium, depending on the gas. In flowing CO_2, the solid reaction product is a complex iron-chromium oxide. The reaction between stainless steel and CO_2 is presently assumed to be as written in the following reaction:

(5) $2Fe + 6Cr + 12CO_2 \rightarrow 3Cr_2O_3 \cdot Fe_2O_3 + 12CO$.

In order to account for the nearly complete reaction between CO_2 and stainless steel under static conditions, a reaction must be written for which no gaseous reaction products remain. If the reaction in flowing CO_2 is valid, secondary reactions leading to consumption of the CO will be involved. These reactions might proceed by several stages, as postulated below:

(6) $Fe_2O_3 + 3CO \rightarrow 2Fe + 3CO_2$,

(7) $42Cr + 9CO \rightarrow 3Cr_2O_3 + 9Cr_4C$;

(8) $16Cr + 3CO_2 \rightarrow 2Cr_2O_3 + 3Cr_4C$.

With respect to chromium, reaction 5 is irreversible at 1500°F, and subsequent reactions will occur only between CO and Fe_2O_3 and between CO and the chromium in the metal. The net reaction between static CO_2 and stainless steel is therefore represented by reaction 8. The reaction between CO and stainless Steel probably proceeds according to reaction 7,

since this accounts for the increase in the carbon content of the steel, the apparent lack of carbon deposition, and the formation of the nonmagnetic film containing no carbon.

Deposition of carbon during the tests could not be detected, although it is postulated from the analytical results. If equilibrium conditions are assumed at the conclusion of the static CO_2-stainless steel test, the CO and CO_2 should be present in a definite ratio. At 1500°F the equilibrium constant for the reaction

(9) $CO_2 + C \rightarrow 2CO$

is 8.91. The total partial pressure of the two gases was 16.4×10^{-6} atm, and it was calculated that the ratio of the CO pressure to the CO_2 pressure under these conditions should be 10.7. The actual ratio obtained from the analytical data was 11.6.

MANUFACTURING DEVELOPMENTS

Inspection of Fuel Capsules. As suggested previously,[6] it is considered that adequate nondestructive inspection of the 3/4-in.-OD, 0.020-in.-wall, type 304 stainless steel tubing for fuel capsule service would consist of eddy-current and dye-penetrant inspections. Since most manufacturers of tubing are equipped to perform such inspections, it would be desirable to confine the inspection of capsule tubing to the tubing manufacturer's plant, with the inspection being performed in accordance with ORNL procedure specifications. An opportunity to gage the effectiveness of inspection in the tubing manufacturer's plant was afforded by the purchase of approximately 1650 ft of capsule tubing for use in a critical assembly. The purchase contract specified the procedures to be used for the dye-penetrant and eddy-current inspections, and specified the minimum acceptable quality. The tubing was accordingly inspected in the manufacturer's plant and at present is being thoroughly reinspected at ORNL by pulse-echo,

[6] The ORNL Gas-Cooled Reactor, ORNL-2500, Part 2, Section 4.3.4 (April 1, 1958).

resonance-ultrasonic, and eddy-current techniques, as well as random sample inspection by radiography and fluorescent penetrants. When completed, this study will provide a much clearer understanding of the quality of tubing that would be available if the only inspection were that made by the manufacturer.

A satisfactory dye-penetrant procedure specification[7] existed prior to issuance of the purchase order and a tentative procedure was written for the eddy-current inspection. The eddy-current procedure was based on recent eddy-current studies with both commercial equipment and special experimental equipment developed for these studies. Briefly, the inspection consists of driving the tubing through a tightly coupled, differential, encircling-coil, eddy-current system; the operating parameters are selected as those appropriate to the dimensional and electromagnetic properties of the tubing. The rejection of tubing is based on a comparison of signal amplitude from questionable regions of the tubing with the signal amplitude produced by a milled longitudinal slot 0.0025 in. deep on the outside surface of a tube used as a reference.

A major difficulty encountered in employing the eddy-current test is the presence of a myriad of signals produced by anomalies in the tubing which are not necessarily detrimental to the intended use. These consist of variations in dimensions, electrical conductivity, and permeability, which in many instances produce "background noise" as large as, or larger than, the signal from the reference slot. This difficulty must be overcome before the eddy-current method can be used confidently as a prime inspection method for capsule tubing. Development efforts are being directed toward desensitizing the eddy-current system to these inconsequential anomalies. A much better approach may be to control the tube manufacturing processes so as to eliminate the sources of the noise.

Evaluation comparisons were made of commercial-grade lots of type 304 stainless steel tubing with diameters of 0.750, 0.800, and 1.00 in., and wall thicknesses of 0.005, 0.010, 0.015, and 0.020 in. which had

---

[7] Reactor Material Specifications, TID-7017, Spec. No. RMIS-2, p 215 (October 1958).

been supplied from four vendors. All tubes were found by fluorescent-penetrant inspection to have pinholes. A few small discontinuities were noted by the pulse-echo ultrasonic technique. The major discrepancies were variations in wall thickness which exceeded the commercial tolerance of ± 10%. Five of the twelve lots examined were totally or partially rejected because of these variations in wall thickness. In addition, two of the lots were far in excess of the straightness tolerance of one part in six hundred.

Approximately 100 ft of 3/4-in.-OD, 0.020-in.-wall type 304 stainless steel tubing was inspected by pulse-echo and resonance-ultrasonic techniques to determine its suitability for fuel capsule service for in-pile tests. The inspection was for the purpose of detecting both defects and excessive wall-thickness variations. Several local measurements were made of the inside diameter by machanically measuring the outside diameter and subtracting the opposing wall thicknesses which were measured by the resonance-ultrasonic technique. A few small discontinuities were noted by the pulse-echo ultrasonic examination, and the measurements of the inside diameter varied from 0.711 to 0.717 in. The tubing was rejected because the diameter variation was too great for the intended use. An additional 150 ft of tubing of the same nominal size was procured and found to be acceptable for the intended use.

In addition to the 3/4-in.-OD tubing, approximately 120 ft of 1/2-in.-OD, 0.014-in.-wall type 304 stainless steel tubing was ultrasonically evaluated. Only a few small defects were located by the pulse-echo technique. The wall thickness was found to be within the ± 10% tolerance.

Two short pieces of 1-in.-dia, type 304 stainless steel tubing with nominal wall thicknesses of 0.002 in. and 0.004 in., respectively, were inspected with liquid penetrants, ultrasonic techniques, and radiography. Small clusters of pinholes were detected on the 0.002-in. tube. The most undesirable characteristics noted were the wall-thickness variations of the type shown in Fig. 5.11. By the use of special radiographic and densitometric techniques, the variations were measured to be as much as 50% from the nominal thickness.

Approximately 16 ft of 1-in.-dia type 304 stainless steel bar was inspected by pulse-echo ultrasound and radiography. This material is being used in the development of fuel capsule end closures. No serious defects were detected in two ultrasonic inspections. In the first inspection, the ultrasound was refracted circumferentially around the bar for the detection of seams and cracks near the surface. In the second, the sound was transmitted diametrically through the bar and a few very small discontinuities (compared with a 1/16-in.-dia flat-bottom hole) were detected.

Fuel Capsule End Closures. The experimental program necessary to achieve a dependable, low-cost fuel element involves the development of a good joint design and a good joining procedure for the end closure. The inert-gas-shielded tungsten-electrode process, which has proved successful for high-quality welding of thin-section materials, was selected for the automatic welding of the caps to the tubes. In the automatic process, the welding variables are easily controlled, and the process can be used in a controlled-atmosphere chamber. Although it is a widely used method of joining metals, tests were required to develop the techniques for this specific application.

The joint designs which could be considered for this application were the three types illustrated in Fig. 5.12: a butt weld, a plug weld, and an edge weld. Each type of end closure has specific advantages with respect to ease of manufacture, integrity, or inspection. The butt weld is favored because of the ease of meaningful radiographic inspection and the absence of notches which might produce stresses in service and bring on premature failure. Reproducible butt welds are dependent on accurate alignment of the joint, however, which may prove difficult in view of the need for assembly in an inert-atmosphere chamber. In assembly of the fuel element capsule by butt welding, the closure made before the MgO spacer and the fuel pellets are inserted may be easily inspected, and the weld may be repaired if necessary. The closure weld to be made after loading of the capsule will be more difficult because contamination of the fuel during the welding process must be avoided. Repairs to the final weld will be limited, and any need for removal of the weld would be cause for rejection of the element on the basis of the length tolerance.

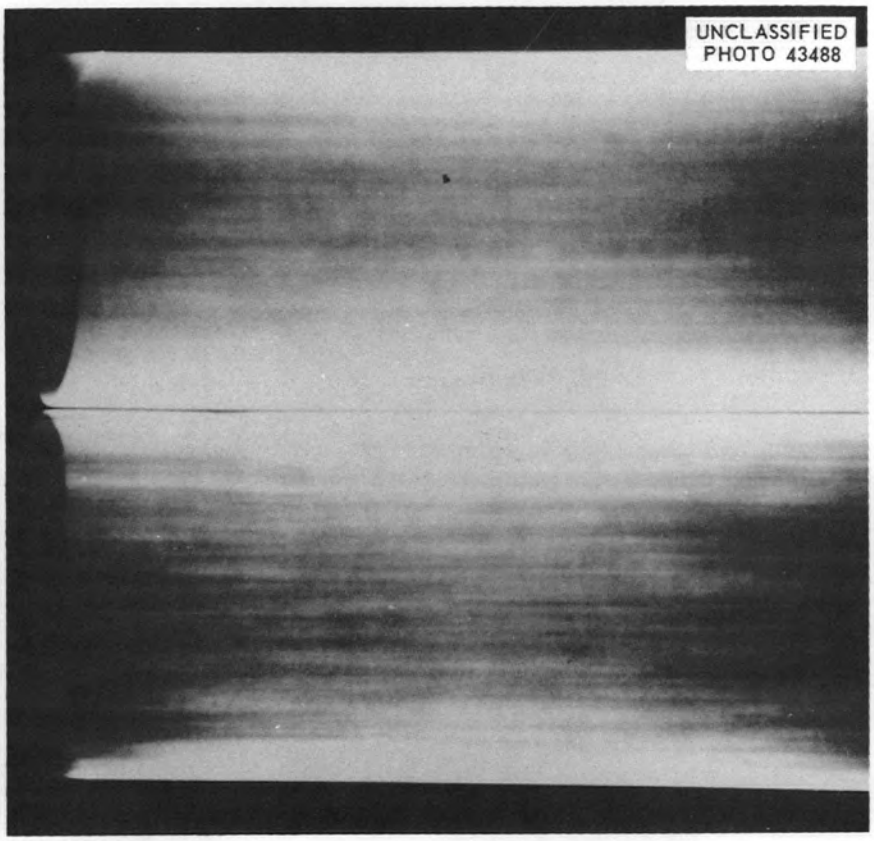

Fig. 5.11. Radiograph of Thin-Walled Tubing.

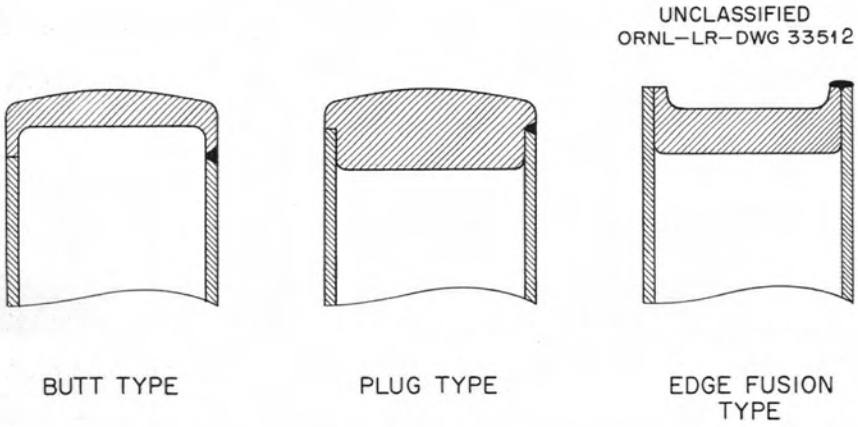

Fig. 5.12. Basic End Cap and Weld Designs.

On the other hand, plug and edge-fusion types of joint are relatively insensitive to alignment, and the weld area is not in the fuel region. With proper fit-up, it might even be possible to eliminate the need for dry-box welding of the final end closure.

In an effort to determine the optimum design for the end closures, a number of experiments are being conducted. These have included the determination of suitable welding conditions for each joint being considered. For these experiments, end caps were machined from type 304L stainless steel bar stock to fit 0.750-in.-ID, 0.020-in.-wall type 304 stainless steel tubing. An interference fit (+0.001, -0.000 in.) was specified for the plug joints. Semiautomatic welding equipment was used throughout the experiments. A rectifier type of welder equipped with a high-frequency pilot circuit and a current-decay attachment was used to provide the welding current. Specimens were held in a chuck in the vertical position and rotated by a variable-speed drive. The welding torch was held fixed during welding, and argon flowing at a rate of 20 cfh was used as a shielding gas.

The results of the experiments are presented in Table 5.8. Metallographic examination of the joints described and numerous other joints indicate that sound welds can be made with relative ease with each of the three basic joint designs. Similar studies will be conducted in a helium-atmosphere chamber to determine the effect of the helium atmosphere on the arc characteristics and the optimum welding conditions.

In order to evaluate the mechanical properties of the various joints, a series of tube-burst tests was conducted. Each specimen consisted of a 4-in. length of tubing with an experimental end closure at each end. One end plug was provided with a 3/16-in.-dia pressure tube. The specimens were heated to 1500°F in a wire-wound box-type furnace and pressurized with argon to 1500 psi. The time to failure was recorded.

Initial tests resulted in violent explosions and extensive damage to the specimen fragments upon collision with the stainless steel lining of the furnace. Thus the origin of failure in these specimens was difficult to determine. For subsequent tests, capsule specimens containing steel slugs that occupied a major portion of the available volume were

Table 5.8. Welding Conditions for End Closure of Fuel Capsules

End plugs: type 304L stainless steel
Tubes: type 304 stainless steel, 0.750 in. ID, 0.020 in. wall
Welding electrode: 1/16-in.-dia, pointed, thoriated tungsten
Arc length: 0.050 in.
Welding speed: 5 1/2 in./min
Welding current: variable
Argon through torch: 20cfh
Backup gas: helium

Joint Type	Current (amp)	Penetration (mils)	Comments
Butt	10	0.014	Incomplete penetration
	12	0.022	Optimum range
	14	0.022	Optimum range
	16	0.018	Excessive weld bead width
	18	0.018	Excessive weld bead width
Edge fusion	10	0.030	Optimum range
	11	0.032	Optimum range
	12	0.040	Optimum range
	13	0.036	Excessive weld overhang
	14	0.038	Excessive weld overhang
	15	0.042	Excessive weld overhang
	25	0.060	Excessive weld overhang
Plug	17	0.014	Incomplete penetration
	20	0.016	Incomplete penetration
	23	0.019	Incomplete penetration
	26	0.020	Optimum range
	30	0.020	Excessive weld bead width
	33	0.020	Excessive weld bead width

used. These capsules did not explode, and post-test examination definitely indicated that failure had initiated in every case in the tube rather than at the weld. A typical post-test example of each of the three joint designs is shown in Fig. 5.13. Metallographic examination of the weld in each specimen indicated that incipient cracking had not occurred during the short-time test. A metallographic section of the weld of a typical butt-welded tube-burst specimen is shown in Fig. 5.14, and similar sections of typical plug and edge welds are shown in Figs. 5.15 and 5.16, respectively.

It was concluded on the basis of these experiments that the testing procedures being used were not selective and that all of the basic joints studied were satisfactory. Long-time tests at lower pressures are now being conducted that will provide a better basis for selection of the final end closure design (see preceding section).

BERYLLIUM INVESTIGATIONS

Welding of Beryllium. Considerable effort is being devoted at other government installations and private laboratories to developing wrought beryllium or beryllium alloys having isotropic mechanical properties. It is not anticipated, however, that such materials will be available immediately, and therefore attempts to fabricate fuel capsule end closures from available materials are in progress.

Since tubing was not available for joining experiments, short lengths of tubing were machined from QMV-grade beryllium, along with end plugs for several different weld designs. An edge-fusion weld sample in which a 0.020-in.-wall tube, 1/2 in. in diameter, was sealed with a plug having an edge thickness of 0.030 in. is shown in Fig. 5.17. The weld was made with the inert-gas-shielded tungsten-arc process in an exhausted hood to prevent the spread of beryllium contamination. A polarized-light photomicrograph of the weld area is shown in Fig. 5.18. Although no mechanical testing has been performed on such welds, it is expected that the cast structure of the weld area is brittle.

UNCLASSIFIED
Y-27511

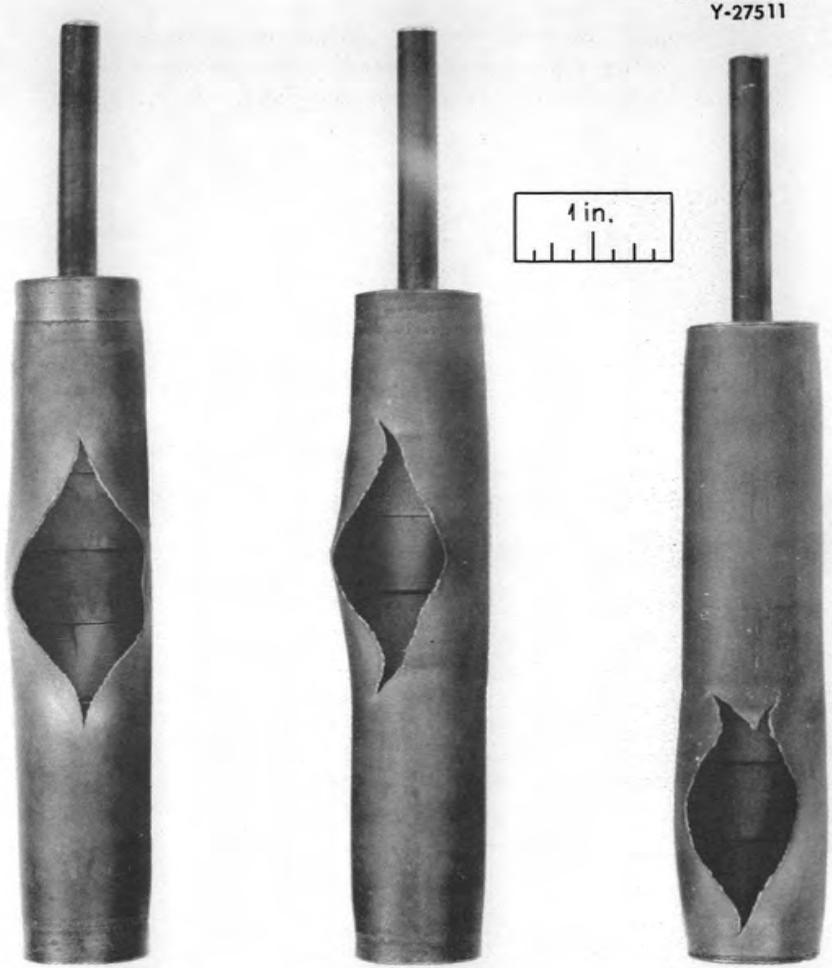

BUTT-WELDED CLOSURES

PLUG-WELDED CLOSURES

EDGE-FUSION-WELDED CLOSURES

Fig. 5.13. Typical Tube-Burst Stress-Rupture Capsules. Failure occurred in 3 min or less when pressurized to 1500 psi at 1500°F.

UNCLASSIFIED
Y-27634

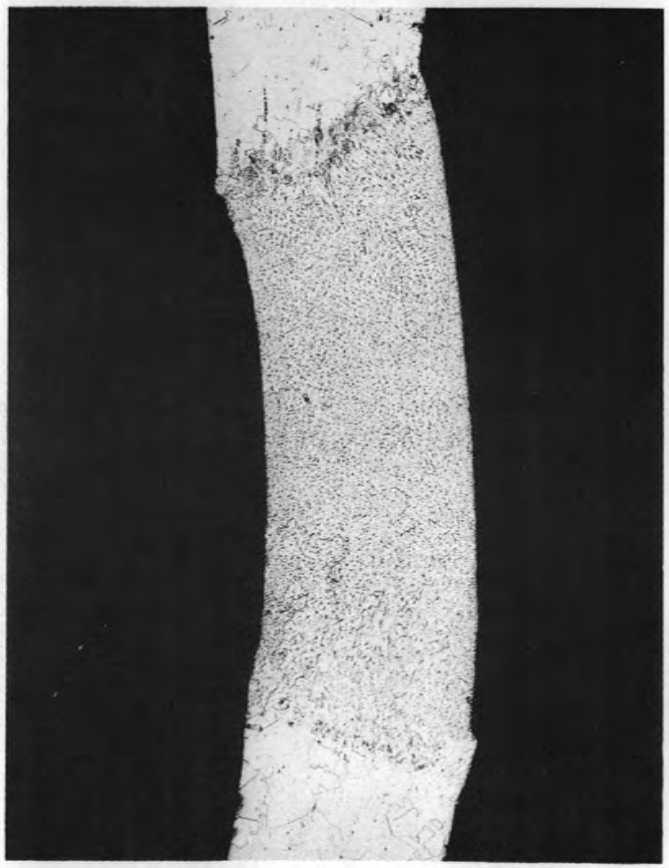

Fig. 5.14. Metallographic Section of a Butt-Welded Tube-Burst Specimen After Test. Failure of tube occurred in 55 sec at 1500°F when pressurized to 1500 psi. Etchant: aqua regia. 50X.

UNCLASSIFIED
Y-27635

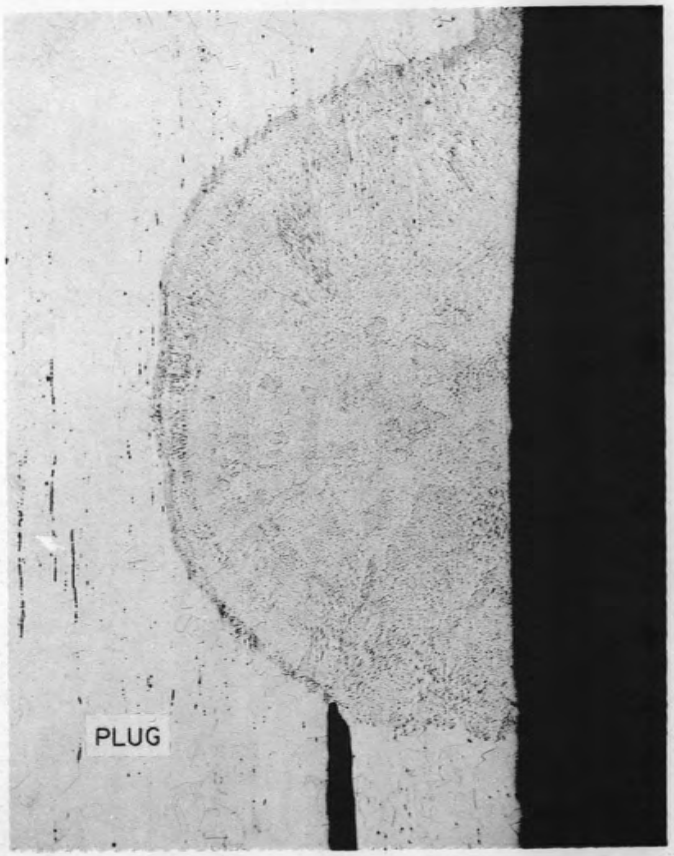

Fig. 5.15. Metallographic Section of a Plug-Welded Tube-Burst Specimen After Test. Failure of tube occurred in 100 sec at 1500°F when pressurized to 1500 psi. Etchant: aqua regia. 50X.

UNCLASSIFIED
Y-27633

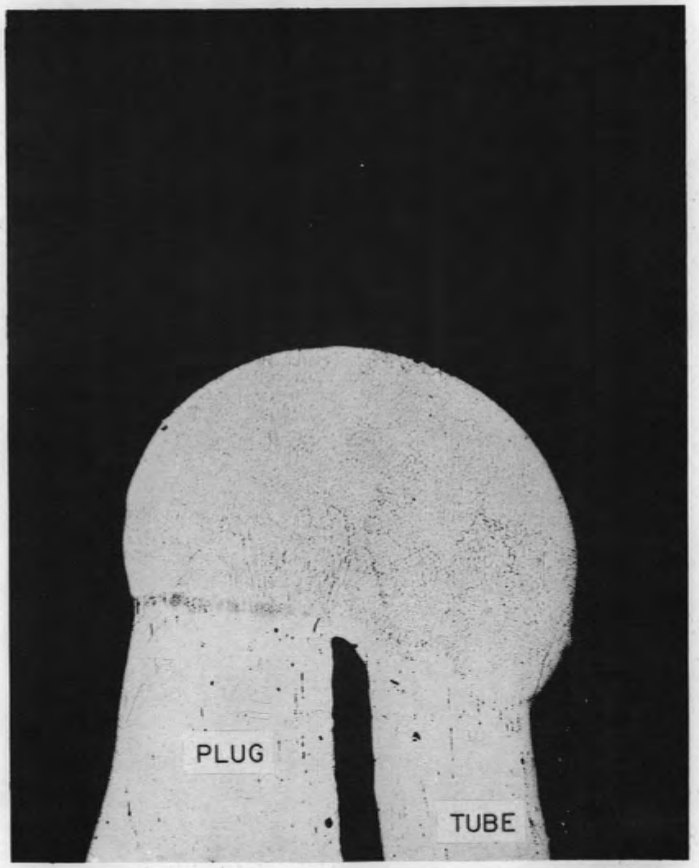

Fig. 5.16. Metallographic Section of Edge-Welded Tube-Burst Specimen After Test. Failure of tube occurred in 30 sec at 1500°F when pressurized to 1500 psi. Etchant: aqua regia. 50X.

UNCLASSIFIED
Y-26282

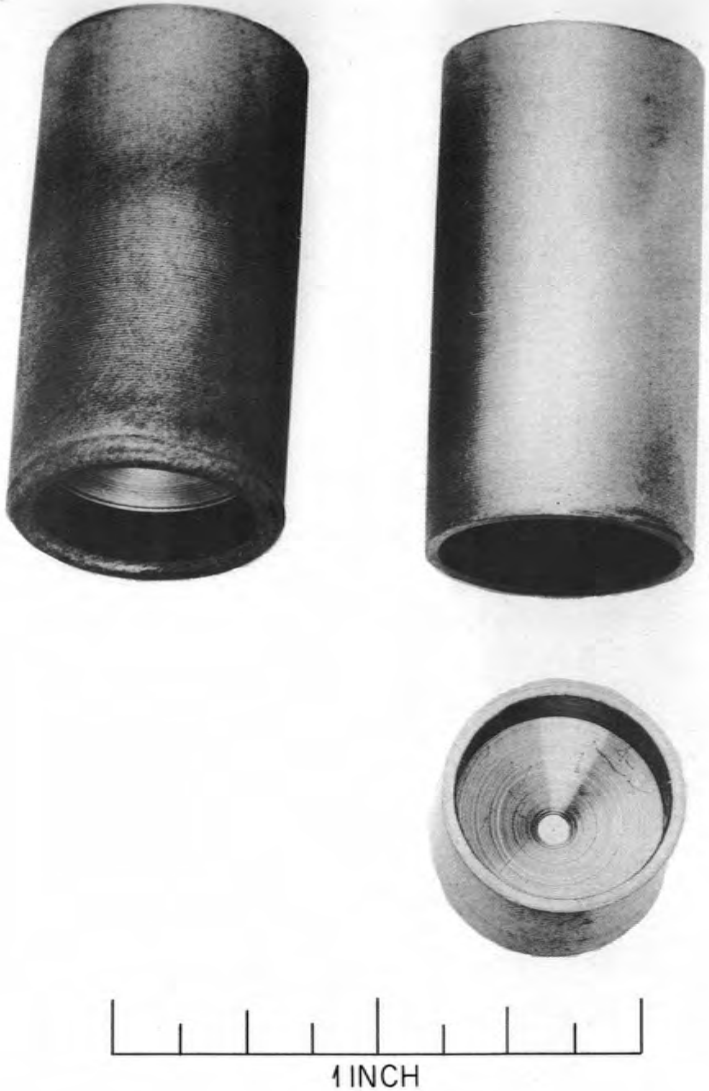

Fig. 5.17. Edge-Fusion-Welded End Closure of Beryllium Tubing.

UNCLASSIFIED
Y-27304

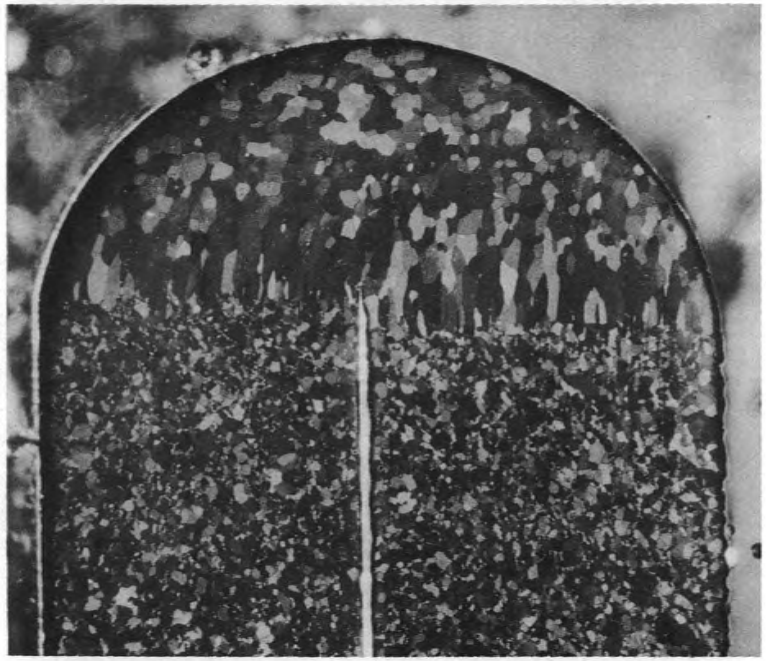

Fig. 5.18. Microsection of Weld Zone of Edge-Fusion-Welded End Closure of Beryllium Tubing. Etchant: oxalic acid. Polarized light. 50X.

A second type of end closure, shown in Fig. 5.19, for which a solid plug was used, was less sensitive to welding variables because of the larger mass of material in the weld area. A bright-field photomicrograph of the weld area is shown in Fig. 5.20. A polarized-light photomicrograph of the same area (Fig. 5.21) shows the large grain structure of the weld.

Welds of this type are inherently brittle, but with proper control they will be made free of cracks and they could be used as leakage seals. Studies of brazing, pressure welding, and other types of recrystallization bonding are being considered.

Compatibility of Beryllium with Coolants. Beryllium-metal samples were exposed in a contaminated helium environment in materials compatibility tests (see chapter 7) in order to evaluate the extent of the compatibility problem with this metal. In the first test (static pot test No. 5), the pot contained stainless and low-alloy steel samples and TSF graphite in addition to the beryllium samples, and the test was scheduled to run for 1000 hr at 1400°F in a helium atmosphere. However, the test was terminated because of a leak in the container vessel after being at temperature less than one day. Upon removal from the pot, the beryllium samples were found to have a loosely adherent, metallic-appearing, gray scale. X-ray diffraction analysis of the scale showed no characteristic lines of beryllium oxide. Three of the weaker lines of beryllium carbide were noted, although the characteristic strong line of beryllium carbide was missing.

Following the failure of pot No. 5, another static pot test (No. 7) with only beryllium specimens, TSF graphite, and helium was run for 100 hr at 500°F and 900 hr at 1400°F to duplicate the temperature conditions of static pot test No. 5. A post-test examination of these beryllium samples showed that the reaction of the beryllium with the test environment was even more severe than in test No. 5. The specimens were covered with a loosely adherent gray scale, as shown in Fig. 5.22, which spalled profusely as the specimens were lifted from the supporting stand. Following the removal of the scale, thickness measurements made on the specimen showed a remaining section thickness of 0.022 in., compared with a thickness of 0.145 in. before the test. The stainless steel rods which supported the beryllium samples had a loosely adherent gray scale

UNCLASSIFIED
Y-26284

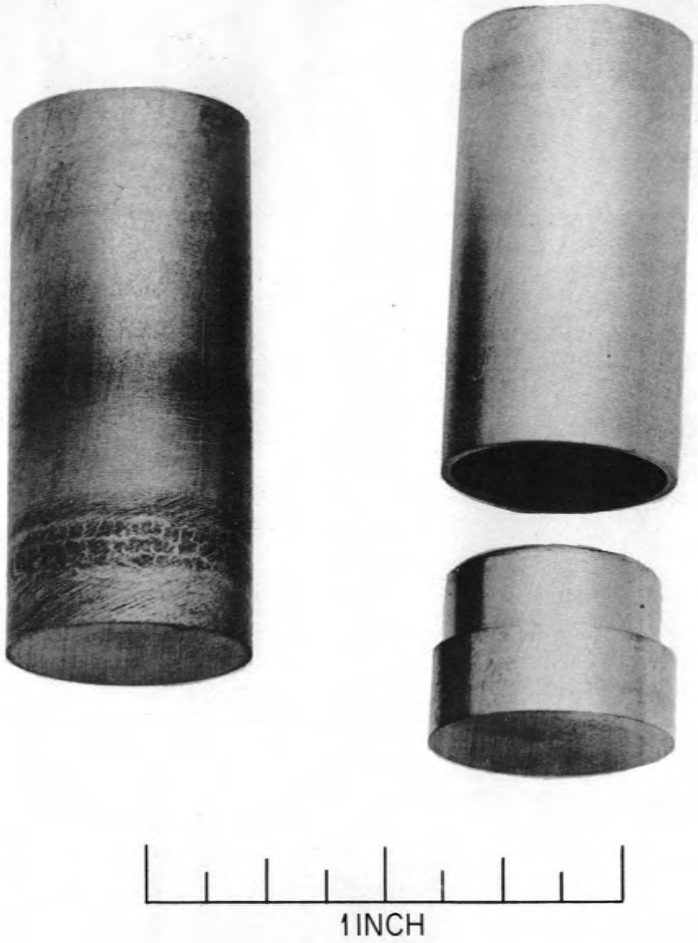

Fig. 5.19. Plug-Welded End Closure of Beryllium Tubing.

UNCLASSIFIED
Y-26661

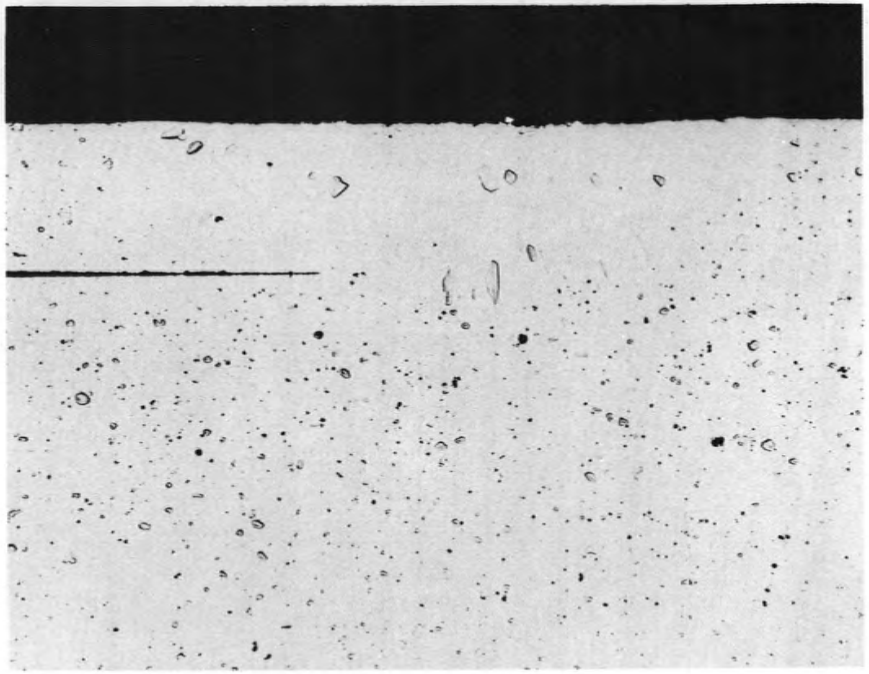

Fig. 5.20. Microsection of Weld Zone of Plug-Welded End Closure of Beryllium Tubing. Etchant: oxalic acid. Bright-field illumination. 50X.

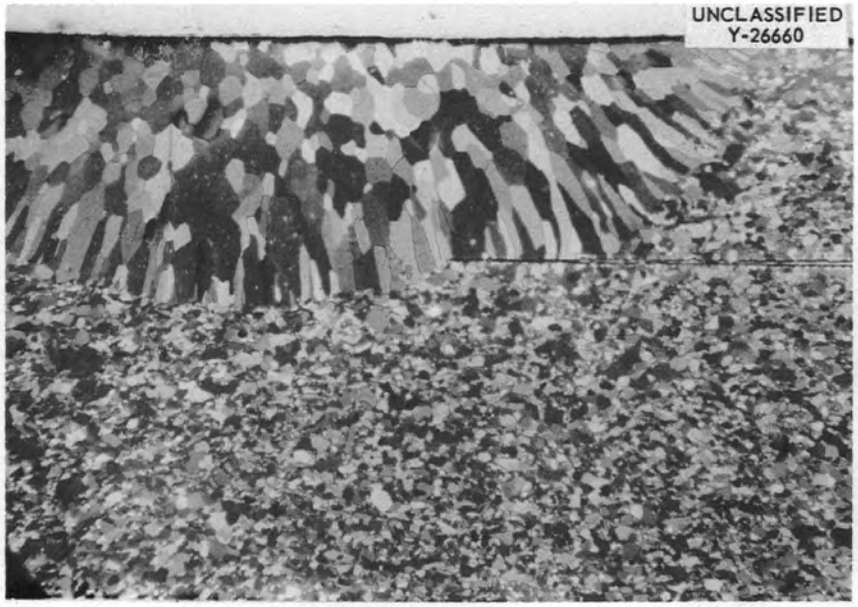

Fig. 5.21. Microsection of Weld Zone of Plug Weld in Beryllium Tubing. Etchant: oxalic acid. Polarized light. 50X.

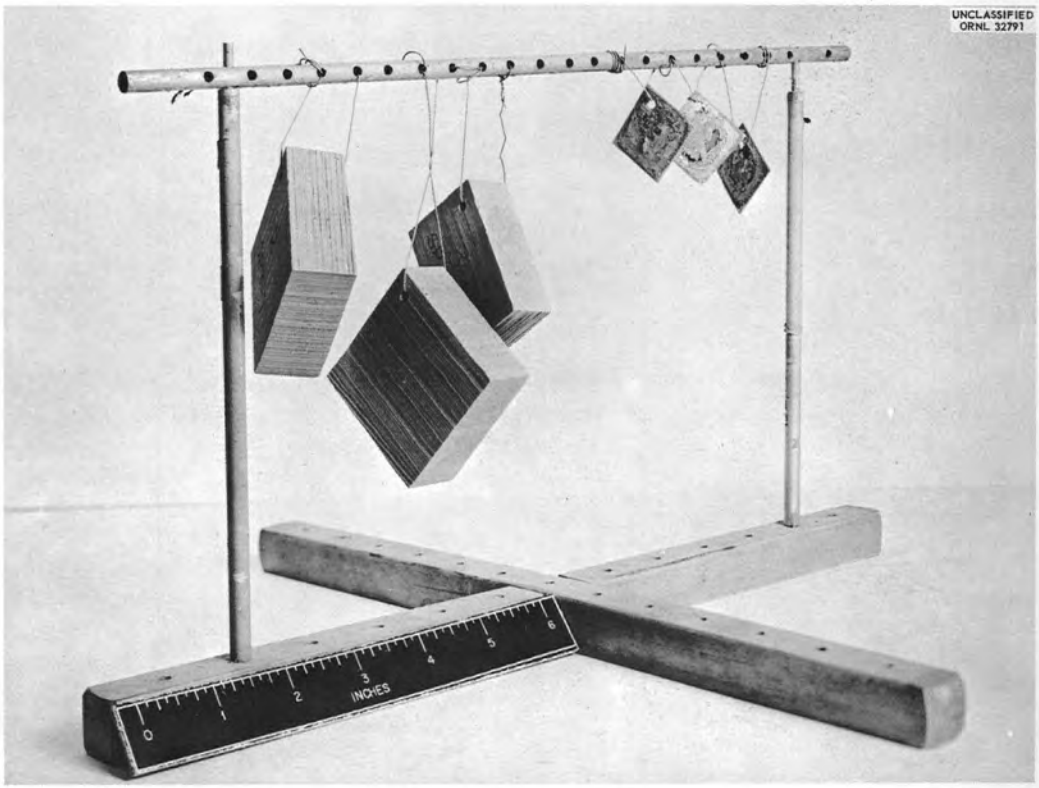

Fig. 5.22. Beryllium Specimens After Exposure in Static Pot No. 7 Which Contained Helium and TSF Graphite for 100 hr at 400°F and 900 hr at 1400°F.

that differed in appearance from the scale on the beryllium. It was difficult to determine by visual inspection whether this scale formed directly on the stainless steel or was deposited there from the pot atmosphere. Samples of all the scales have been submitted for x-ray diffraction analysis. The results of analysis of the gas used in this static pot test were similar to the results of analyses of the gas used in other similar tests at 1400°F without beryllium.

6. IN-PILE TESTING OF COMPONENTS AND MATERIALS

FUEL ELEMENT IRRADIATION PROGRAM

Full-size (diameter only) and reduced-size single fuel rod specimens consisting of UO_2 pellets in stainless steel capsules are being irradiated in the LITR, ORR, ETR, and GETR to study parameters controlling the design of the GCPR seven-rod-cluster fuel element. Since no facility exists for the irradiation of a full-size seven-rod cluster, flow and heat transfer tests are being simulated in out-of-pile tests (see chapters 3 and 7). Correlation of the results from both types of experiments will, it is believed, be adequate for evaluating the design.

The irradiation experiments designed to test the mechanical stability of the capsule and of the UO_2 fuel pellets and to examine the integrity of at least two types of capsule end closure are listed in Table 6.1.

Table 6.1 GCPR Irradiation Program

Reactor	No. of Experiments	Type of Specimen	Environment of Specimen	Variables Under Study
ETR	14	Prototype	NaK	Pellet geometry Oxide density Clearance between pellets and capsule Oxide temperature Burnup
ORR	8	Prototype	NaK	Pellet geometry Thermal cycling
GETR	15	Reduced prototype	Helium	Thermal cycling Pellet geometry Oxide density Crushed oxide Capsule temperature Burnup
LITR	12	Miniature	Air	Fission gas release as a function of time and burnup

Variations in parameters such as pellet geometry, temperature, density, burnup, and thermal cycling have been confined to those of practical interest in the design of the GCPR fuel element. Thermal cycling, where indicated, will be accomplished by the insertion and removal of neutron-absorbing shutters.

In order to complete the experimental program within the proposed reactor time schedule, it has been necessary to utilize the four reactors listed. Further details of these irradiation programs are presented in Tables 6.2, 6.3, and 6.4.

For convenience NaK will be used as the primary heat transfer medium surrounding the full-diameter capsules to be irradiated in the ETR and ORR. Fission and gamma heat will be dissipated to the reactor or pool cooling water through a thin gas annulus which will serve as a heat barrier. Temperature control will be achieved by adjusting the helium and nitrogen gas mixture in the annulus to obtain the proper thermal conductivity. Tests at the GETR will be conducted with smaller diameter pellets at accelerated burnup rates in a forced-circulation loop. The circulated gas will be helium. Small-diameter capsules will be irradiated in the LITR to obtain fission-gas release data as a function of burnup in the temperature range from 2000 to 3000°F.

Full-Diameter Prototype Fuel Capsule Irradiations. As indicated in Fig. 6.1 the apparatus for irradiations in the ORR and ETR consists of UO_2 pellets in a capsule immersed in a NaK-filled pressure vessel which, in turn, is contained in a gas-filled tube. The unassembled parts of the apparatus are shown in Fig. 6.2. Helium at 315 psia pressurizes the NaK to simulate the GCPR coolant pressure, and the helium and nitrogen control gas mixture at 300 psia reduces the pressure stress in the hot NaK vessel and minimizes creep in the stainless steel walls. Each experiment will be run independently and without purging of the gas regions except during temperature transients or leak checks, and all the experimental apparatus will be joined in common control systems outside shielded block and check valves.

The pressurized gases will be supplied through manually controlled pressure and flow regulators. The composition of the gas mixture introduced for heat flux and temperature regulation will be determined at the instrument panel with the use of a thermal conductivity cell. For ORR irradiations, equipment directly associated with the capsule will be enclosed in a lead shielded box near the pool. Check valves on inlet lines

Table 6.2. Proposed Program of Irradiations of Prototype Fuel Capsules

Capsule dimensions: 0.750 in. OD, 0.020 in. wall, 6 in. long
Pellet dimensions: 0.705 or 0.700 in. OD, 0.5 in. long
Fission power: 30,000 Btu/hr·ft
Fission heat flux: 162,500 Btu/hr·ft^2
Capsule surface temperature: 1300°F

Irradiation Facility	Experiment No.	Diameter of Hole in UO_2 Pellet (in.)	UO_2 Density (% of Theoretical)	Neutron Flux, Average Perturbed (n/cm^2·sec)	UO_2 Enrichment (%)	Total Burnup (Mwd/tonne)	Actual Time of Irradiation (days)	Clearance Between Capsule and Pellet (in.)	Thermal Cycling
ETR Reflector	E1	0	95	3.9×10^{13}	Natural	3,000	255	0.0025	
	E2	0	95	3.9×10^{13}	Natural	3,000	255	0.0025	
	E3	0	95	3.9×10^{13}	Natural	6,000	510	0.005	
	E4	0	95	3.9×10^{13}	Natural	6,000	510	0.005	
	E5	0.323	95	3.9×10^{13}	1.00	3,000	202	0.005	
	E6	0.323	95	3.9×10^{13}	1.00	3,000	202	0.005	
	E7	0.323	95	3.9×10^{13}	1.00	13,000	875	0.0025	
	E8	0.323	95	3.9×10^{13}	1.00	13,000	875	0.0025	
	E9	0.323*	95	3.9×10^{13}	1.00	6,000	404	0.0025	
	E10	0.323*	95	3.9×10^{13}	1.00	6,000	404	0.0025	
	E11	0.323*	95	3.9×10^{13}	1.00	13,000	875	0.005	
	E12	0.323*	95	3.9×10^{13}	1.00	13,000	875	0.005	
	E13	0	75	3.9×10^{13}	1.00	3,000	200	0.0025	
	E14	0	75	3.9×10^{13}	1.00	3,000	200	0.0025	
ORR Pool	01	0.323*	95	8.0×10^{12}	4.00	2,000	135	0.0025	Yes
	02	0	95	7.6×10^{12}	3.00	2,000	165	0.0025	Yes
	03	0.323	95	8.0×10^{12}	4.00	2,000	135	0.0025	Yes
	04	0.323	95	8.0×10^{12}	4.00	2,000	135	0.0025	No
	05	0.323	95	8.0×10^{12}	4.00	2,000	135	0.0025	Yes
	06	0.323*	95	8.0×10^{12}	4.00	2,000	135	0.0025	Yes
	07	0.323	95	8.0×10^{12}	4.00	2,000	135	0.0025	No
	08	0	95	7.6×10^{12}	3.00	2,000	165	0.0025	Yes

*Beryllium oxide rod inserted in hole.

Table 6.3. Proposed Program of Irradiations of Reduced-Size Prototype Fuel Capsules in GETR Pool

Capsule dimensions: 0.533 in. OD, 0.014 in. wall, 6 in. long
Pellet dimensions: 0.467 in. OD, 0.5 in. long
Clearance between capsule and pellet: 0.0025 in.
Fission power: 30,000 Btu/hr·ft
Fission heat flux: 229,000 Btu/hr·ft^2
UO_2 enrichment: 0.92%

Experiment No.	Diameter of Hole in UO_2 Pellet (in.)	UO_2 Density (% of Theoretical)	Neutron Flux, Average Perturbed (n/cm^2·sec)	Total Burnup (Mwd/tonne)	Actual Time of Irradiation (days)	Capsule Surface Temperature (°F)	Thermal Cycling
G1	0.230	95	8×10^{13}	6000	208	1300	Yes
G2	0.230	95	8×10^{13}	3000	104	1300	Yes
G3	0.230	95	8×10^{13}	6000	208	1300	No
G4	0.230	95	8×10^{13}	3000	104	1300	No
G5	0	95	6×10^{13}	6000	244	1300	Yes
G6	0	85	6×10^{13}	3000	122	1300	Yes
G7	0	85	6×10^{13}	6000	244	1300	No
G8	0	75	6×10^{13}	3000	122	1300	No
G9	0.230*	95	8×10^{13}	6000	208	1300	Yes
G10	0.230*	95	8×10^{13}	3000	104	1300	Yes
G11	0.230*	95	8×10^{13}	6000	208	1300	No
G12	0.230*	95	8×10^{13}	3000	104	1300	No
G13	0	95	6×10^{13}	3000	122	1300	Yes
G14	0	75	6×10^{13}	3000	122	1300	Yes
G15	0	75	6×10^{13}	3000	122	1300	Yes
G16	**	95	6×10^{13}	3000	122	1300	Yes
G17	**	95	6×10^{13}	3000	122	1300	No
G18	**	95	6×10^{13}	3000	122	1300	No
G19	**	95	6×10^{13}	3000	122	1300	Yes
G20	**	95	6×10^{13}	3000	122	1500	Yes
G21	**	95	6×10^{13}	3000	122	1500	No
G22	**	95	6×10^{13}	3000	122	1500	No
G23	**	95	6×10^{13}	3000	122	1500	Yes

*Beryllium oxide rod inserted in hole.
**To be determined later.

Table 6.4. Program of Irradiations of Miniature Fuel Capsules in the LITR Core

Pellet dimensions: 0.156 in. OD, 1 in. long
Diameter of central hole in UO_2 pellet: 0.078 in.
Capsule surface temperature: 1300°F

Experiment No.	UO_2 Density (% of Theoretical)	Total Power (Btu/hr·ft)	Total Heat Flux (Btu/hr·ft^2)	Neutron Flux, Average Perturbed (n/cm^2·sec)	UO_2 Enrichment (%)	Total Burnup (Mwd/tonne)	Actual Time of Irradiation (days)	Clearance Between Capsule and Pellet (in.)	Irradiation Period Starting Date
L1	95	7,235	177,149	2.1×10^{13}	10	7,000	97	0.001–0.0015	10/21/58
L2	85	12,947	317,007	2.1×10^{13}	20	7,000	49	0.001–0.0015	2/24/59
L3	75	6,775	165,886	2.5×10^{13}	10	7,000	81	0.0025–0.003	
L4	95	7,934	194,264	2.3×10^{13}	10	13,000	164	0.001–0.0015	9/30/58
L5	85	10,357	253,951	1.7×10^{13}	20	13,000	112	0.001–0.0015	
L6	75	6,776	165,910	2.5×10^{13}	10	13,000	151	0.001–0.0015	10/21/58
L7	95	10,278	251,657	1.5×10^{13}	20	7,000	68	0.0025–0.003	
L8	85	12,947	317,007	2.1×10^{13}	20	7,000	49	0.0025–0.003	
L9	75	13,552	331,820	2.5×10^{13}	20	7,000	41	0.001–0.0015	
L10	95	8,931	218,676	1.3×10^{13}	20	13,000	145	0.0025–0.003	
L11	85	12,947	317,007	2.1×10^{13}	20	13,000	91	0.0025–0.003	
L12	75	12,527	306,723	2.3×10^{13}	20	13,000	82	0.0025–0.003	
L13	95	7,934	194,264	2.3×10^{13}	10	13,000	164	0.001–0.0015	11/11/58
L14	95	10,278	251,657	1.5×10^{13}	20	7,000	68	0.001–0.0015	12/23/58
L15	95	8,932	218,700	1.3×10^{13}	20	7,000	79	0.001–0.0015	12/23/58
UO_2-1-1	95	7,000	118,000	2.0×10^{13}	10	6,000	73	0.001–0.0015	3/17/58
UO_2-1-2	95	7,000	118,000	2.0×10^{13}	10	6,000	73	0.001–0.0015	6/17/58

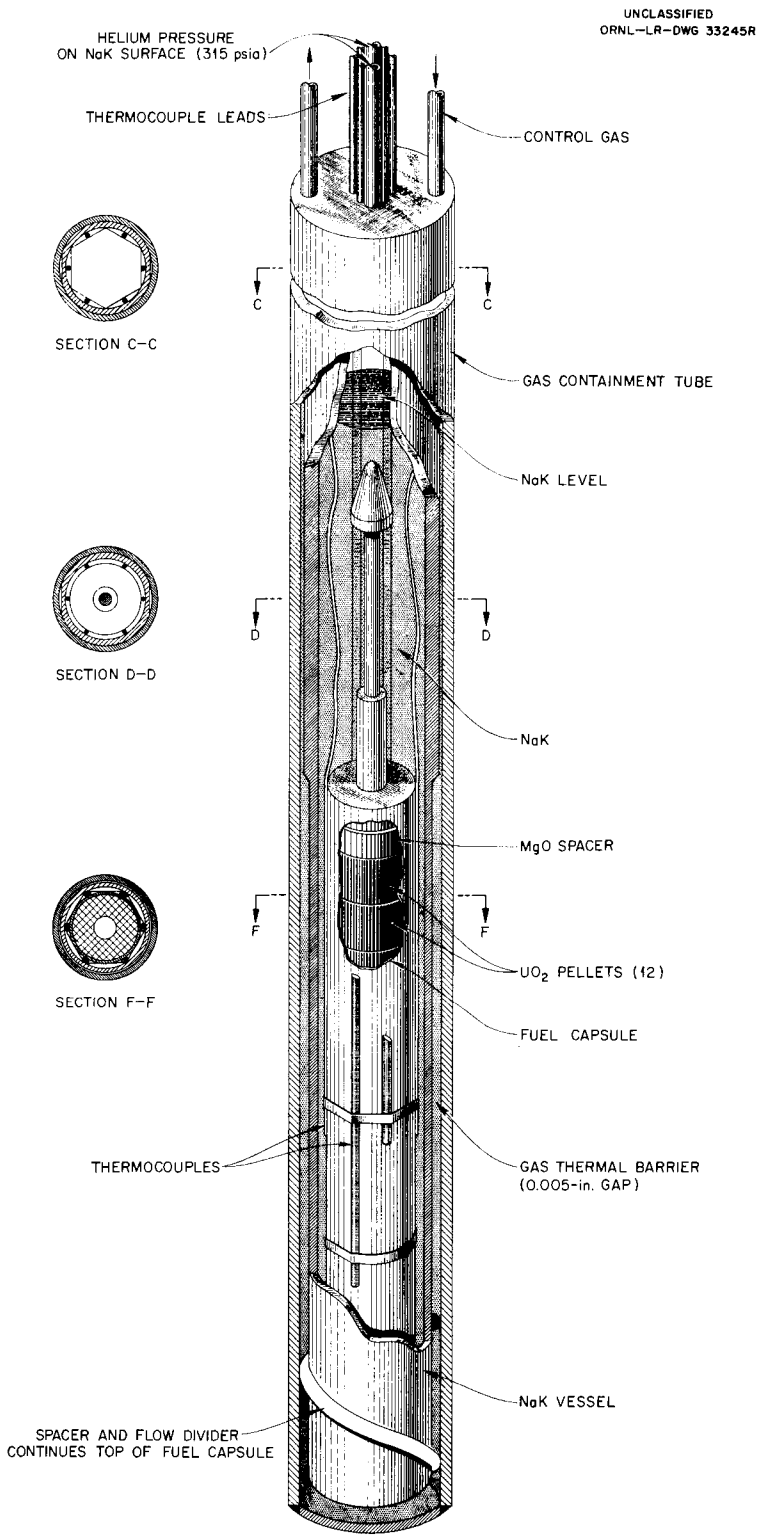

Fig. 6.1. Apparatus for Fuel Capsule Irradiations in the ORR and ETR.

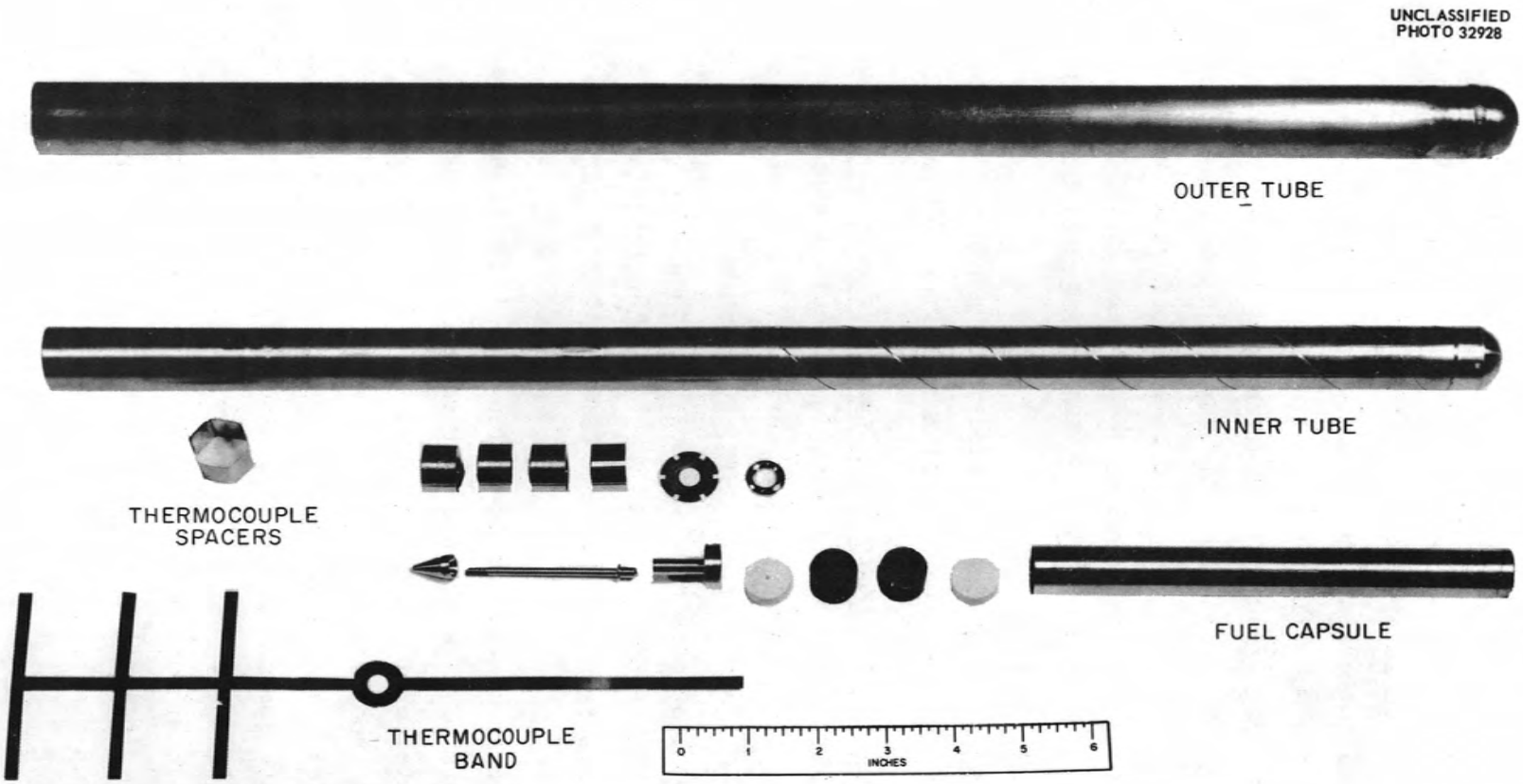

Fig. 6.2. Unassembled Parts of Apparatus for Fuel Capsule Irradiations in the ORR and ETR.

and activated charcoal traps in the stack exhaust line will prevent release of activity in the event of capsule rupture or other equipment failure. Eight facilities for irradiation of prototype-size UO_2 pellets in NaK-cooled capsules are being provided in the ORR poolside area. The experiment installation is approximately 65% complete.

ETR irradiations are to be conducted by the Phillips Petroleum Company, except that the NaK-filled and instrumented capsules will be furnished by ORNL and the post-irradiation examinations to be performed will be specified by ORNL. The capsules will be positioned in the beryllium reflector region of the ETR, and they will be equipped with pressure and temperature control systems comparable to those provided at the ORR. The first ETR capsule has been delivered to the Phillips Petroleum Company, and two others are nearly completed.

The results of an initial experiment conducted with a somewhat different apparatus are described in a following section.

Reduced-Size Prototype Fuel Capsule Irradiation. A contract was negotiated with the General Electric Vallecitos Atomic Laboratory on September 1, 1958 which provides for: (1) installation of a helium-cooled loop in the GE test reactor (GETR), (2) fabrication and irradiation in the GETR of capsules containing slightly enriched UO_2, (3) post irradiation examination and testing of the fuel capsules irradiated in the GETR and other capsules irradiated at the LITR and ORR at ORNL and in the ETR at NRTS.

The design of the helium-cooled loop includes an irradiation section that consists of five experiment tubes in parallel which are installed in the pool outside of and adjacent to the GETR pressure vessel. Each of the 1.5-in.-dia (nominal) experiment tubes will accommodate three end-on-end fuel capsules. The helium compressor, precooler, and regenerative heat exchanger are common to all five experiment tubes and are located external to the reactor shield. An auxiliary helium compressor assembly is provided to maintain coolant flow in the event of failure of the primary compressor. In addition, the GETR facility is equipped with an emergency diesel-driven electric generator to protect against power failure.

Individual 15-kw-capacity electric heaters are provided in the inlet section of each of the experiment tubes to provide additional flexibility in maintaining the correct inlet gas temperature.

An irradiation assembly contains three capsules, and each capsule contains 12 UO_2 fuel pellets. The over-all length of the capsule assembly is 23.25 in.

Aluminum-clad cadmium cylindrical shutters are installed on each of the experiment tubes. The shutters are arranged so that by means of hydraulic cylinders they can be individually lowered or raised over the fuel capsules on any predetermined program in order to provide thermal cycling. The shutters also serve as protective devices; they will be automatically lowered on a signal of low helium flow, high activity level of the helium, or high fuel capsule surface temperature. Further, the reactor will scram on a signal of high fuel capsule surface temperature or high activity level of the helium.

Design parameters of the loop are:

Loop heat removal capacity	90 kw
Bulk coolant temperature at	
Inlet to experiment tube	720°F
Fuel capsule assembly outlet	800°F
Compressor discharge	160°F
Helium mass flow rate per experiment tube	2800 lb/hr
System pressure at irradiation position	400 psia
Helium velocity at experiment facility	355 fps
Maximum capsule surface temperature	1500°F
Maximum rate of system contamination from hydrocarbons	2 g/1000 hr

The initial loading of the loop, which is scheduled for early 1959, will consist of 15 capsules which will be tested at a power output of 30,000 Btu/ft·hr and a capsule surface temperature of 1300°F.

Miniature Capsule Fission-Gas-Release Experiments. Irradiations of miniature capsules were initiated early in 1958, and the results of two experiments are described in the next section. Equipment was constructed for

six additional experiments and the irradiations are under way. The new equipment provides two axially separated sealed cavities for UO_2 pellets.

EXAMINATIONS OF IRRADIATED CAPSULES

Prototype Capsules. Irradiated prototype capsules are examined to determine the quantity of fission-gas release and the effect of irradiation on the capsule and the UO_2 pellets as functions of various design and operation parameters, such as power density, fuel burnup, operating temperature, and pellet geometry. The experimental results will provide a basis for a choice of pellet shape. Tests are to be made with solid pellets, pellets with central holes, and pellets with beryllium oxide rods inserted in the central holes.

The initial prototype capsule irradiation was conducted in the LITR with the apparatus shown in Fig. 6.3. Future irradiations will be performed as described in the preceding section.

The initial experiment was terminated on August 6, 1958 because of failure of a gas seal. The capsule used in this experiment was fabricated of type 304 stainless steel and it contained 12 UO_2 pellets with central holes. The capsules were filled with purified helium before they were sealed.

The steel spring at the bottom of the capsule was loaded to apply a stress equal to that of the GCR-2 full-size fuel element, about 2.75 lb. Heat generated in the UO_2 during irradiation was transferred to the outer jacket, which was cooled by the reactor water, through a 0.020-in. annulus filled with helium at a pressure of 400 psi. A rack-and-pinion mounting allowed vertical positioning of the apparatus so that predetermined temperatures (measured by Chromel-Alumel and platinum-platinum-10% rhodium thermocouples) could be maintained during operation.

In the preparation of the UO_2 pellets by the Ceramics Laboratory of the Metallurgy Division, ammonium diuranate was precipitated from UO_2F_2, and UO_2 was recovered by successive calcinations and pressing at 15,000 psi. Pellets formed by pressing the UO_2 at 7500 psi were statically pressed at 35,000 psi and sintered for 1 hr at 3180°F in an atmosphere of 7 parts of nitrogen to 3 parts of hydrogen. The resulting pellets were 0.705 in. OD,

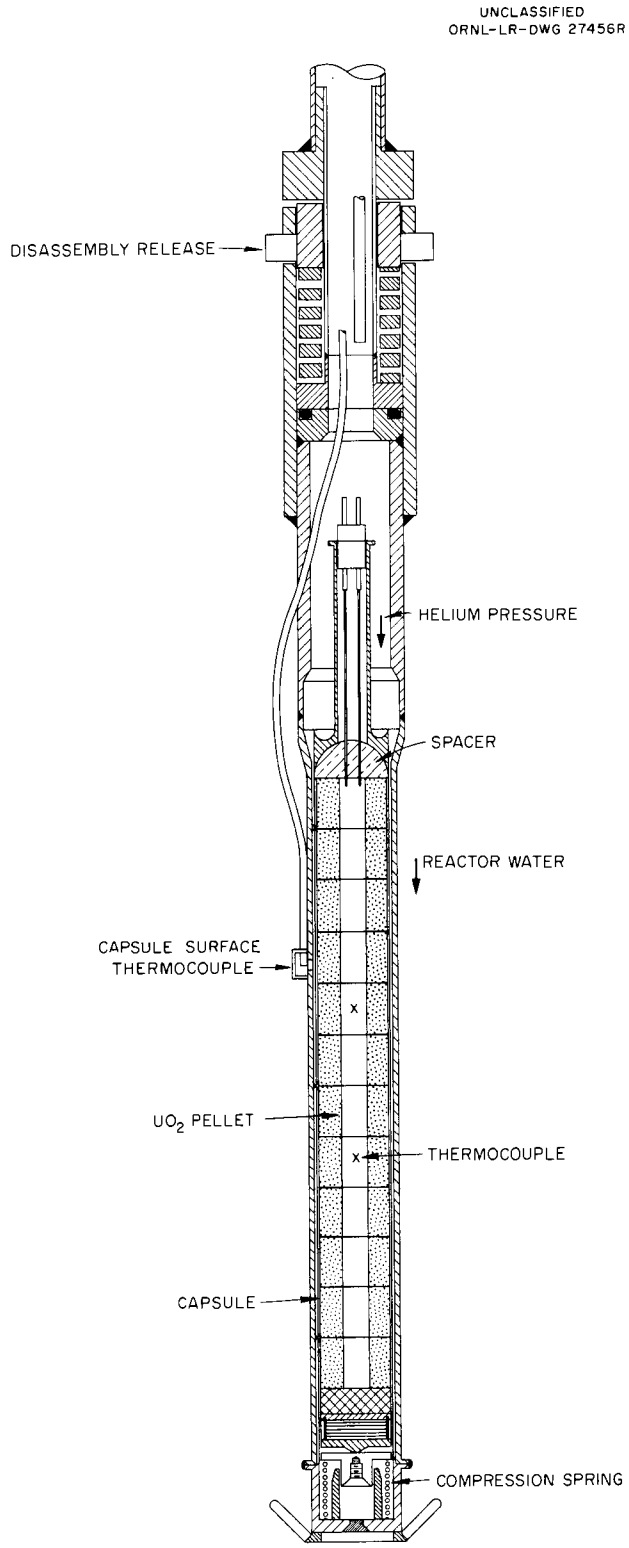

Fig. 6.3. Apparatus for Fuel Capsule Irradiation in the LITR.

0.250 in. ID, and 0.500 in. long; they each weighed approximately 27.5 g; and the density was 10.4 g/cm^3. The U^{235} content was 1.91%, and the U:O ratio, by stoichiometric analysis, was 1:2.005. Spectrographic analysis showed traces (less than 0.1 wt %) of Al, B, Be, Ca, Cr, Cu, Fe, Mg, Mo, Ni, Si, and Ti. A chemical analysis for fluorine showed less than 10 ppm.

The pellets were irradiated to a total exposure of 0.43×10^{18} n/cm^2 at the top, 3.1×10^{18} n/cm^2 at the center and 10.4×10^{18} n/cm^2 at the bottom. The maximum capsule surface temperature was 950°F and the central pellet temperature was 1850°F. The capsule will be examined in a hot cell for dimensional changes. The information obtained during operation of this first experiment verified the heat transfer calculations used in the design.

Miniature Capsules. The extent to which the fission gases are released from the UO_2 crystal lattice into the fuel capsule is important because the gas could cause distortion or swelling of the capsule by pressure buildup and it could cause an increase in the temperature of the UO_2 by reducing the thermal conductivity of the helium atmosphere in the capsule. Fission-gas release is considered to be primarily the result of solid-state diffusion.[1] Normally, diffusion is affected by temperature, concentration, total surface area, and time. The total surface area available for adsorption of gas, as measured by the Brunauer-Emmett-Teller method (using krypton instead of nitrogen for high-density UO_2), is a function of density. Therefore this series of experiments was designed for measurement of the fission gas released by UO_2 pellets of the several densities considered usable for fuel elements and for examination of the pellets to determine whether they will fracture under the high thermal stresses expected during operation.

Two capsules, designated UO_2-1-1 and UO_2-1-2, were irradiated in the LITR. The apparatus for the first irradiation is shown schematically in Fig. 6.4. The apparatus for the second experiment was like that for the the first experiment except that the design was changed to provide for the simultaneous irradiation of two capsules. The nominal clearance

[1] J. D. Eichenberg et al., Effects of Irradiation on Bulk UO_2, WAPD-183, p 25 (Oct. 1957).

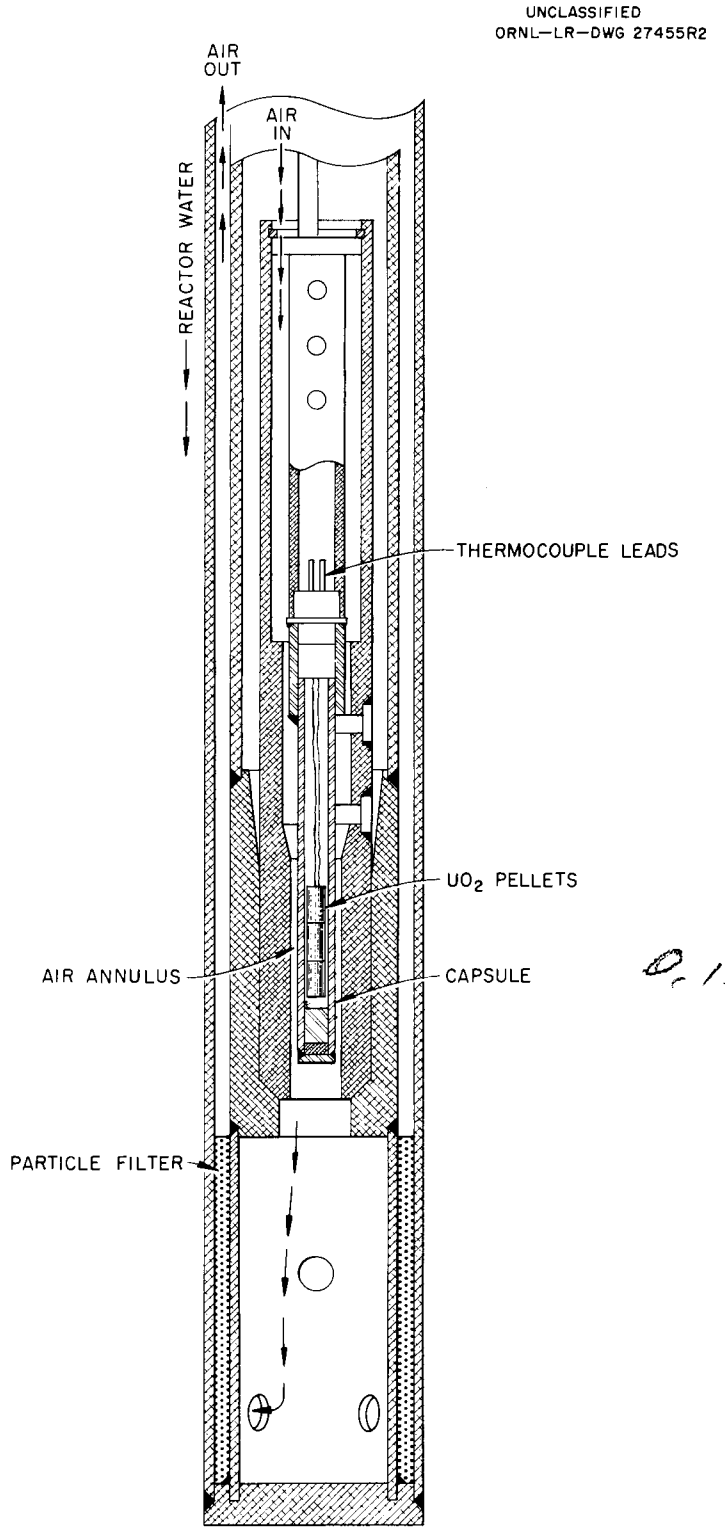

0.156"

Fig. 6.4. Apparatus for Irradiation of Miniature Capsules in the LITR.

between the pellets and the inner surface of the sealed capsule was 2 mils. The capsule was filled with a helium atmosphere before it was sealed. Some titanium sponge was included in the assembly to getter residual oxygen.

The pellet specimens, which were prepared as described above, were cylinders, with central holes, that measured 0.156 in. OD, 0.078 in. ID, and 0.250 in. long. Pellet specimens with and without central holes are shown in Fig. 6.5. In the first two tests the pellet specimens had average densities of 10.52 g/cm^3, or 96% of theoretical; the U:O ratio was 1:2.008; the U^{235} content was 15 wt %; and the gas surface area was 0.002 m^2/g, or three times the geometric area. Spectrographic analysis showed traces (less than 0.01 wt %) of Al, B, Ca, Cr, Cu, Fe, Mg, Mo, and Ni.

The conditions of the tests are given below:

	UO_2-1-1	UO_2-1-2	
		Top	Bottom
Time at 3000-kw reactor power, hr	1,829	1,964	1,964
Integrated flux (cobalt foil, uncorrected), n/cm^2	7×10^{19}	20×10^{19}	20×10^{19}
Power dissipation, w/cm^3	780	1,020	1,020
UO_2 central temperature, °F	1,770	1,770	2,000
UO_2 outer surface temperature, °F	1,670	1,490	1,720
Thermal stress, psi	12,500	35,000	35,000

A bench test was made to determine the variation in the actual temperature of the capsule surface from that indicated by thermocouples spot-welded to the surface in the annular space required for the cooling air stream. The bench test was conducted with power generation, temperature, and air flow that simulated operating conditions in the reactor. Temperatures were recorded on a Brown recorder and checked with an optical pyrometer. The total variation was less than 10°F, which is less than the error that may be expected with this equipment, and therefore may be disregarded.

After irradiation, fission-gas samples were taken in a hot cell by puncturing the capsule with a tube-piercing valve. The gas was allowed to flow into an evacuated system from which an aliquot was valved off into a

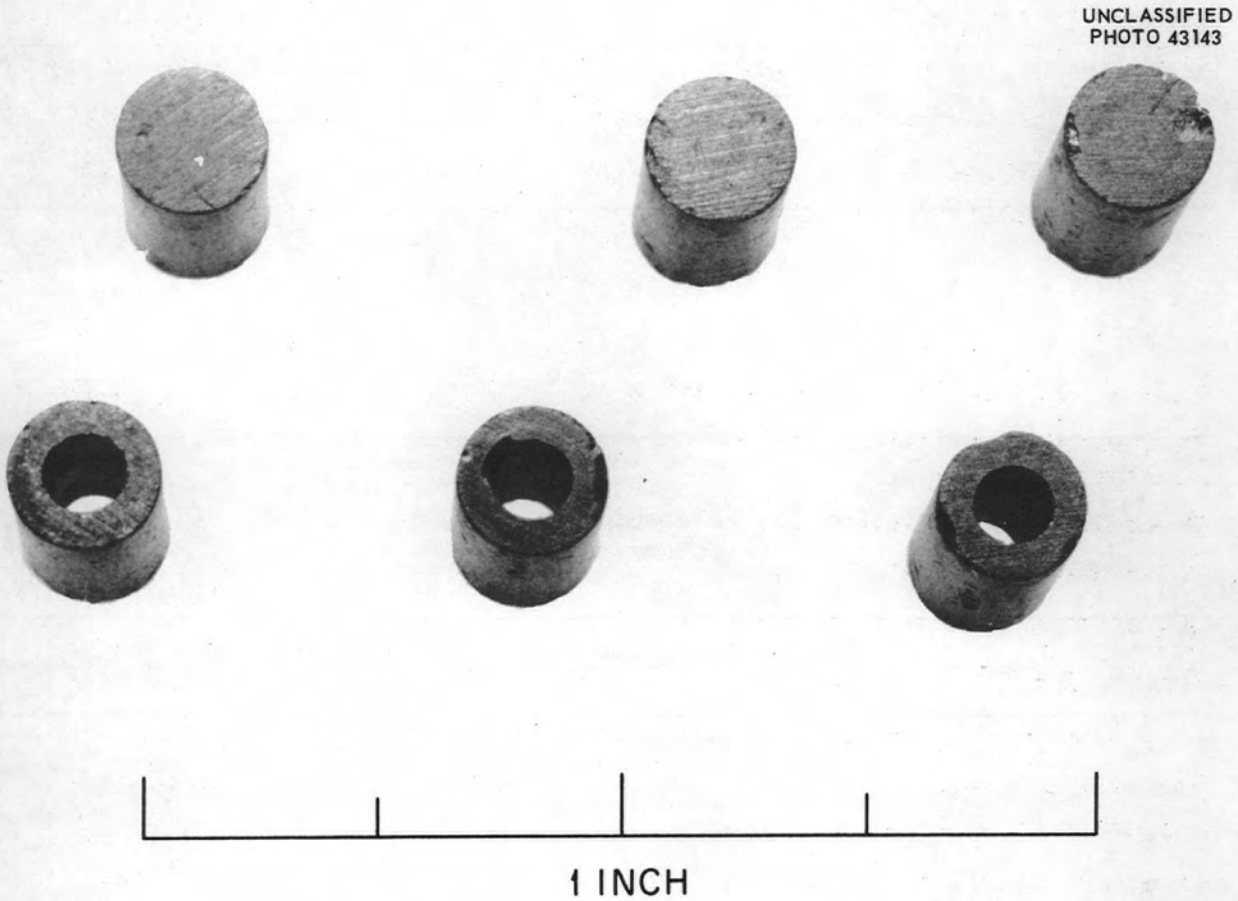

Fig. 6.5. UO_2 Pellets Used in Irradiation Experiments.

glass bulb. The gas samples were analyzed with a sodium iodide gamma-ray scintillation spectrometer. The fission-gas sampling apparatus is shown in Figs. 6.6 and 6.7. Results of the fission-gas analyses are presented in Tables 6.5 and 6.6. Further irradiations are planned, as described in the preceding section, for which 1-in.-long pellets will be used.

Table 6.5 Results of Analyses of Fission Gas Released in Miniature Capsule Experiments UO_2-1-1 and UO_2-1-2

Fission Gas Analyzed for	Quantity Found (cm^3) UO_2-1-1	UO_2-1-2 (top)	UO_2-1-2 (bottom)	Accuracy of Measurement (%)
Kr^{88}		4×10^{-8}	8×10^{-8}	±30
I^{131}	3×10^{-7}	1.4×10^{-8}	2.5×10^{-8}	±30
Xe^{133}	3×10^{-5}	2.0×10^{-5}	2.7×10^{-5}	±10
Xe^{135}	3×10^{-7}	1.6×10^{-6}	2.3×10^{-6}	±10

Table 6.6 Fission Gas Released as Percentage of Total Gas Volume of Capsule

Fission Gas	Ratio of Fission Gas Released to Total Gas Volume (%) UO_2-1-1	UO_2-1-2 (top)	UO_2-1-2 (bottom)
Kr^{88}		0.5	1.0
I^{131}	0.08	0.02	0.03
Xe^{133}	0.7	1.8	2.3
Xe^{135}	0.2	0.7	1.0

CLOSED-CYCLE-LOOP IRRADIATION FACILITY

An experimental facility is being constructed at the ORR to study radiation effects on ceramic fuels at high temperatures. The locations of both the in-pile and auxiliary components of the facility are shown in Fig. 6.8.

The design consists of concentric in-pile tubes containing a removable test capsule cooled by recirculated gas. The concentric tubes enter the reactor tank at flange V2 and extend downward with a 17-in. horizontal

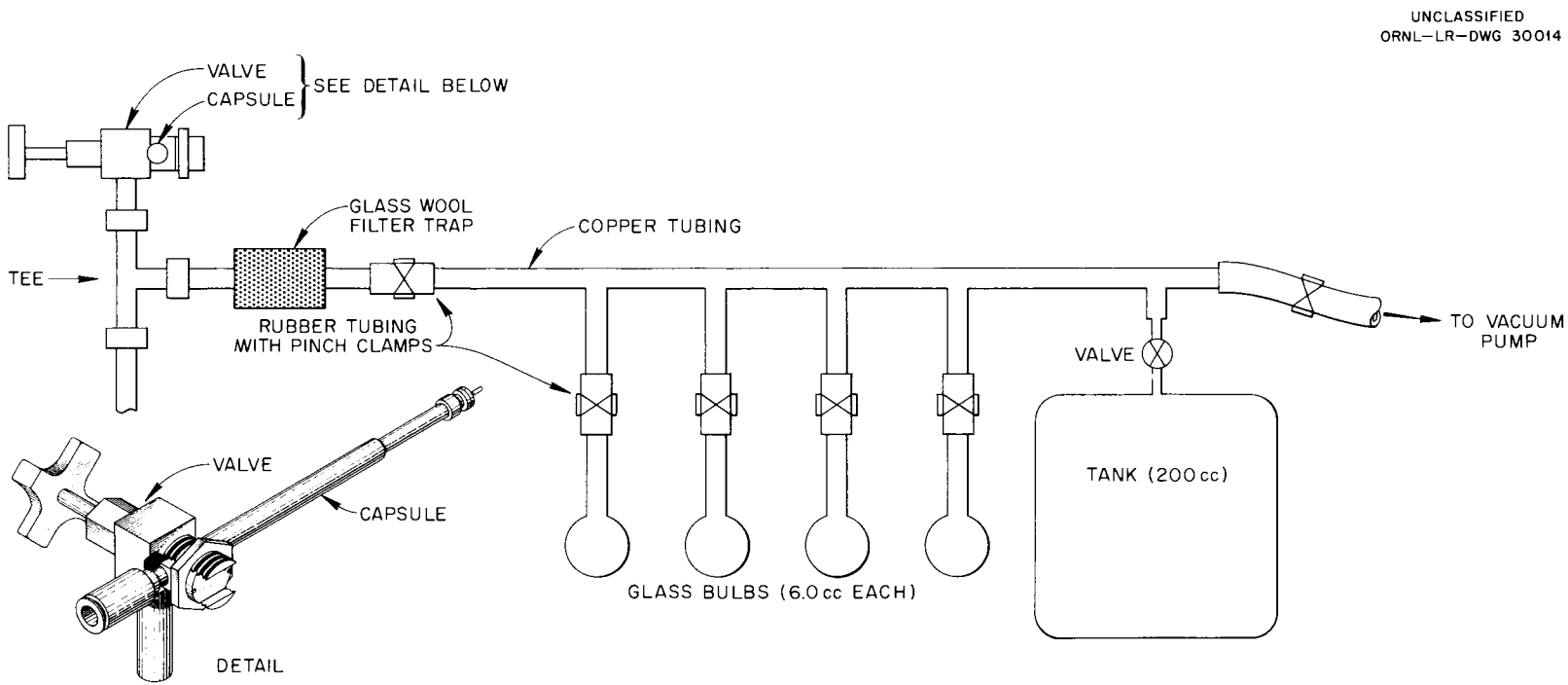

Fig. 6.6. Fission Gas Collection Apparatus.

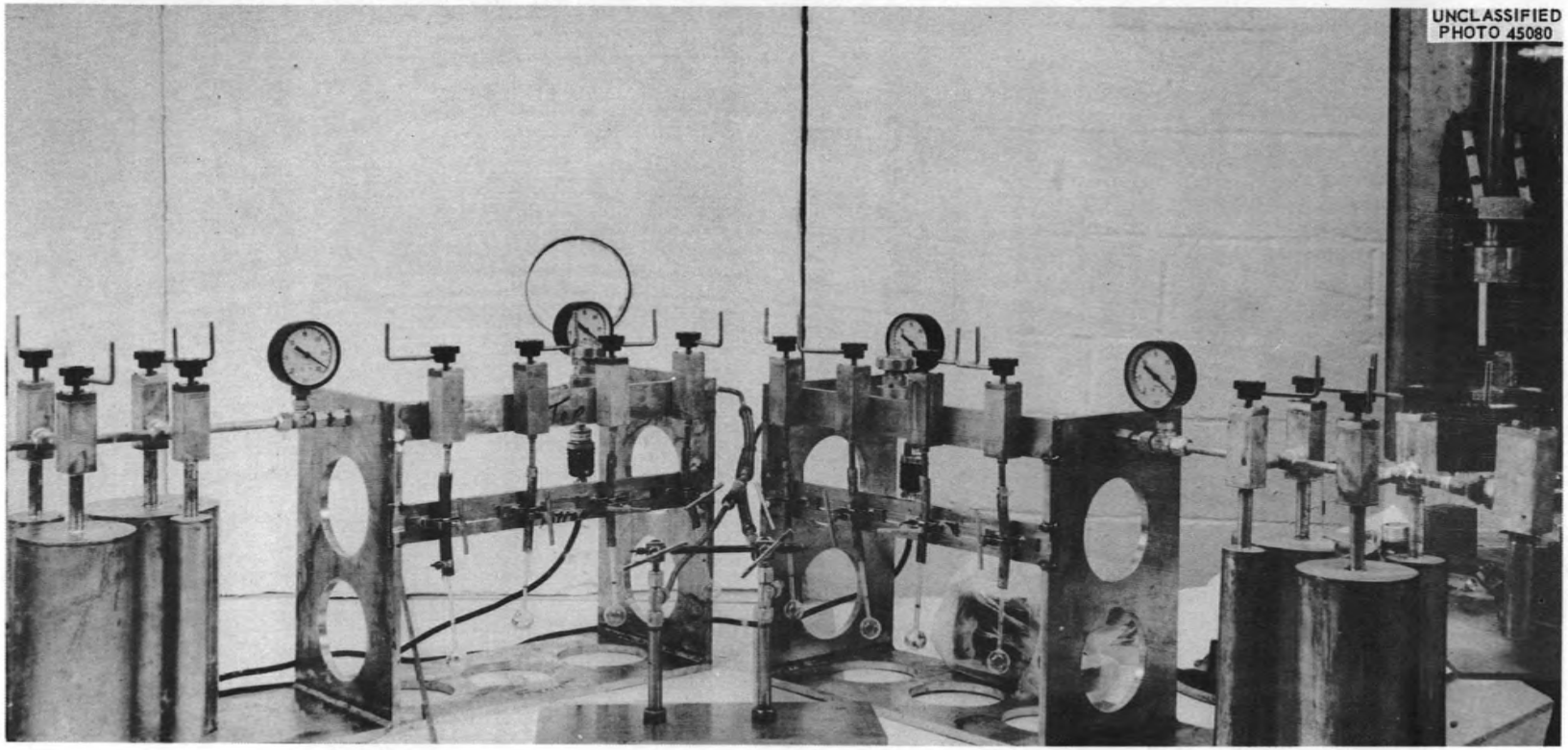

Fig. 6.7. Apparatus for Collecting Fission Gas Samples from Irradiated Fuel Capsules.

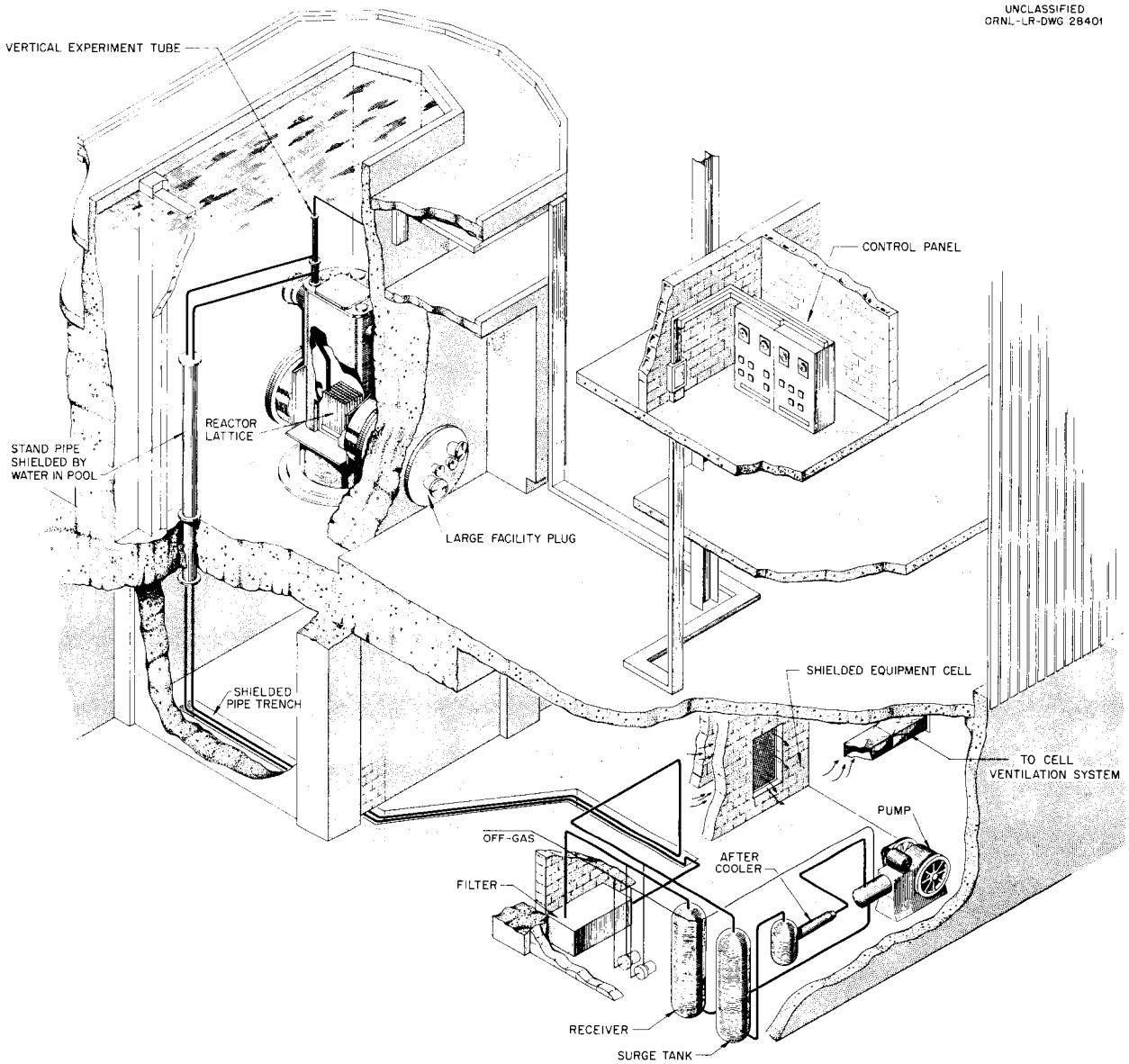

Fig. 6.8. Closed-Cycle-Loop Irradiation Facility in ORR.

offset into the reactor lattice position B-9. A thermal-neutron flux of approximately 0.7×10^{14} $n/cm^2 \cdot sec$ is expected at a reactor power of 20 Mw. The gas coolant to be used in the first tests will be nitrogen, but air and other gases could be used. The entire loop will contain 160 ft^3 of gas, which will be forced through the in-pile tubes by a 30-hp oil-free compressor. The compressor and other auxiliary components are located within a shielded compartment in the ORR basement. Coolant lines between this compartment and the reactor pool are shielded. This facility is expected to be put into operation early in 1959.

This loop, in contrast to other larger loops which are to be used for testing prototype fuel elements, was designed primarily for studying fuel materials at high temperatures. Of immediate interest are graphite-clad UO_2 compacts. These elements may also be inserted into thin stainless steel capsules or coated with Si-SiC. For future studies it is anticipated that fuel elements of the following types will be available: Si-SiC-UO_2 clad with Si-SiC, and Cr-Al_2O_3-UO_2 clad with Cr-Al_2O_3, MgO-UO_2 clad with MgO, and BeO-UO_2 clad with BeO. An equivalent list of fuel element materials may also be made with ThO_2-UO_2 mixtures.

HOT CELL MODIFICATIONS

Structural design studies have been completed for the modifications of Cell 6, Building 3025, required for the examination of irradiated samples containing plutonium, such as the low-enrichment UO_2 pellets used in the fuel capsule experiments described above. The plan of the existing cell is shown in Fig. 6.9 and the plan of the altered cell is shown in Fig. 6.10. As may be seen, cell 6 is to be expanded to include former cell 5B. The new cell will be equipped with two viewing windows, and the interior operating area will be serviced by three model-8 master-slave manipulators. The rear rotary door will provide access for radioactive samples into the cell. Samples will be removed from the cell through the same door after being canned and passed through an automatic scrubber and air lock. The cell will be provided with a bridge crane, rear access sleeves, and a rear gamma shield door for access into the decontamination room. The decontamination room and cell have a filtered ventilation system separate

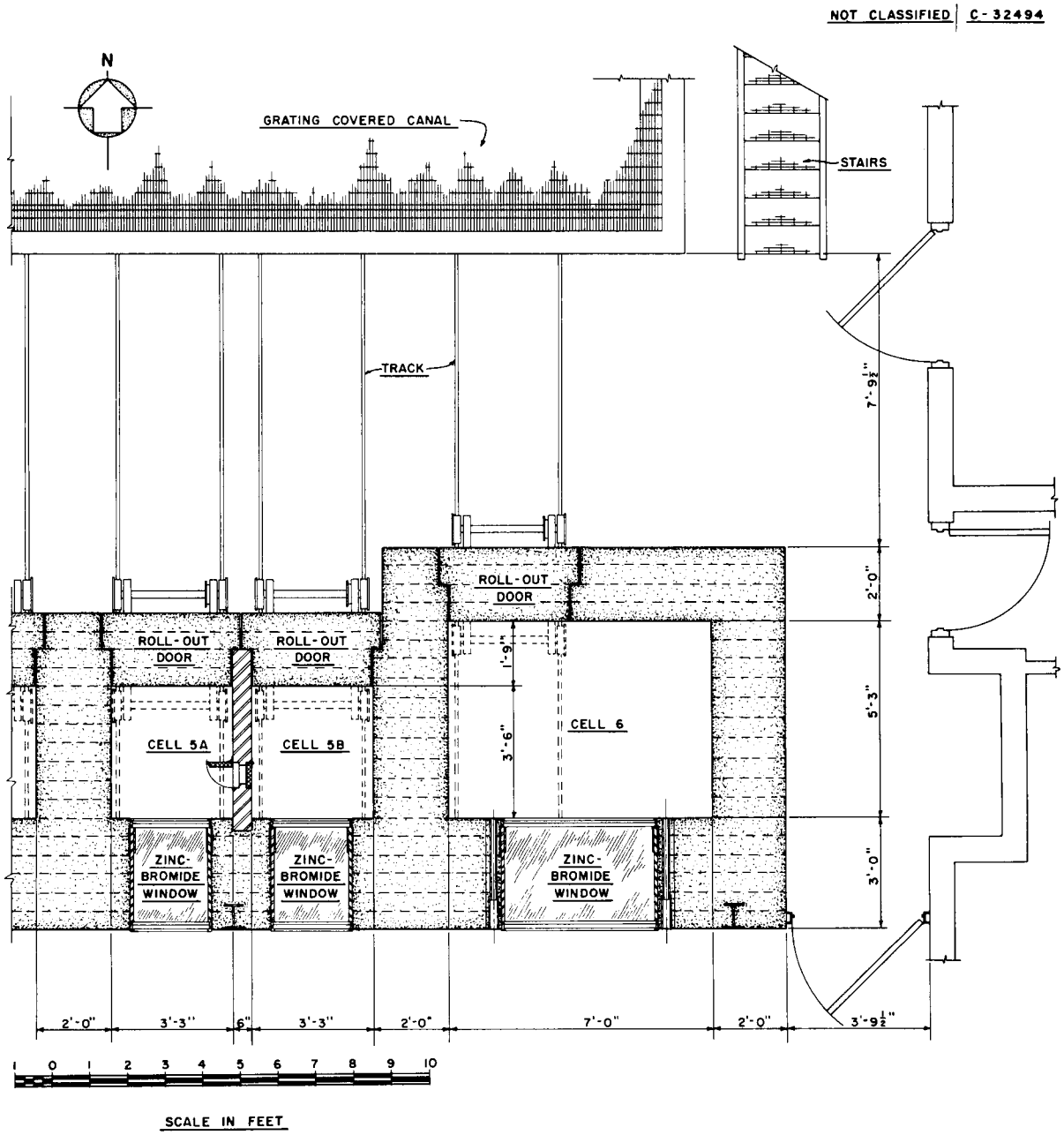

Fig. 6.9. Plan of Existing Cells.

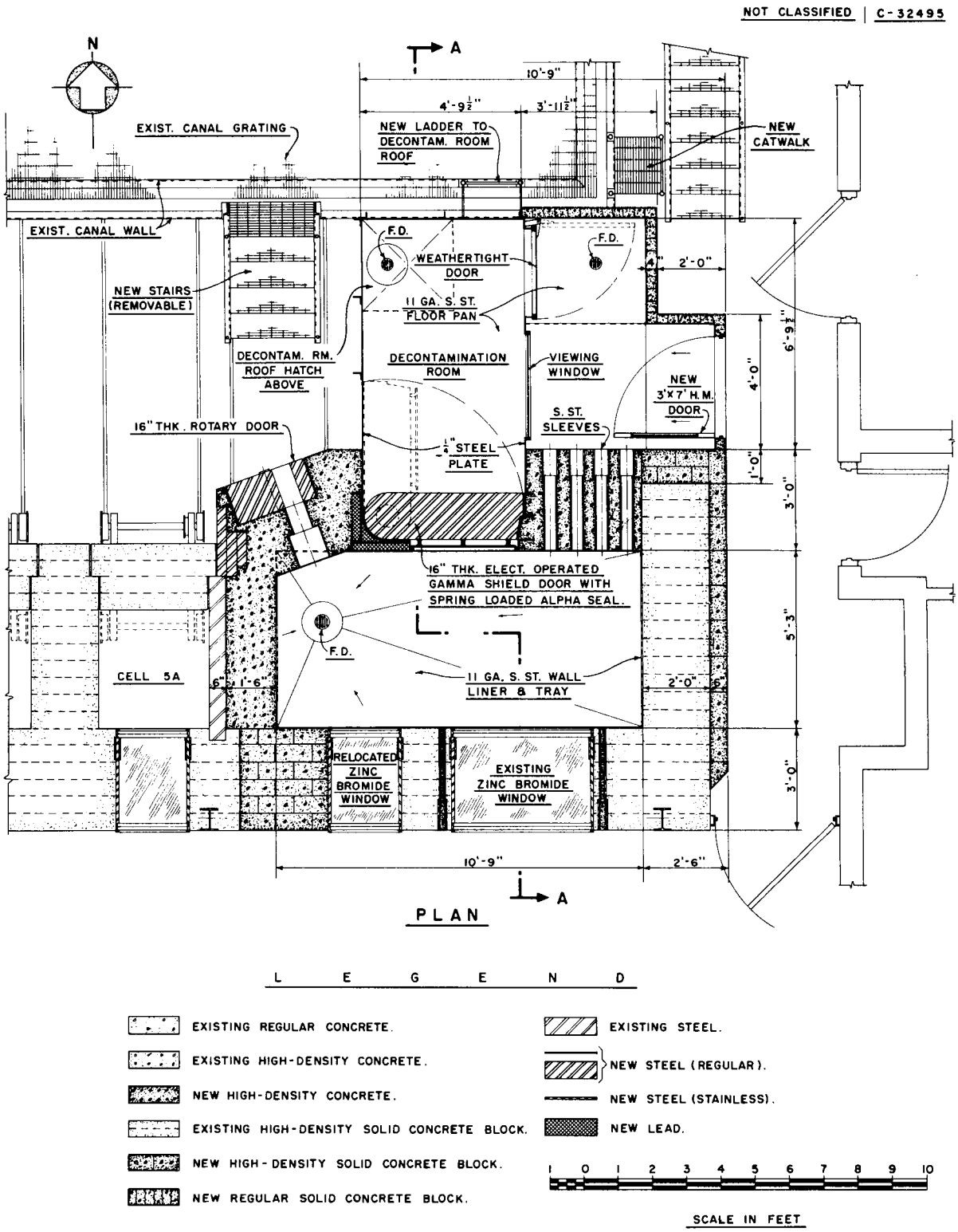

Fig. 6.10. Plan of Altered Cell 6.

from that of the rest of the cells. Glove ports and a viewing window (Fig. 6.11) will make it possible for the operator to perform equipment maintenance without entering the contaminated area. This room may be decontaminated by a water spray. Equipment will be removed or brought in by an overhead hatch and access door. The extension crane will move the equipment by remote control into the cell. Personnel will be restricted to the decontamination room; there will be no personnel access to the cell.

The ORR hot cell will be used to remove the ORR-irradiated prototype fuel capsules from their NaK-filled irradiation tubes. The facility tubes will be cut off under water and transferred through the canal into the ORR hot cell, where the outer tubes will be cut away; the NaK will be drained off and reacted with butyl alcohol. The samples will then be transferred to modified cell 6, Building 3025, or shipped to the General Electric Vallecitos Atomic Laboratory for further examination. Design work has been completed on the cell off-gas system and on the remote cutters and saws.

THERMOCOUPLE IRRADIATION STUDIES

Noble-metal thermocouples will be required at the temperatures that will be used in the studies of ceramic fuel elements. The noble-metal thermocouple in common usage at ORNL is platinum – platinum-10% rhodium. Rhodium has a rather large thermal-neutron absorption cross section (150 barns), with a large resonance at about 1 ev. Thus, for reasonable exposure periods, there may be appreciable rhodium burnup (for example, 1.5% per 10^{20} n/cm^2) which may seriously affect the thermocouple calibration. Therefore measurements are being made of the effect of neutron exposure on the calibration of platinum – platinum-rhodium and Chromel-Alumel thermocouples.

Bare and ceramic-insulated platinum – platinum-10% rhodium and Chromel-Alumel thermocouples have been irradiated in a water-cooled hollow beryllium piece in the C-47 location adjacent to the active core in the LITR. The thermocouples are about 18 in. long and are encased in 3/8-in.-OD aluminum tubes, as shown in Fig. 6.12. After being irradiated

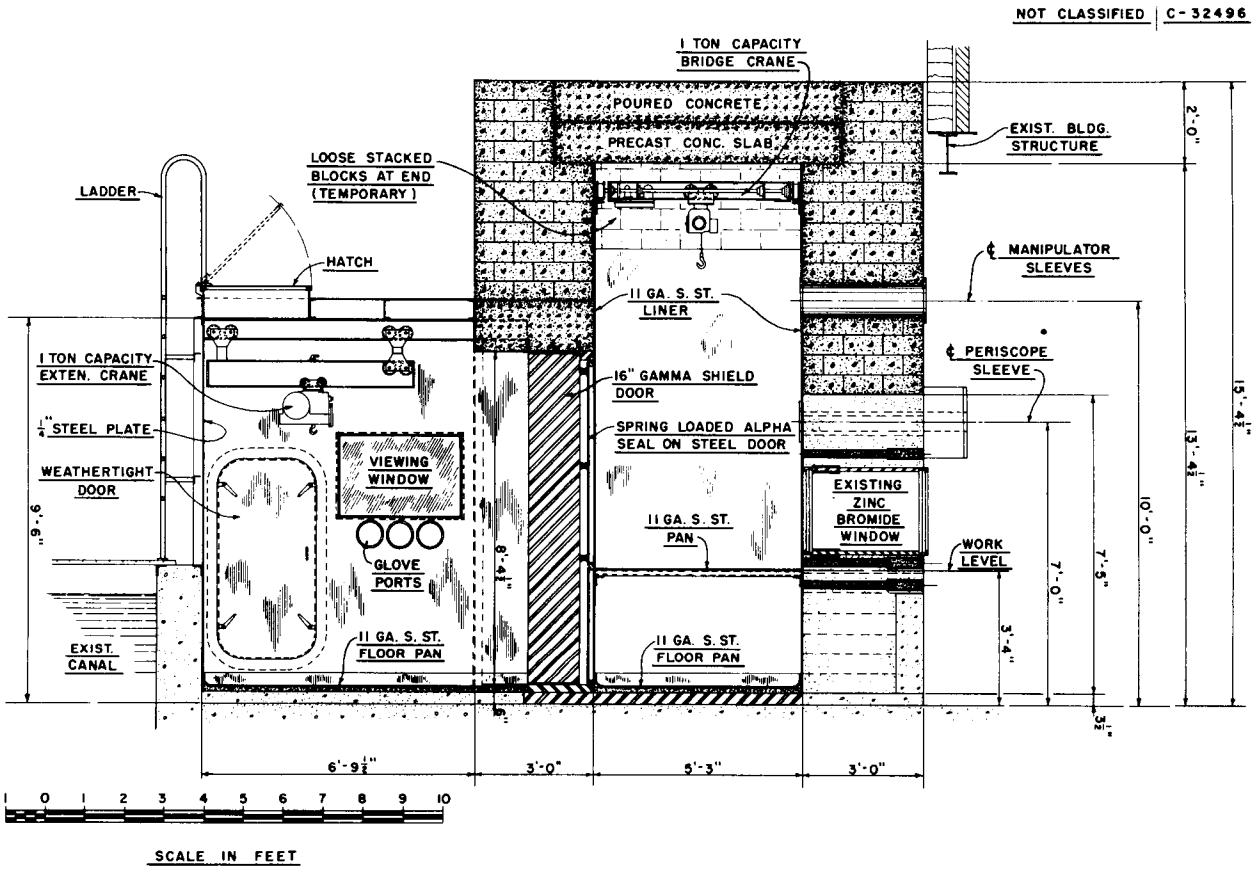

Fig. 6.11. Section A-A of Fig. 6.10.

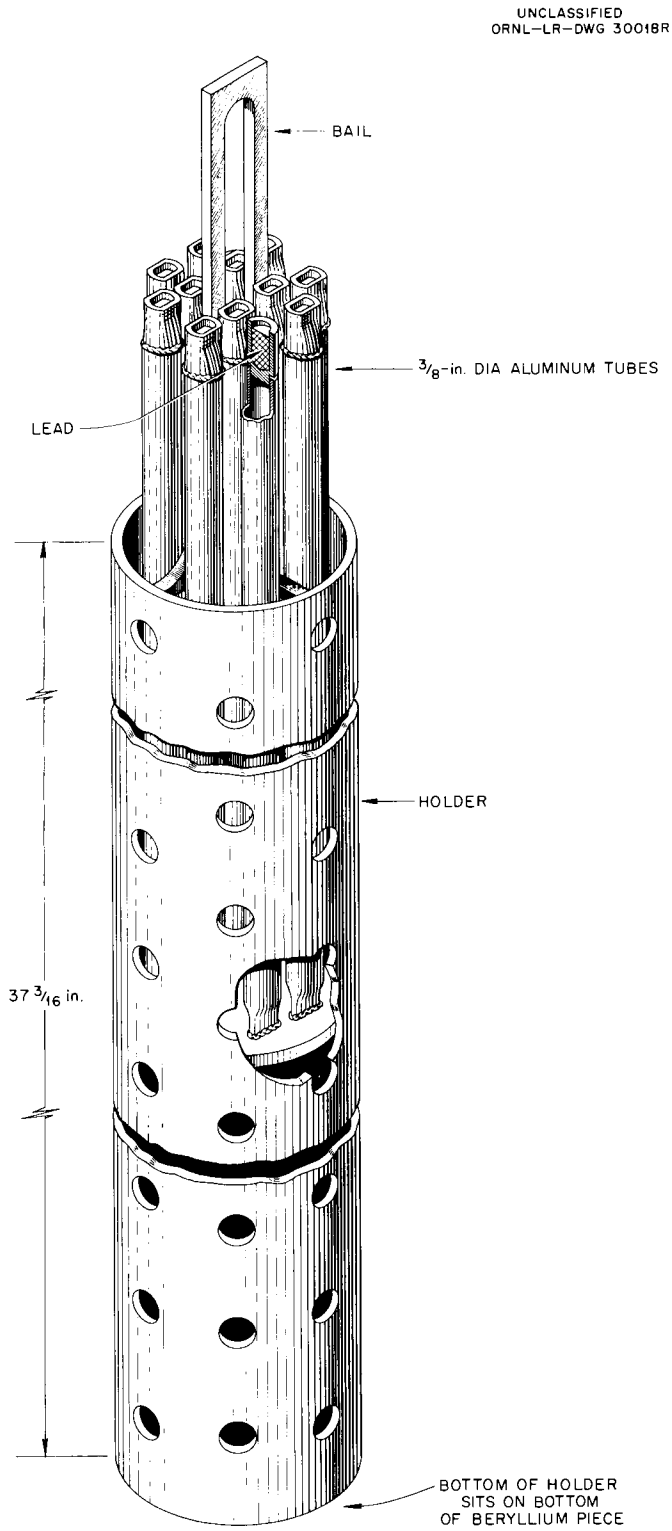

Fig. 6.12. Apparatus of Irradiation of Thermocouples in the LITR.

for the desired period, the tubes were removed from the holder; the short-time activity is being allowed to decay before the thermocouples are removed from the tubes for calibration.

Only bare platinum – platinum-10% rhodium thermocouples have been calibrated thus far, since the remaining wires are too radioactive to handle outside hot cells. The calibrations have been made by the Standards Laboratory of the Instrument Department by using the routine method and equipment for calibrating standard platinum – platinum-rhodium thermocouples. The method used and the equipment are essentially those recommended by the National Bureau of Standards.[2] The method may have to be revised, however, because it appears that the relative location of the furnace temperature gradient with respect to the irradiated wire may affect the calibration.

Most of the platinum – platinum-rhodium thermocouples irradiated in the LITR have been calibrated by the above-described means (with relative location of the furnace temperature gradient and wire held constant), and the results are as presented in Figs. 6.13 and 6.14. The thermal-neutron exposures given on the curves are approximate.

Supplementary measurements have indicated that most, if not all, of the difference between irradiated and nonirradiated thermocouples occurs in the platinum-10% rhodium leg. It is apparent that there is a difference in performance in the wire from the two manufacturers for exposures less than approximately 3.6×10^{20} n/cm^2. The Sigmund Cohn platinum-10% rhodium wire is very much more radioactive than the similar Bishop wire. A gamma-ray spectrum analysis made after several weeks of decay indicated that most of the long-lived activity in all the wires is due to Ir^{192}. Additional samples are being prepared for identification of the short-lived activity.

Additional thermocouples are being irradiated in the ORR to obtain higher exposures. Techniques for calibrating the Chromel-Alumel and high-exposure platinum – platinum-rhodium thermocouples in a hot cell are being developed.

---

[2] NBS Circular 590.

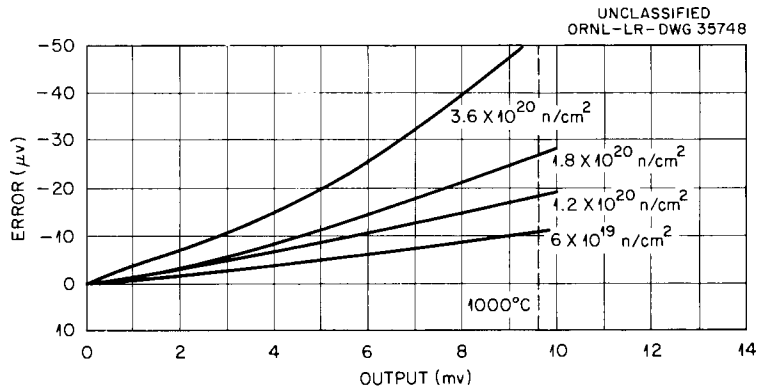

Fig. 6.13. Effect of Reactor Irradiation on Platinum–Platinum-10% Rhodium Thermocouple – Bishop Wire. Error (μv) indicates difference from an unirradiated thermocouple of the same wire.

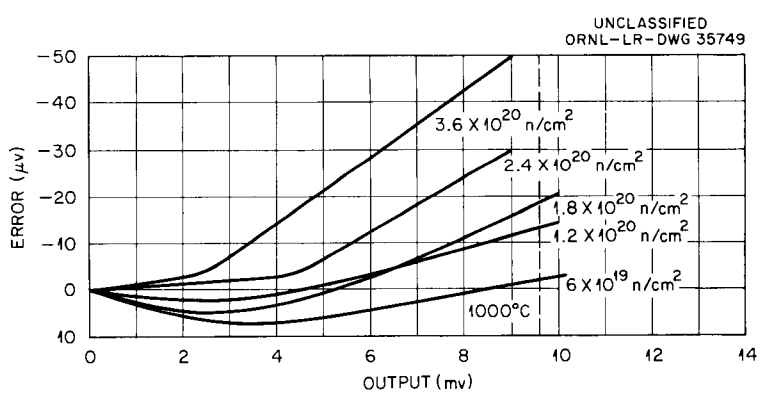

Fig. 6.14. Effect of Reactor Irradiation on Platinum–Platinum-10% Rhodium Thermacouple – Sigmund Cohn Wire. Error (μv) indicates difference from an unirradiated thermocouple of same wire.

SiC-Si CLADDING FOR HIGH-DENSITY GRAPHITE

In the interest of developing a moderator capable of withstanding high temperatures in an oxidizing atmosphere, SiC-Si clad graphite[3] is being examined for oxidation and erosion resistance outside the reactor in preparation for subsequent experiments in the reactor. Four different samples of graphite coated with SiC-Si have been subjected to out-of-pile tests.

The first experiment was designed primarily as a destructive erosion test. A needle-point blast of air was directed at one portion of the specimen, which contained a core of UO_2. The air blast impinged on the surface at a temperature of 1830°F with a near-sonic velocity. Because of the small area of the jet, erosion at this point could be compared with the surrounding surface of the sample. After 1000 hr of testing, the only observed change was a slight discoloration at the point of air impact.

The sample was periodically weighed, and a gradual weight increase was noted. This may have been due to impurities in the air blast which embedded into or adhered to the hot sample.

When the sample was weighed, it was removed directly from the furnace and cooled in an air blast. No evidence of cracking, spalling, or any thermal shock damage was observed.

The experiment was terminated after more than 1000 hr when a platinum thermocouple was inadvertently placed in direct contact with the specimen. The Pt-Si reaction that resulted formed a porous section in the SiC-Si cladding, and the graphite oxidized beneath the cladding. Only a hollow shell was left in the vicinity of the Pt-Si reaction area, as shown in Fig. 6.15. A metallographic section of the specimen is shown in Fig. 6.16; the light material is Si and the darker gray area is the SiC phase.

A second experiment was conducted primarily as an oxidation test. Three graphite specimens clad with SiC-Si, each 1/4 in. in diameter and 1 in. long, were placed in an Inconel holder and inserted into an Inconel tube in a furnace. Air was forced through the tube and over the specimens, as shown in Fig. 6.17. Because of the excellent resistance of the first specimen to oxidation, the temperature was increased to 2000°F, and the

[3]Developed by J. R. Johnson of Minnesota Mining and Manufacturing Corporation.

UNCLASSIFIED
RMG 2316

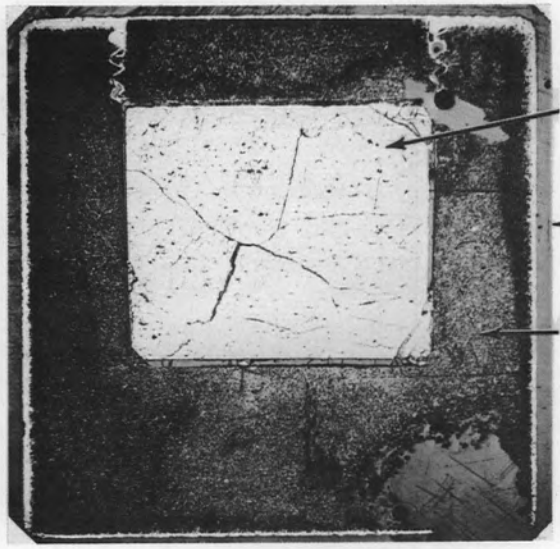

Fig. 6.15. Section Through SiC-Si Clad Graphite Sample After Failure of Cladding.

UNCLASSIFIED
RMG 2315

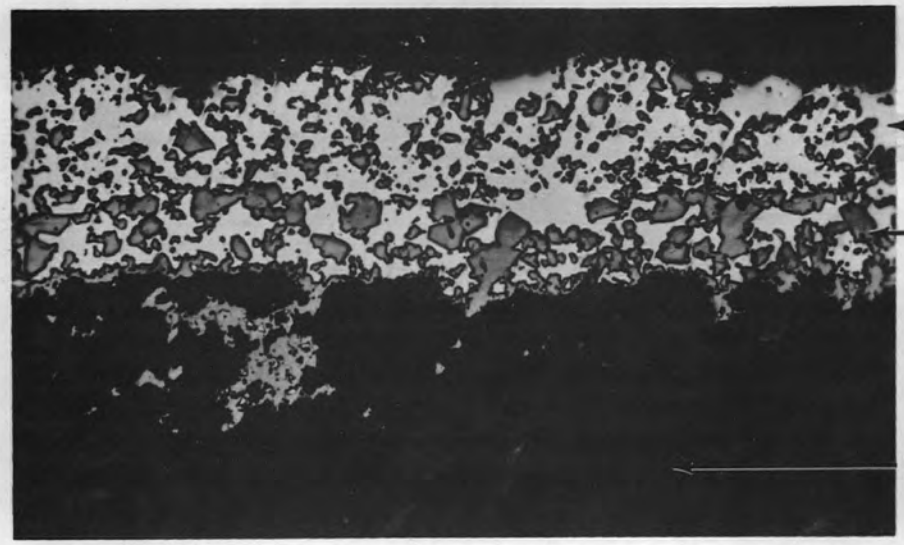

Fig. 6.16. Metallographic Section of SiC-Si Clad Graphite After 1000 hr at 1830°F in an Air Blast. 250X.

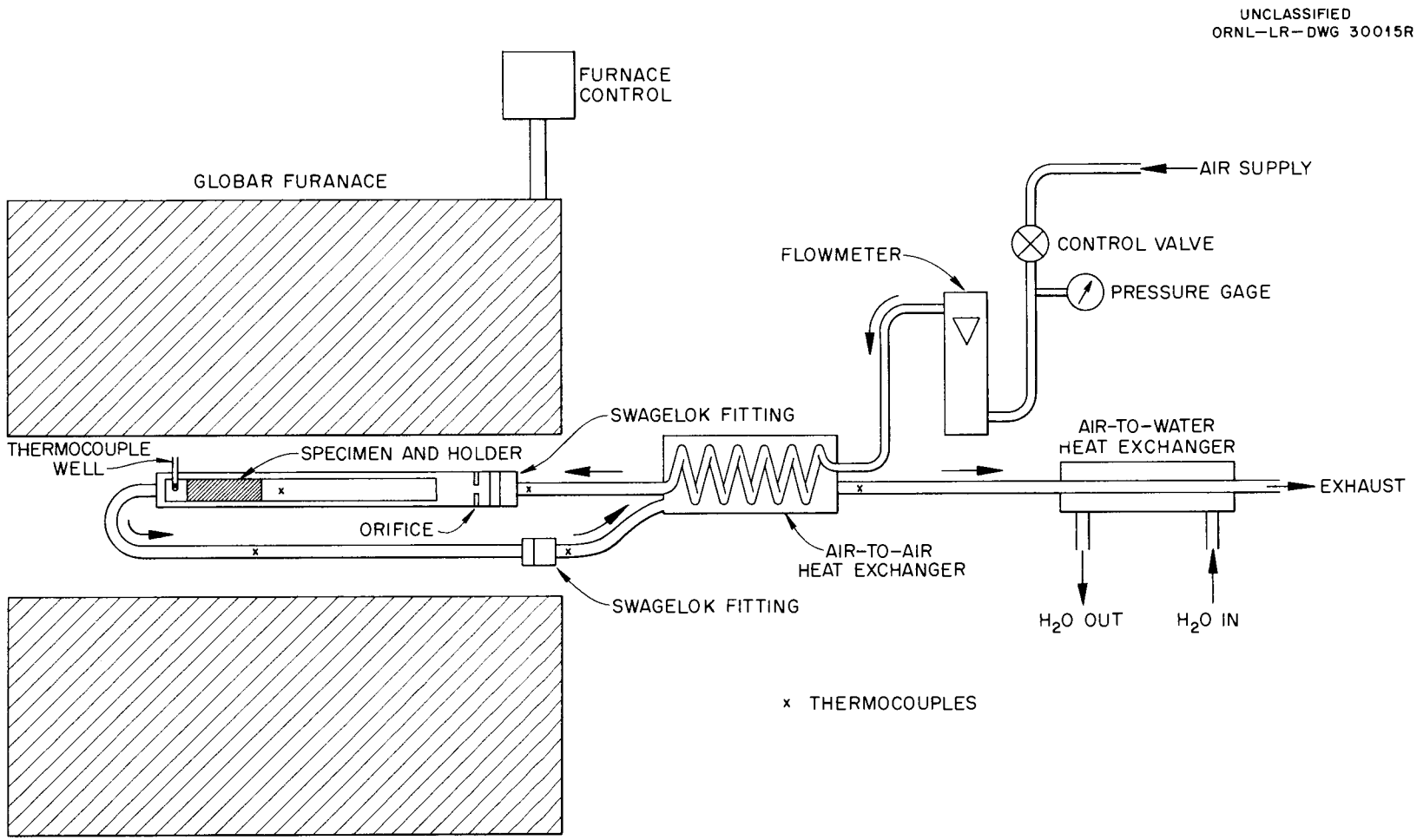

Fig. 6.17. Apparatus for Oxidation Tests of SiC-Si Clad Graphite Specimens.

average velocity of the air stream past the specimens was increased to 140 fps with a volume flow of 0.95 scfm. Two of the specimens withstood 897 hr of this test without detectable change of weight or appearance. One specimen lost weight after 30 hr of the test, and after 700 hr only a shell of SiC-Si was left.

The two sound specimens and two untested specimens of the same construction were encapsulated and inserted in the ORR. One capsule containing a tested and an untested specimen was removed after a thermal-neutron exposure of 9×10^{19} n/cm^2 at reactor water temperature.

The irradiated specimens showed no changes in weight or density. They were again placed in the oxidation testing apparatus and tested at 1100°C for 193 hr. No weight or appearance changes were observed after this test. The specimens were then again encapsulated and placed in the ORR. They will be retested in the oxidation testing apparatus after a further thermal-neutron exposure of approximately 5×10^{20} n/cm^2.

A reactor experiment is planned to test the ability of SiC-Si clad graphite to retain gaseous fissions products at high temperatures and high heat fluxes. The sample will be heated by fission heat to the desired temperatures and the evolved fission gases will be analyzed. Initial tests will be made with unclad UO_2 and ThO_2-UO_2 in order to establish the rate and amount of gaseous evolution as a function of temperature, burnup, and power. Subsequent tests will be made with the fuel clad in high-density graphite and in SiC-Si clad graphite.

INSTANTANEOUS FISSION-GAS STUDY

A determination of ability to retain gaseous fission products is important in the evaluation of any fuel material, but it is of particular concern in the case of ceramics, which have poorer gas retention properties than metals at normal temperatures. The mechanisms by which the gases are released are not well known and apparently these mechanisms are influenced by several variables.

A reactor experiment is planned in an attempt to determine the effect of temperature, power, time, and ratio of surface area to volume on UO_2 of 95% theoretical density. In subsequent tests, density and method of formation may be included as variables.

It is planned to utilize position C-1 of the ORR reactor for the experiment. The UO_2 sample will be placed within a capsule and hung vertically within the lattice of the reactor. The power generated in the sample will be regulated by moving the capsule up or down until the desired neutron flux is obtained. Sample temperatures will be continually recorded by attached thermocouples. The fission gas evolved will be swept from the sample to an analyzer by a moving stream of gas. The temperature of the sample will be regulated by cooling the outside of the capsule with an air blast.

A hydraulic positioning device has been constructed to position the sample within the reactor. This positioner, which will move the sample over a total vertical traverse of 18 in., is controlled by solenoid valves and is normally operated manually. However, the instrumentation is arranged so that an approach to a dangerous condition will result in automatic withdrawal of the sample from the high flux region of the reactor. The sample position will be indicated on a control panel by a Selsyn motor arrangement.

The cooling system will provide air flow at a rate of 30 scfm. The air will flow down an inner concentric tube, over the sample capsule, and up the outer tube. Because of the high gamma-ray heating expected in the reactor, cooling will be necessary at all but the extreme withdrawn position. This gamma-ray heating will result in the capsule and facility tube walls evolving considerably more heat than that evolved by the specimen.

Fission gases released from the UO_2 sample will be entrained in a helium stream that will continuously sweep the sample. The tubes for carrying the sweep gas will support and position the sample in the reactor. The thermocouple lead wires will also run through the sweep gas tubes. Helium will be used as the sweep gas to avoid oxidation of the sample and activation of the sweep gas. The helium will be passed through a NaK bubbler and a charcoal trap to remove oxygen and water vapor contaminants. The helium containing gaseous fission products will pass through a quartz-wool filter, which will remove any solid particles, especially those fission products which are gaseous at the sample temperature but which will solidify in the gas stream.

The gases emerging from the filter will pass over a high-level Geiger-Mueller tube for a continuous total activity measurement and then to a scintillation counter. At this point the gas may either be continuously analyzed or collected in a liquid-nitrogen-cooled charcoal trap for half-life measurements. The output of the scintillation counter will be fed to a continuously recording, single-channel, pulse-height analyzer. In the event that too many short-lived products are evolved to permit analysis with a single-channel instrument, provisions are being made to feed the amplifier signal to a 200-channel analyzer located in the ORR reactor building. This instrument would be used only to identify the various components of the evolved gases.

In experiments conducted at other laboratories, all the samples used to evaluate fission-gas evolution at other than low specific power levels have fractured. Specimens in the form of rectangular slabs 0.030 in. thick will be used in these experiments in an attempt to avoid sample fracture from thermal stresses. Calculations have indicated that a power density of 300 w/cm^3 can be generated in UO_2 of this thickness without exceeding the rupture stress. The temperature drop across the slab, with heat flow from only one face, will be less than 100°F. The advantage of this small temperature differential will be that evolution of the fission gas as a function of temperature can be more easily evaluated.

The first samples will be in the form of rectangles 1 in. long, 0.7 in. wide, and 0.030 in. thick. Two samples will be placed together so that the thermocouples can be sandwiched between them. Thermocouples will also be pressed against the outer surfaces of the samples, and the temperature difference between the inner and outer surfaces can be utilized for a comparative flux level evaluation in the initial part of the experiment. This method can also be used to evaluate thermal conductivity as a function or irradiation by comparing the changes in temperatures as a function of time. It is planned in the first experiments to irradiate the sample at constant power and to vary the temperature.

7. OUT-OF-PILE TESTING OF MATERIALS AND COMPONENTS

A series of reactor materials compatibility tests is under way in which reactor conditions are simulated, insofar as possible, in order to determine the extent of reactions of graphite and the impurities evolved from the graphite and the various other materials required in helium-cooled reactor systems. With these experiments, metals and alloys of interest for core structural components and reactor grades of graphite are heated together in vessels containing static helium or in helium-filled natural convection and forced-circulation loops. A complementary test with CO_2 as the coolant was completed.

Measures of the chemical reactivity of the various test specimens with the gaseous impurities evolved from graphite upon heating are obtained from these tests. Both TSF and AGOT grades of reactor graphite have been used to obtain a comparison of their gas impurity contents and degassing rates. Since oxygen, CO, or CO_2 impurities could cause mass transfer of carbon from the hot graphite to the cooler steam generator region of the reactor, thermal-convection loops with cold legs were designed to obtain evidence of carbon mass transfer. A forced-circulation loop is being built for investigating graphite erosion and the aerodynamic characteristics of fuel element bundles previously subjected to the collapsing forces of the reactor coolant gas at 300 psig. High-pressure thermal-convection loops are also being built to assist in these investigations. Experimental studies designed to yield quantitative information on the gases evolved by different types of graphite at various temperatures have also been initiated.

REACTOR MATERIALS COMPATIBILITY TESTS

Seven pot-type static-gas materials-compatibility tests and six low-pressure thermal-convection tests have been completed in the test facilities described previously.[1] Summaries of operating conditions and results of these tests are presented in Tables 7.1 and 7.2. Representative gas impurity data obtained by mass spectrometer analyses during the course of these tests

[1] The ORNL Gas-Cooled Reactor Materials and Hazards, ORNL-2505, p 12.33 (June 19, 1958).

Table 7.1. Summary of Conditions and Metallurgical Results of Pot-Type Static-Helium Materials-Compatibility Tests

Test No.	Maximum Temperature (°F)	Grade of Graphite	Total Elapsed Time of Test (hr)	Maximum Observed Impurity Concentration of Gas (vol %)	Specimens Included and Metallurgical Results
1	1400	TSF	1000	1.8 to 2.0	Stainless and low alloy steels, an Fe-Al alloy, columbium, Inconel, molybdenum, zirconium, and zirconium base-alloys: Zirconium and zirconium-base alloys showed heavy reaction layers comprised of ZrO_2 with minor amounts of ZrN; columbium and molybdenum specimens showed negligible weight changes and excellent resistance to attack; stainless steels ond Inconel exhibited na surface changes other than a very light tornish; low-alloy steels and an Fe-Al alloy were noticeably darkened along exposed surfaces, but weight changes were extremely small
2	1400	AGOT	1000	12.33	Specimens same as those of test No. 1: Zirconium and zirconium-base alloys showed somewhat heavier attack than in test No. 1; other specimens were similar in appearance and properties to comparoble specimens in test No. 1
3	1400	TSF	1000	6.66	Stainless and low-alloy steels: Small zone of decarburization noted along exposed surfaces of type 310 stainless and low-alloy steel specimens; other stainless steels were unaffected, except for slight tarnishing (identified as Fe_3O_4)
4*	1400	TSF	1000	3.72	Stainless and low-alloy steels: Light oxide films formed an all specimens; no other effects noted
5	1400	TSF	120	5.06	Stainless and low-alloy steels and beryllium: Test terminated after 20 hr at temperature because of a gas leak; beryllium specimens showed heavy ottack; other specimens not examined
6	1250	TSF	1000	1.39	Stainless and low-alloy steels and an Fe-Al alloy: All stainless steel specimens exhibited a thin (0.1 to 0.5 mil decarburizatian zone along exposed surfoce; type 304 stainless steel specimens exhibited an ocicular phase (presumably ferrite) below the decarburized layer; the Fe-Al alloy and the low-alloy steels showed very light oxide films but no evidence of decarburization
7	1400	TSF	1000	3.85	Beryllium: as described in chap. 5, a loosely adherent gray scale formed on the specimens; after-test thickness of metal was 0.022 in. compared with on initial thickness of 0.145 in.; film has not been positively identified but is believed to be a mixture of hydroxides and carbides of beryllium
8	1100	TSF	1000	3.62	Stainless and low-alloy steels and Fe-Al base allays: Data processing not yet completed

*A side arm was added to the pot and maintained at 500°F to promote circulation of the helium.

Table 7.2. Summary of Conditions and Metallurgical Results of Low-Pressure Thermal-Convection Loop Materials Compatibility Tests

Test No.	Maximum Temperature (°F)	Grade of Graphite	Total Elapsed Time of Test (hr)	Maximum Observed Impurity Concentration of Gas* (vol %)	Specimens Included and Metallurgical Results
1	1400	TSF	1000	2.78	Specimens same as those of static test No. 1: Results similar to those of static test No. 1; no apparent deposition of carbon in cold leg
2	1400	AGOT	1000	11.76	Specimens same as those in static test No. 1: Amount of attack of the various materials was heavier than in test No. 1; no apparent deposition of carbon in cold leg
3	1400	TSF	2100	7.59	Stainless and low-alloy steels: Light attack evident; no apparent deposition of carbon in cold leg
4	1000	TSF	350 (with helium) 1000 (with CO_2)	2.18 (with helium) 0.5 (with CO_2)	Stainless and low-alloy steels: Surface reactions evidenced by dark gray films on the low-alloy steels and black-irridescent films on the stainless steels; while not excessive, reaction layers (oxide films) were noticeably heavier than for comparable tests with helium at 1400°F; black deposits found in cold leg
5	1300	TSF	1000	4.43	Stainless and low-alloy steels: Data processing not yet completed

*Helium was used initially in all tests, but in test No. 4 the helium was replaced with CO_2 after 350 hr.

are presented in Figs. 7.1, 7.2, and 7.3. The quantities of impurities present in the gas are plotted rather than the total impurities evolved from the graphite because the impurities are constantly consumed by reaction with the metal test specimens and the metal containment vessel. Two reactor grades of graphite, National Carbon types AGOT and TSF, have been evaluated. The AGOT graphite was found to evolve approximately three to four times more impurities than were evolved by type TSF graphite. The procedure for all the tests with helium included heating to 500°F followed by 100 hr of steady-state operation, followed by heating to the final operating temperature, and then steady-state operation for the remainder of the test.

The gas analysis data indicate rapid outgassing of the graphite impurities during heating, with a slight increase in the impurity concentration of the gas during steady-state operation at 500°F. It thus appears that the impurities are not readily consumed by the metal at 500°F. Following heating to the maximum operating temperature, the impurity concentration of the gas was observed to decrease in each test. The maximum impurity concentration was found to be dependent on the maximum temperature and the grade of graphite. Following the initial impurity reduction, H_2 and the N_2 and Co mixture were found to represent approximately 80% of the total remaining impurities. Since N_2 and Co have the same mass numbers, they cannot be individually identified accurately by mass spectrometer analysis. In all tests the gaseous impurity trends were well established during the first 13 days. Therefore, the data plots presented are not extended beyond that time. The amount of each impurity present at the end of each test is listed in Table 7.3.

The reactions that occurred between structural metals and the gaseous environments in these tests were studied by means of weight-change determinations and metallographic examinations of the metal specimens. X-ray and electron diffraction studies were also made of the surface films formed on the specimens. With the exception of the zirconium and the beryllium specimens, evidences of reaction at the exposed surfaces of the specimens were slight and the weight changes were usually of the same magnitude as the limits of weighing precision. The low-alloy steels showed somewhat more surface film formation than the stainless steels, but the data indicate that they would be suitable as structural materials for helium-graphite systems.

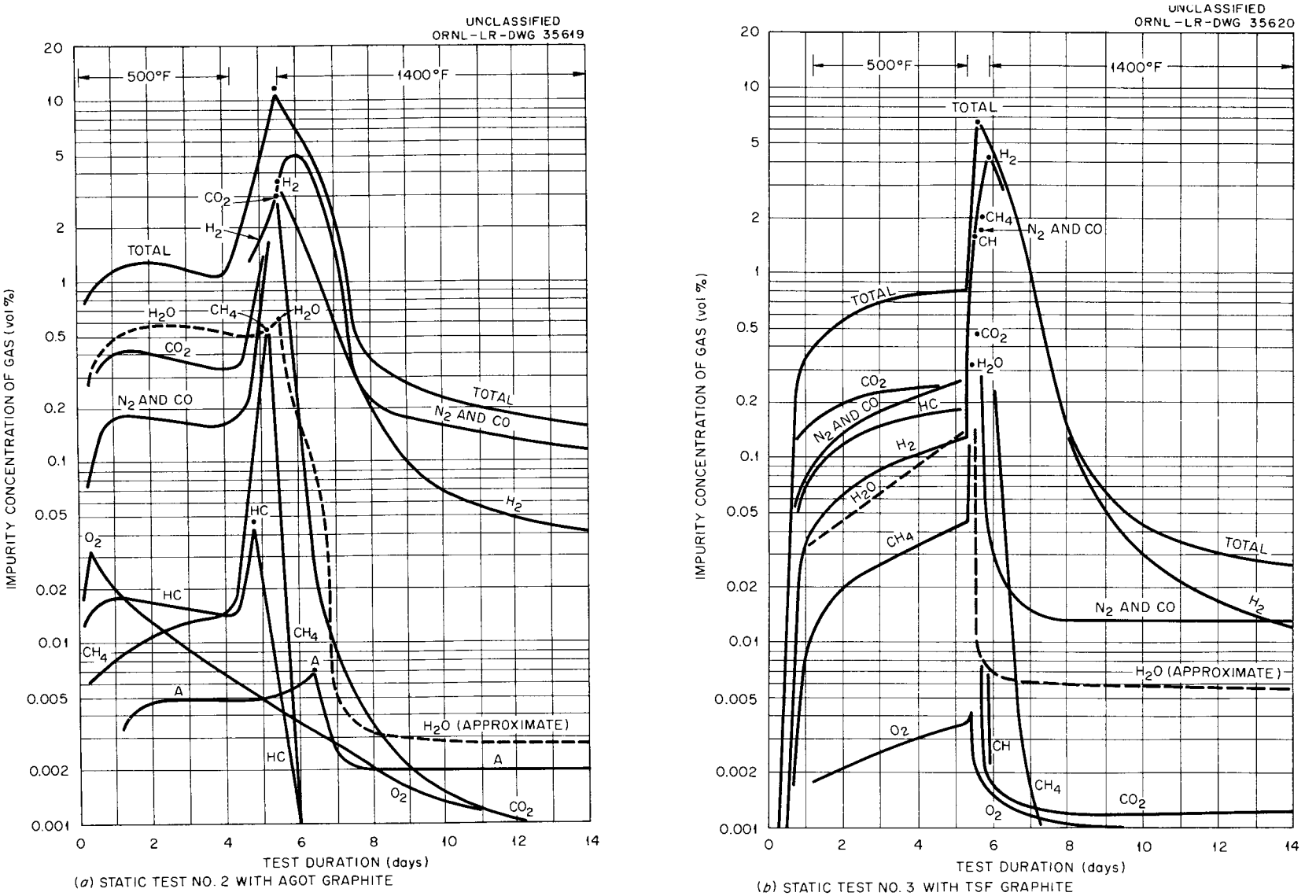

Fig. 7.1. Representative Impurity Concentration vs Time Curves from Static Helium Tests with AGOT and TSF Graphite at 1400°F.

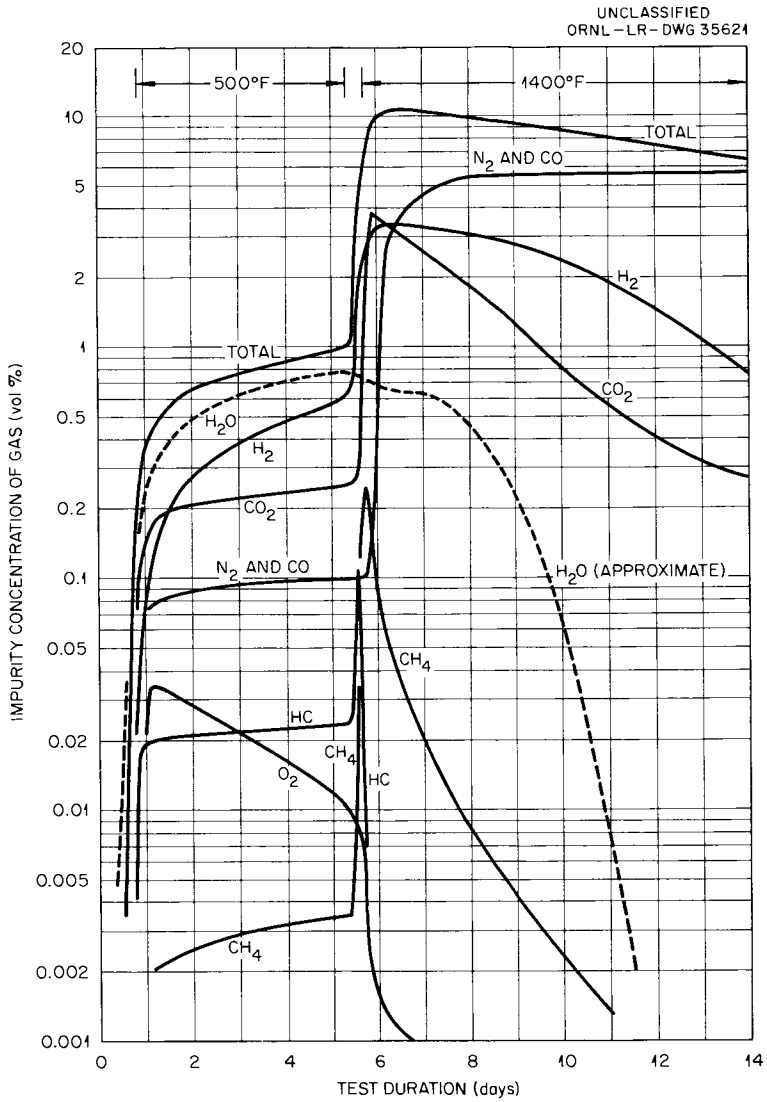

(*a*) THERMAL-CONVECTION TEST NO. 2 WITH AGOT GRAPHITE

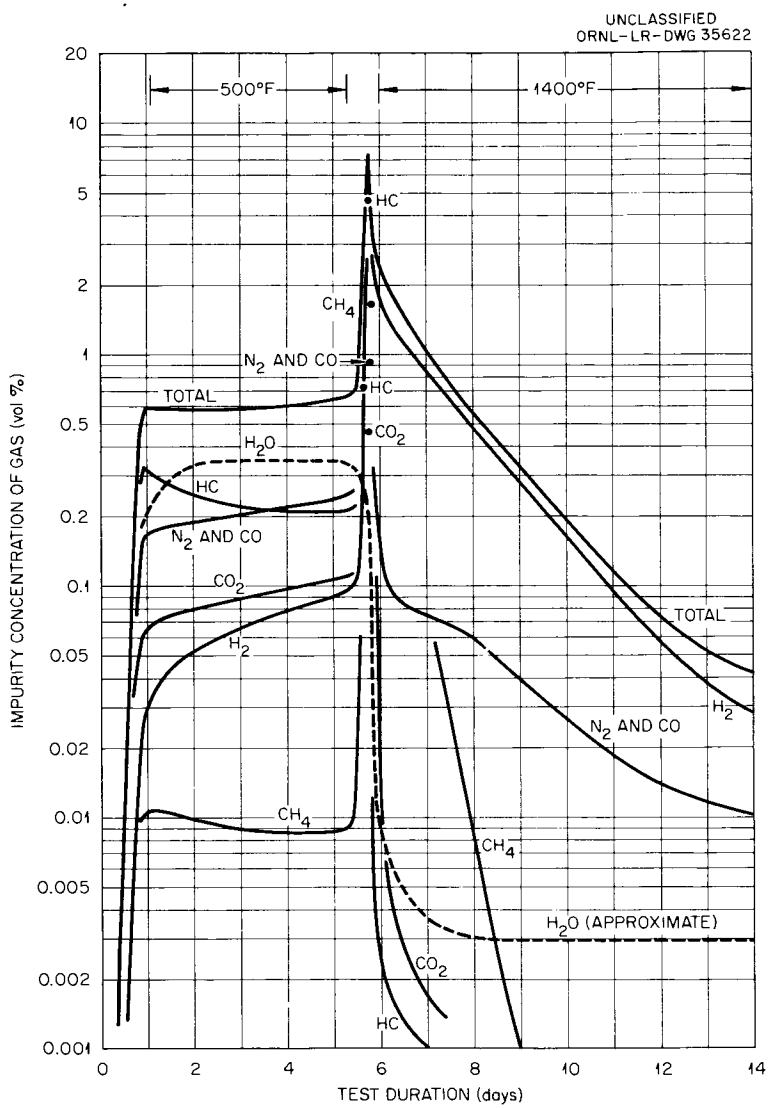

(*b*) THERMAL-CONVECTION TEST NO. 3 WITH TSF GRAPHITE

Fig. 7.2. Representative Impurity Concentration vs Time Curves from Low-Pressure Thermal-Convection Tests with AGOT and TSF Graphite at 1400°F.

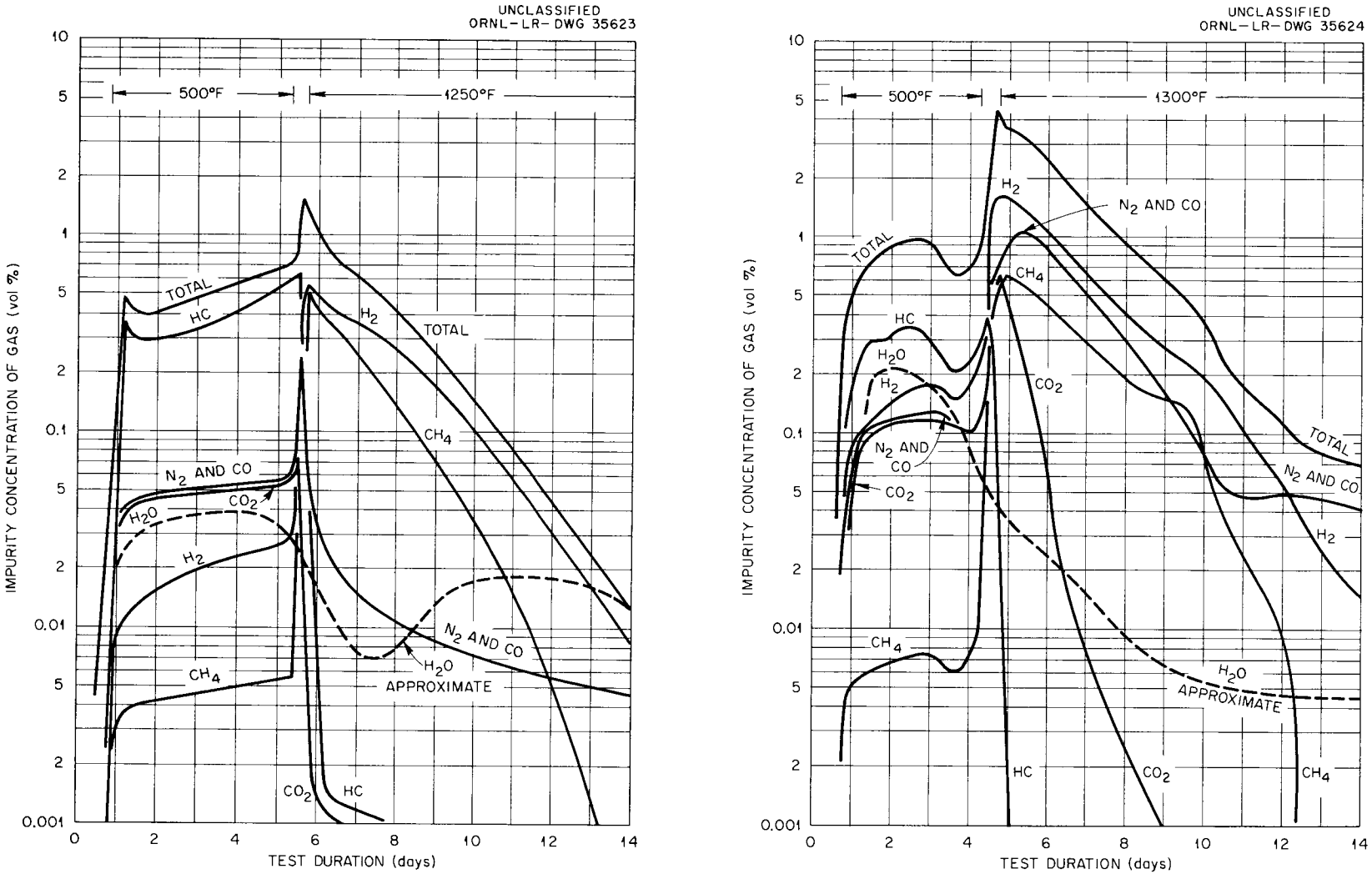

(*a*) STATIC TEST NO. 6 WITH TSF GRAPHITE.

(*b*) THERMAL-CONVECTION TEST NO. 5 WITH TSF GRAPHITE.

Fig. 7.3. Comparison of Representative Impurity Concentration vs Time Curves from Static Test No. 6 at 1250°F and Thermal-Convection Test No. 5 at 1300°F. TSF graphite was used in both tests.

Table 7.3. Results of Mass Spectrometer Analyses of Gases Remaining at Completion of Each Materials Compatibility Test

Test No.	Test Temperature (°F)	Gas Composition (vol %)									
		H_2	He	CH_4	H_2O	N_2 and/or CO	O_2	A	CO_2	Hydrocarbons	Total Impurities
						Static Tests					
1	1400	0.0069	99.981	<0.0001	0.0017	0.0086	0.0014	0.0006	<0.0001	<0.0001	0.0192
2	1400	0.0114	99.980	<0.0001	0.0017	0.0051	<0.0001	0.0018	<0.0001	0.0003	0.0203
3	1400	0.0046	99.990	<0.0001	0.0014	0.0039	<0.0001	0.0004	0.0001	<0.0001	0.0104
4	1400	0.0032	99.993	<0.0001	0.0009	0.0023	<0.0001	0.0003	0.0001	<0.0001	0.0068
5	Not analyzed; test terminated prior to completion										
6	1250	0.0009	99.978	<0.0001	0.0177*	0.0025	<0.0001	0.0002	0.0004	<0.0001	0.0217
7	1400	0.0027	99.990	<0.0001	0.0046	0.0020	<0.0001	0.0003	0.0001	<0.0001	0.0097
						Thermal-Convection Tests					
1	1400	0.0099	92.219	<0.0001	<0.0001	0.0032	<0.0001	7.77**	0.0003	<0.0001	0.0134
2	1400	0.0035	99.828	<0.0001	0.0009	0.1640	<0.0001	0.0022	0.0009	<0.0001	0.1715
3	1400	0.0034	99.990	<0.0001	0.0006	0.0046	<0.0001	0.0011	0.0009	<0.0001	0.0106
4	1000		0.56		0.06	0.9300	0.01	0.01	98.43		
5	1300	Data processing not yet completed									

*Value known to be high due to residual water in mass spectrometer; not included in total impurities.

**Argon was used during welding operations and approximately 8 to 9 vol % remained in the vessel throughout the test.

No evidence of carburization as a result of direct contact of stainless or low-carbon steels with graphite was found.

Low-pressure thermal-convection loop test No. 4 was performed to determine the compatibility of CO_2 and specimens of stainless and low-alloy steels in a loop containing TSF graphite at 1000°F. The metal specimens showed more oxidation than those tested with helium at 1400°F. In addition, the cold leg, which was maintained at 500°F, contained traces of carbon.

The effects of the test on the mechanical properties of the various stainless steels were evaluated in microhardness tests and tensile tests at 70 and 1400°F. In general, it was found that the changes in mechanical properties were only those which could be attributed to the annealing that occurred at the relatively high test temperatures. The dummy fuel element assemblies and support structures included in the thermal-convection loops showed no evidences of mechanical distortion or failure.

Construction has been started on a forced-circulation loop designed for studying the effects of high gas velocities and erosion by gas-borne dust particles. It is also proposed to utilize this facility to perform impurity addition studies in which conditions that might exist in a reactor because of in-leakage of impurities or the use of a nonstandard grade of graphite can be simulated. In addition, the facility will be utilized to evaluate various types of gas purification systems. The final loop design is essentially the same as that described previously,[2] except that it includes the GCPR fuel channel design rather than the GCR-2 design. All major components of the loop are on hand, except the compressor, which is being supplied by the AiResearch Division of the Garrett Corporation.

Two high-pressure thermal-convection loops are also being constructed for evaluating the effects of high gas pressures on graphite outgassing characteristics and on fuel capsule materials. These loops, in conjunction with the forced-circulation loop, will provide facilities for evaluating the integrity of full-scale fuel element assemblies under all proposed reactor operating conditions except nuclear radiation.

---

[2] Ibid., p 12.41.

GAS EVOLUTION BY GRAPHITE

The possible materials problems associated with projected use of helium as the coolant at high outlet temperatures in graphite-moderated reactors are being investigated. Although pure helium is available, it is anticipated that contamination of the helium by water vapor, carbon dioxide, carbon monoxide, oxygen, hydrogen, nitrogen, and hydrocarbons may occur from such sources as leaks in the valves, seals, heat exchanger tubes, and the outgassing of the graphite, as in the experimental systems described in the preceding section. The contaminants resulting from the outgassing will probably be the most important during startup and early stages of operation of the reactor. The reaction

$$C + CO_2 \rightleftharpoons 2\ CO \quad ,$$

which can produce burnout of graphite in the hot regions and deposition of carbon in the cooler areas of the reactor, is of particular importance, since most of the oxygen present in the gas either as oxygen or in the water vapor will react with the graphite to yield carbon dioxide. The possible interaction of the contaminants with the metal surfaces, especially the fuel element cladding, must also be considered, as discussed in Chapter 5.

Experimental studies designed to yield information on the quantity and composition of the gas evolved by different types of graphite at various temperatures have been started. It is planned to investigate such factors as the geometry of the graphite specimen and the effect of exposure of graphite specimens to various atmospheres. The results of these experiments should permit an evaluation of the level of contaminants likely to occur in the helium, assist in an appraisal of the interaction of these contaminants with the graphite and the metal surfaces, and aid in the design of the purification system for the helium.

A general view of the apparatus used in the gas evolution studies is presented in Fig. 7.4. In the use of this equipment, the graphite specimen is loaded into a quartz tube and the entire system is pumped down to 1 to 2-μ with the graphite specimen at room temperature and the sample bulbs in place. The specimen is heated by means of a tube furnace to temperatures in the range 200 to 1000°C. The heating period at any particular temperature is

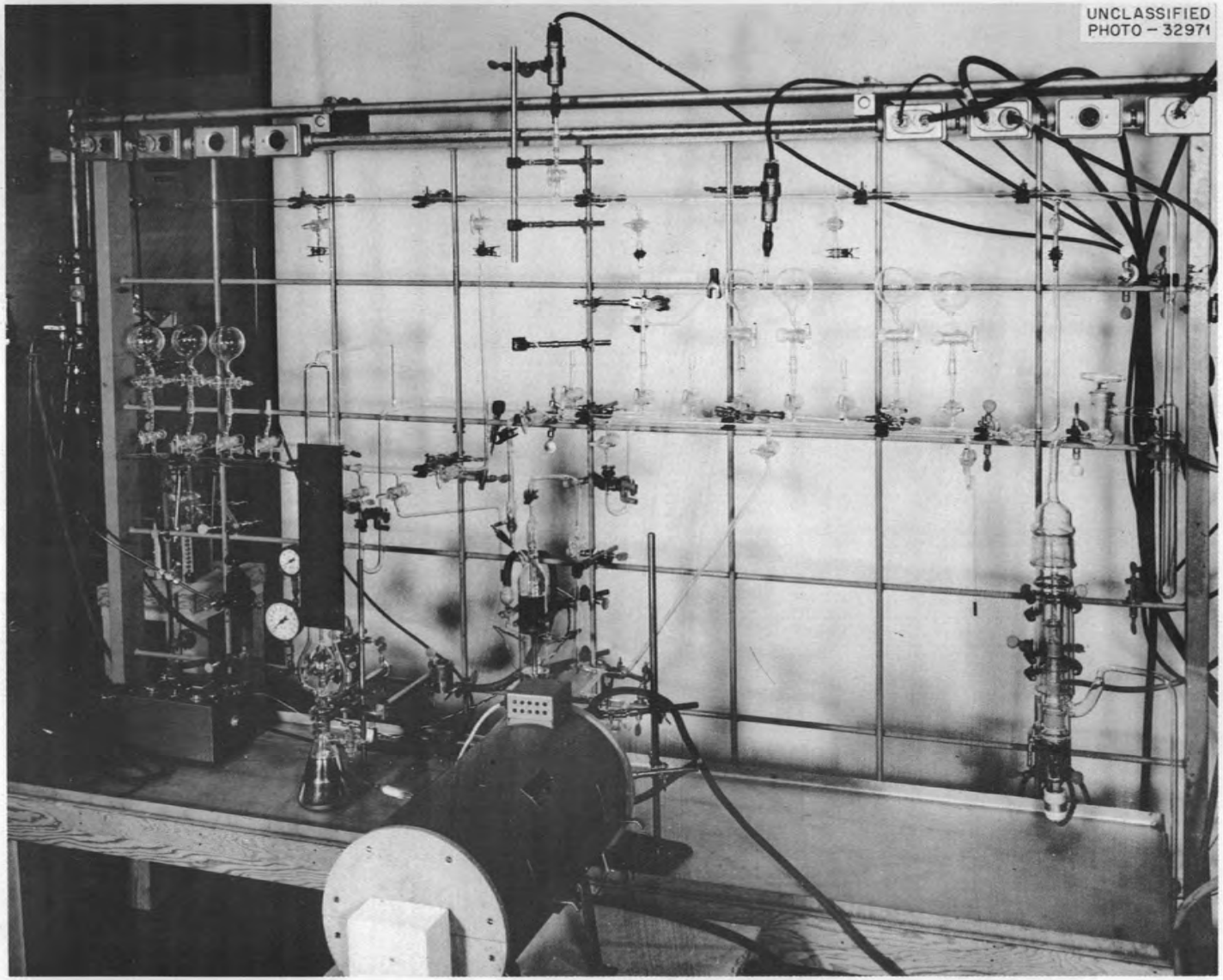

Fig. 7.4. Apparatus for Studying the Gas Evolution of Graphite at Various Temperatures.

1 1/2 to 3 hr; usually a longer time is required for evolution of the gas at the higher temperatures than at the lower temperatures for the same specimen. (Most of the gas is evolved in the first 30 min.) The evolved gas is pumped out of the quartz tube by a Toepler pump into the previously evacuated manifold and attached gas sample bulbs. The volume of collected gas is determined from the volume of the system and the pressure as measured by a McLeod gage, and the composition of the gas is obtained by mass spectrometer analysis. An additional manifold is provided for use in collecting the gas evolved by induction heating of graphite at temperatures above the 1000°C limit of the tube furnace now in use.

All the data presented here were obtained for graphite specimens 3/4 in. in diameter and 2 in. in length. Studies have been started recently for which 1 1/2- by 2-in. specimens are used, and it is planned to investigate larger specimens in the future. Gas sample bulbs of approximately 200-cm^3 capacity are normally used, although larger bulbs may be utilized if necessary. As mentioned previously the composition of the evolved gas is determined by mass spectrometer analysis which routinely gives mass 28 values that do not distinguish between nitrogen and carbon monoxide. The limited data available indicate, however, that at temperatures above 700°C mass 28 is principally carbon monoxide and below 600°C it is mainly nitrogen. It is planned to supplement the mass spectrometer analysis with gas chromotography in the future to obtain more reliable values for carbon monoxide and nitrogen.

The evolved gas is pumped away from the graphite sample at the designated temperature and then pumped out of the manifold before collection of gas begins at the next higher temperature. This means that the volume of gas reported for any given temperature is the quantity collected between that temperature and the next lower temperature. The volume of gas is arbitrarily reported as cubic centimeters at standard conditions per 100 cm^3 of graphite. The densities of the graphite samples studied ranged from 1.65 to 1.75 g/cm^3.

Information concerning the graphite samples used in these studies is presented below:

AGOT-I.- This graphite was manufactured by National Carbon Company in July 1957, stored indoors with a cover over the stack, and wrapped in paper just prior to shipment to ORNL in December 1957. The bars were cut shortly

after arrival, and the pieces were stored in polyethylene bags until machined in late October 1958 just prior to initiation of the gas evolution studies.

AGOT-II.- This graphite was received in May 1958 as 8 x 8 x 51-in. bars shortly after its manufacture by National Carbon Company. The bars arrived wrapped in paper and remained covered until machined in late October 1958. The specimens were stored in polyethylene bags until used.

TSF-I - This gas-purified graphite was manufactured by the National Carbon Company in December 1956. The pieces were individually wrapped in paper and stored for approximately one year prior to receipt at Y-12. The bars were cut shortly after arrival in December 1957, and the pieces were stored in polyethylene bags before and after machining in late October 1958.

TSF-II - This material arrived at Y-12 in August 1958 shortly after its manufacture by National Carbon Company. The 8 x 8 x 51-in. bars had been individually wrapped in paper immediately after being cooled under argon. Specimens for the gas-evolution studies were machined from pieces previously machined for use in the engineering studies described above. The specimens were stored in polyethylene bags until degassed.

TSF-III - Less is known about the history of this graphite. It was obtained as 4 x 4 x 51-in. bars in late November 1957 from the National Carbon Company. It was stored wrapped for approximately six months and then exposed to laboratory atmosphere for nearly six months prior to machining for use in the gas-evolution studies.

Great Lakes Graphite.- This material was manufactured by Great Lakes Carbon Company in May 1958 at the Morganton, North Carolina, plant. It was wrapped in paper soon after removal from the furnace and stored intact until specimens were cut from the 4 x 4 x 6-in. block in late October 1958. No details of manufacture are available, but it is probably a gas-purified graphite that was cooled under argon.

The results of the gas-evolution studies in the temperature range 200 to 1000°C are presented in Tables 7.4 through 7.9 for all the types of graphite studied. The data for AGOT-I and TSF-II are compared in Figs. 7.5 and 7.6.

Excluding the data obtained from TSF-III, it may be seen that there is no marked difference in the volume of gas evolved by the AGOT and TSF types of graphite. The TSF probably evolves somewhat less gas. There are some

Table 7.4. Volume and Composition of Gas Evolved by AGOT-I

Temperature (°C)	Volume of Gas (cm^3/100 cm^3 of Graphite)	Gas Constituents[a]											
		H_2		H_2O		CO_2		N_2 + CO		O_2		CH_4 + Other Hydrocarbons	
		vol %	cm^3	vol %	cm^3	vol %	cm^3	vol %	cm^3	vol %	cm^3	vol %	cm^3
200[b]	1.2	1.0	0.0	70	0.8	3.0	0.0	11.0	0.1	3.0	0.0	6.0	0.1
400[c]	1.8	(3)	(0.1)	(50)	(0.9)	(20)	(0.4)	(14)	(0.3)	(3)	(0.1)	(10)	(0.2)
500	2.2	7.0	0.2	12.0	0.3	39	0.9	29	0.6	2.0	0.0	8.0	0.2
600	2.6	11.0	0.3	3.0	0.1	50	1.3	32	0.8	0.5	0.0	3.0	0.1
700	2.5	15.0	0.4	6.0	0.2	37	0.9	41	1.0	0.2	0.0	0.4	0.0
800	5.7	28	1.6	2	0.1	25	1.2	48	2.7	0.1	0.0	0.6	0.0
900	6.3	44	2.8	5.0	0.3	1.0	0.1	50	3.2	0.1	0.0		0.0
1000	10.1	55	5.6	0.2	0.0	0.3	0.0	43	4.4	0.1	0.0		0.0
Total	32.4		11.0		2.7		4.8		13.1		0.1		0.6

[a]All cubic centimeter values normalized to 100 cm^3 of graphite and rounded off.
[b]3.0% H_2S reported at 200 and 500°C.
[c]Sample leaked prior to analysis; composition estimated from other data for AGOT-I.

Table 7.5. Volume and Composition of Gas Evolved by AGOT-II

Temperature (°C)	Volume of Gas (cm^3/100 cm^3 of Graphite)	Gas Constituents[a]											
		H_2		H_2O		CO_2		N_2 + CO		O_2		CH_4 + Other Hydrocarbons	
		vol %	cm^3	vol %	cm^3	vol %	cm^3	vol %	cm^3	vol %	cm^3	vol %	cm^3
200	1.2	0.9	0.0	74	0.9	0.2	0.0	20	0.2	3.9	0.0	0.6	0.0
300[b]	0.8	(1)	(0.0)	(70)	(0.6)	(10)	(0.1)	(16)	(0.1)	(2)	(0.0)	(1)	(0.0)
400[c]	1.0	1.3	0.0	77	0.8	9.8	0.1	6.7	0.1			1.8	0.0
500	1.0	2.8	0.0	27	0.3	42	0.4	17	0.2	0.3	0.0	5.6	0.1
600	2.8	2.1	0.1	7.4	0.2	71	2.0	9.8	0.3			1.3	0.0
700	1.4	7.5	0.1	14	0.2	49	0.7	13.6	0.2			2.3	0.0
800	4.1	6.8	0.3	3.6	0.1	55	2.3	22	0.8			0.8	0.0
900	5.2	32	1.7	1.5	0.1	2.6	0.1	63	3.3	0.1	0.0	0.5	0.0
1000	5.8	36	2.1	1.2	0.1	0.4	0.0	59	3.4	0.1	0.0		
Total	23.3		4.3		3.3		5.7		8.6				0.1

[a]All cubic centimeter values normalized to 100 cm^3 of graphite and rounded off.

[b]Sample leaked prior to analysis; composition estimated.

[c]1.5% H_2S reported at 400 and 500°C; 1 to 13% SO_2 reported in range 400–700°C, equivalent to 0.8 cm^3/100 cm^3 of graphite.

Table 7.6. Volume and Composition of Gas Evolved by TSF-I

Temperature (°C)	Volume of Gas (cm^3/100 cm^3 of Graphite)	Gas Constituents[a]											
		H^2		H_2O		CO_2		$N_2 + CO$		O_2		CH_4 + Other Hydrocarbons	
		vol %	cm^3	vol %	cm^3	vol %	cm^3	vol %	cm^3	vol %	cm^3	vol %	cm^3
200	1.0	5.0	0.1	16	0.2	8.0	0.1	61	0.6	9.0	0.1	1.0	0.0
400	1.9			55	1.0	7.0	0.1	38	0.7				
600	2.2	30	0.7	5.0	0.1	21	0.5	36	0.8	1.0	0.0	6.0	0.1
800	4.1	75	3.1	4.0	0.2	2.0	0.1	15.0	0.6	0.1	0.0	4.0	0.2
1000	9.1	92	8.4	1.0	0.1	0.1	0.0	6.0	0.6			1.0	0.1
Total	18.3		12.3		1.6		0.8		3.3		0.1		0.4

[a]All cubic centimeter values normalized to 100 cm^3 of graphite and rounded off.

Table 7.7. Volume and Composition of Gas Evolved by TSF-II

Temperature (°C)	Volume of Gas (cm^3/100 cm^3 of Graphite)	Gas Constituents[a]											
		H_2		H_2O		CO_2		$N_2 + CO$		O_2		CH_4 + Other Hydrocarbons	
		vol %	cm^3	vol %	cm^3	vol %	cm^3	vol %	cm^3	vol %	cm^3	vol %	cm^3
200	1.6	1.4	0.0	73	1.2	0.6	0.0	11.9	0.2	2.2	0.0	11	0.2
300	1.1	2.7	0.0	52	0.6	2.9	0.0	12.4	0.1	0.3	0.0	30	0.3
400	1.1	3.7	0.0	40	0.4	9.8	0.1	20	0.2	0.3	0.0	25	0.3
500	1.4	8.1	0.1	34	0.5	19.7	0.3	23	0.3	0.2	0.0	15	0.2
600	2.4	16.2	0.4	11.3	0.3	25	0.6	35	0.8	0.05	0.0	12	0.3
700[b]	3.2	55	1.8	6.6	0.2	7.7	0.2	18.4	0.6			12	0.4
800	3.5	82	2.9	1.3	0.0	0.8	0.0	11.5	0.4	0.1	0.0	4	0.1
900	4.8	88	4.2	0.4	0.0	0.2	0.0	10.0	0.5			0.6	0.0
1000	7.2	94	6.8	0.3	0.0	0.1	0.0	5.8	0.4				
Total	26.3		16.2		3.2		1.2		3.5				1.8

[a]All cubic centimeter values normalized to 100 cm^3 of graphite and rounded off.
[b]0.6% of A reported at 700°C, not determinable at other temperatures.

Table 7.8. Volume and Composition of Gas Evolved by TSF-III

Temperature (°C)	Volume of Gas (cm^3/100 cm^3 of Graphite)	Gas Constituents[a]											
		H_2		H_2O		CO_2		N_2 + CO		O_2		CH_4 + Other Hydrocarbons	
		vol %	cm^3	vol %	cm^3	vol %	cm^3	vol %	cm^3	vol %	cm^3	vol %	cm^3
200	0.7	2.3	0.0	36	0.3	2.7	0.0	52	0.4	6.0	0.0		
400	0.5	2.7	0.0	55	0.3	5.0	0.0	27	0.1	1.3	0.0	8.1	0.0
500	0.3	9.5	0.0	18	0.1	9.1	0.0	39	0.1	1.6	0.0	22	0.1
600	0.3	20	0.1	36	0.1	7.8	0.0	20	0.1	0.8	0.0	15	0.0
700[b]	0.7	29	0.2	19	0.1	3.7	0.0	19	0.1	0.5	0.0	27	0.2
800	1.0	58	0.6	5	0.1	1.0	0.0	16.0	0.2	0.3	0.0	18	0.2
900	1.0	71	0.7	10	0.1	0.6	0.0	12.0	0.1	0.1	0.0	5.7	0.1
1000	1.0	76	0.8	5	0.1	0.4	0.0	16.5	0.2	0.1	0.0	1.6	0.0
Total	5.5		2.4		1.2		~0.1		1.3				0.6

[a]All cubic centimeter values normalized to 100 cm^3 of graphite and rounded off.
[b]1.3% of A reported at 700°C, other temperatures gave A values ranging from 0.1 to 1.0%.

Table 7.9. Volume and Composition of Gas Evolved by Great Lakes Company Graphite

Temperature (°C)	Volume of Gas (cm^3/100 cm^3 of Graphite)	Gas Constituents[a]											
		H_2		H_2O		CO_2		N_2 + CO		O_2		CH_4 + Other Hydrocarbons	
		vol %	cm^3	vol %	cm^3	vol %	cm^3	vol %	cm^3	vol %	cm^3	vol %	cm^3
200	0.3	2.3	0.0	48	0.1	4.1	0.0	21	0.1	2.1	0.0	22	0.1
400	0.6	2.1	0.0	38	0.2	11.3	0.1	23	0.1	0.5	0.0	25	0.2
600[b]	1.6	15.8	0.3	15.4	0.3	18.5	0.3	34	0.5	0.3	0.0	15	0.2
800	2.8	74	2.1	0.5	0.0	2.3	0.1	18.6	0.5	0.1	0.0	4	0.1
1000	5.1	85	4.3	0.9	0.0	0.2	0.0	13.1	0.7	0.1	0.0	0.3	0.0
Total	10.4		6.7		0.6		0.5		1.9				0.6

[a]All cubic centimeter values normalized to 100 cm^3 of graphite and rounded off.
[b]0.4% H_2S reported at 600° C; approximately 0.5% of A reported at 200, 400, and 600° C.

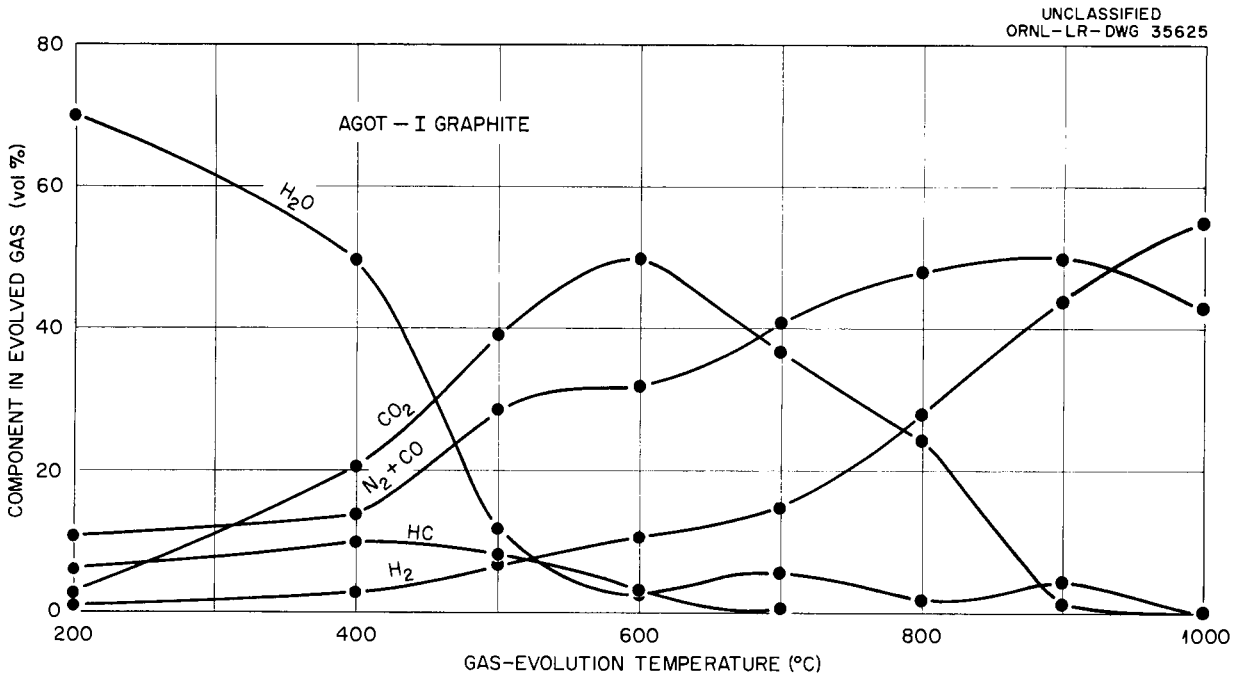

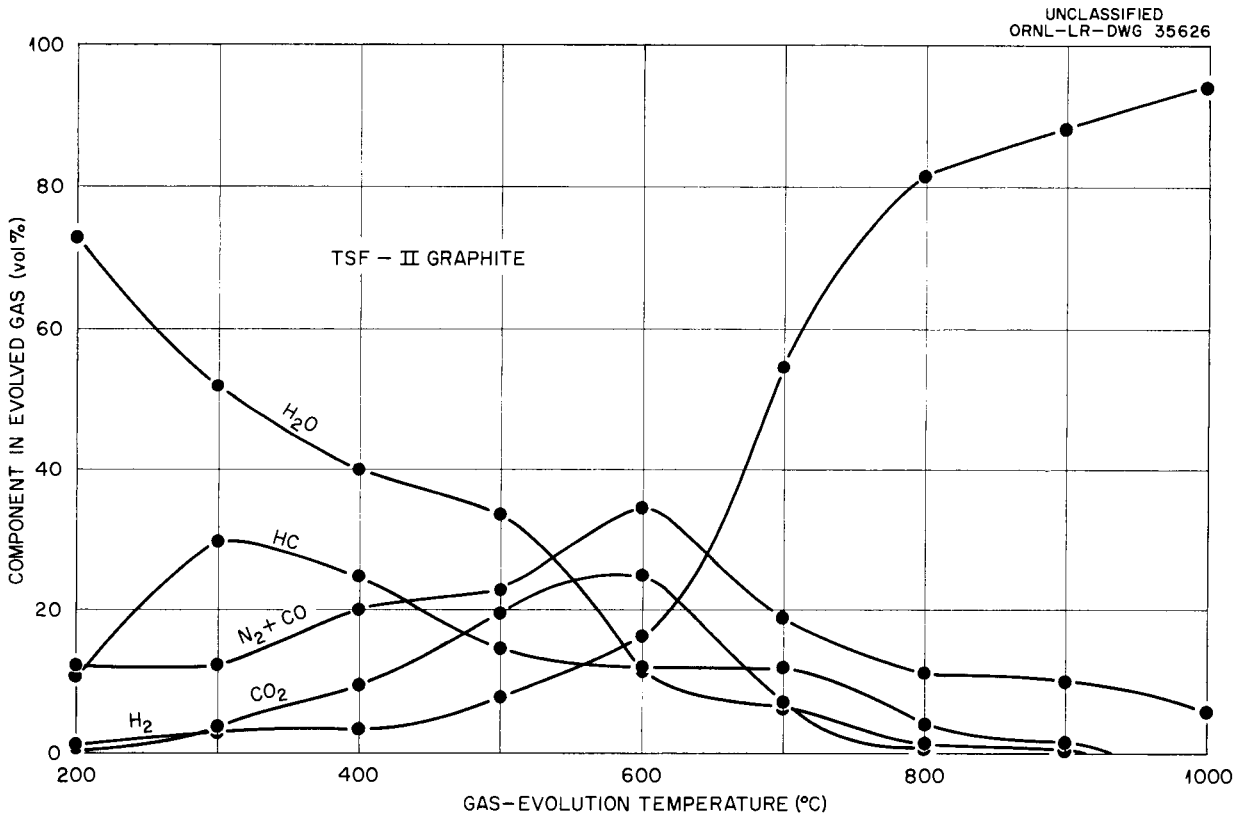

Fig. 7.5. Volume and Composition of Gases Evolved by AGOT-I and TSF-II Graphite at Various Temperatures.

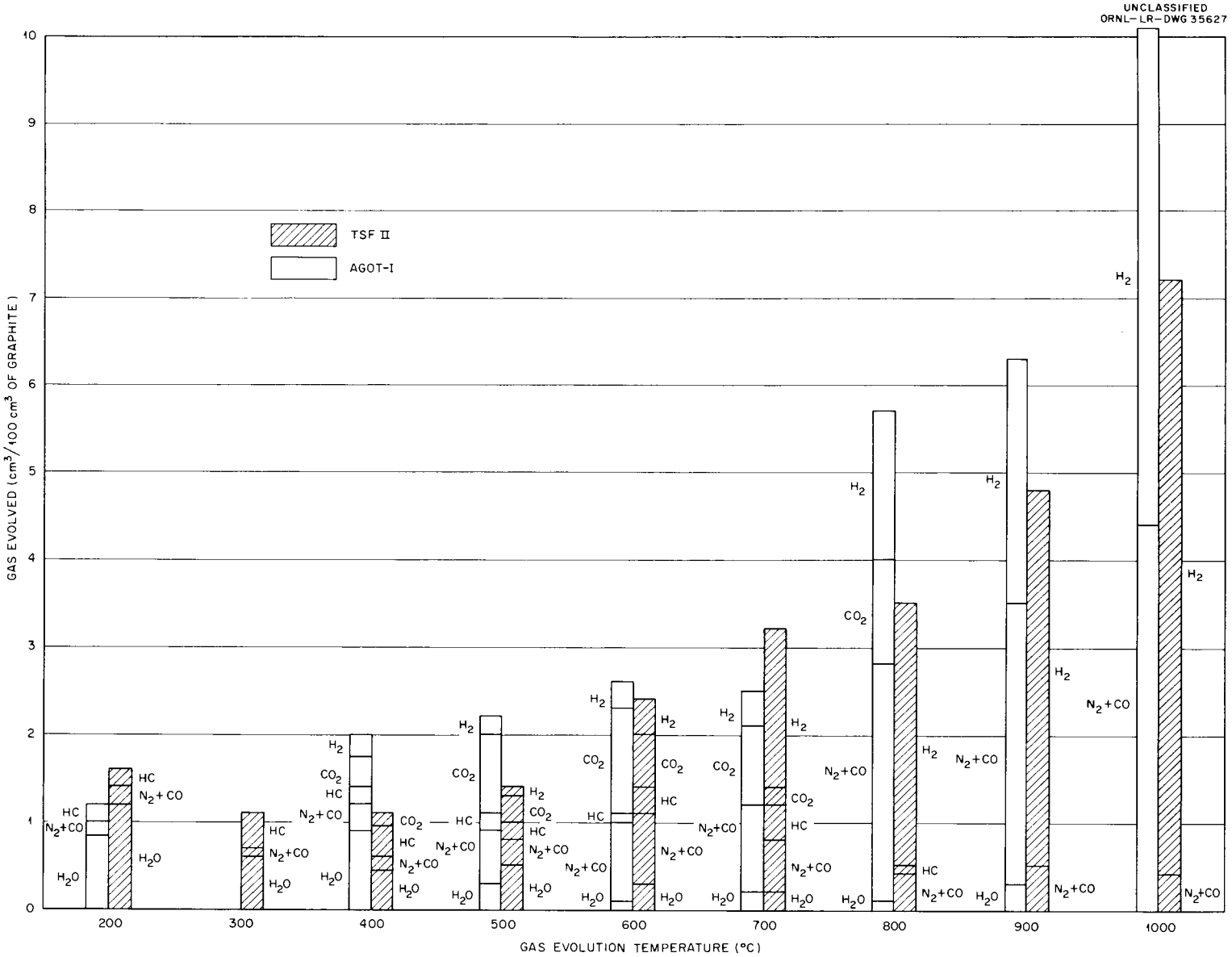

Fig. 7.6. Volumes of the Various Gases Evolved by AGOT-I and TSF-II Graphite in the Temperature Range 200 to 1000°C.

important differences in the compositions of the gases evolved, however, as may be seen in Figs. 7.5 and 7.6. The percentages of hydrogen and hydrocarbons are higher in the gas evolved by TSF graphite than in that evolved from AGOT graphite. The percentage of carbon dioxide is less for the TSF graphite at most temperatures and the percentage of carbon monoxide is considerably lower in the case of TSF graphite at the higher temperatures. It appears that AGOT graphite contains considerably more oxygen (as water or chemisorbed oxygen) than does the TSF graphite, as evidenced by the large quantities of carbon monoxide evolved by AGOT graphite at 700°C and above; TSF graphite evolves principally hydrogen above 700°C. The behavior of the water vapor is comparable for the two graphites in that it is not evolved as such to any extent above 600°C because of interaction with the graphite, and it is essentially absent from the gas evolved above 700°C. A maximum in the carbon dioxide content of the evolved gas is noted at 600°C for both types of graphite. At higher temperatures, conversion to carbon monoxide through the reaction $C + CO_2 \rightleftharpoons 2CO$ is particularly evident in the case of AGOT graphite.

A comparison of the total volume of gas evolved by the two AGOT graphites shows that AGOT-II evolved less gas than did AGOT-I. Such variations in heterogeneous materials probably should be expected. The very low values for the total gas evolved by TSF-III compared to values found for TSF-I and TSF-II is not readily explainable when it is remembered that this particular piece of graphite had been exposed to the atmosphere for an extended period of time.

As mentioned above, little is known about the manufacturing process used for the production of the graphite sample from Great Lakes Carbon Company. The relatively large volume of hydrogen evolved suggests that it is a gas-purified graphite (as is TSF), and the presence of argon in the evolved gas indicates that this graphite was cooled in an argon atmosphere.

Degassing studies of 1 1/2 x 2-in. specimens have been started. The data obtained for this size specimen, as well as that obtainable from larger specimens, should provide information concerning the effect of geometry on the volume of gas evolved in the temperature range 200 to 1000°C. Data will also be obtained at temperatures up to about 2000°C through the use of an induction heater. This apparatus is nearly complete and should be in operation shortly.

8. DEVELOPMENT OF TEST LOOPS AND COMPONENTS

LARGE ORR IN-PILE LOOP

A test facility is being designed for operation in the ORR that will provide data on radiation damage and heat transfer characteristics of advanced, experimental, gas-cooled reactor fuel elements. The present design criteria are a power generation rate of 40,000 Btu/ft·hr for a single 3/4-in.-dia rod at loop pressures from 300 to 400 psig and gas coolant temperatures of up to 1500°F. Flow sheets, test section and loop components designs, preliminary specifications for compressor and loop auxiliaries, and an estimated schedule and budget for detail design and construction are being prepared.

Considerable work was done previously on the design of similar facilities for the ORR to test fuel elements for specific reactor projects. The first of these was supported by the Army. The concept utilized two ORR vertical holes, with long pipe runs from the reactor to a room external to the reactor pools that housed most of the major loop components. This facility was designed to test fuel elements with a variety of gas coolants (N_2, He, CO_2, air) at a gas outlet temperature of 1500°F and pressure of 300 psig, with 100 kw maximum power generation in the fuel sample. Work on this concept had proceeded through the detailed design and into the procurement phase when a redesign of the facility was undertaken to make it suitable for operation at conditions of interest to the GCPR. For these considerations, a gas outlet temperature of 1000 to 1100°F was selected, with a pressure of 400 psig. Helium and CO_2 were both considered for the coolant gas, and a power generation rate comparable to that of the GCPR was contemplated. The design was conceived as a "package" to contain all loop components and the test section, and it was to be located in the ORR pool and to be removable and replaceable in one piece. Details of this concept have been reported.[1] A review of this preliminary design study brought about a change in the objectives, and the loop is now being designed, as stated above, to provide a facility for irradiation and study of advanced fuel elements.

---

[1] J. R. McWherter et al., Proposed Gas-Cooled In-Pile Facility, ORNL CF-58-12-42 (December 15, 1958).

SPECIAL GAS COMPRESSORS

A number of small (100 to 500 cfm) gas compressors needed for in-pile and out-of-pile forced-circulation loop tests are being developed because commercially available compressors are not sufficiently leaktight and cannot be operated at the required pressures and temperatures.

Since gas temperatures in the loops will exceed 1000°F heat transfer equipment will be most economical if the gas temperature at the compressor is as high as possible. Although suction temperatures of 1000 to 1400°F are desired, development initially of compressors for operation at 600°F appeared to be more certain. Low leakage requirements are being met by enclosing the centrifugal compressors, motors, and bearings in a housing containing the process gas for the loop.

Grease-Lubricated Compressors. The compressors for the large ORR in-pile loop were designed to each provide a flow of 210 cfm at 600°F and 400 psig for a pressure rise of 8 psi. No more than 0.4 g of contaminants were to be introduced into the system by the compressor in any 1000-hr period. A minimum maintenance-free operating period of 3000 hr was required. The compressor design was integrated with that of the loop package, since the space for it will be quite small, and fabrication is under way.

The ambient temperature of 600°F imposed the need for cooling the electric motor, and water cooling was selected so that rolling element bearings and conventional lubricants could be used. A compromise between aerodynamic design considerations and grease-lubricated-bearing life led to an impeller speed of 12,000 rpm. Bearing manufacturers predict useful lifetimes substantially in excess of 1000 hr.

A cross section of the compressor is shown in Fig. 8.1. Assembly of one unit is scheduled to start in February 1959.

Gas-Bearing Compressors. A need exists for reliable gas compressors capable of maintenance-free operation for periods approaching 10^4 hr, which is substantially longer than can be expected with grease-lubricated bearings. Compressors having gas-lubricated bearings should be ideal for this application. Initial design studies have been completed, and layout work will continue when data become available from the bearing tests discussed below.

A compressor with gas-lubricated bearings is being purchased for testing from the Armstrong-Siddeley Company, Great Britain, which has had extensive

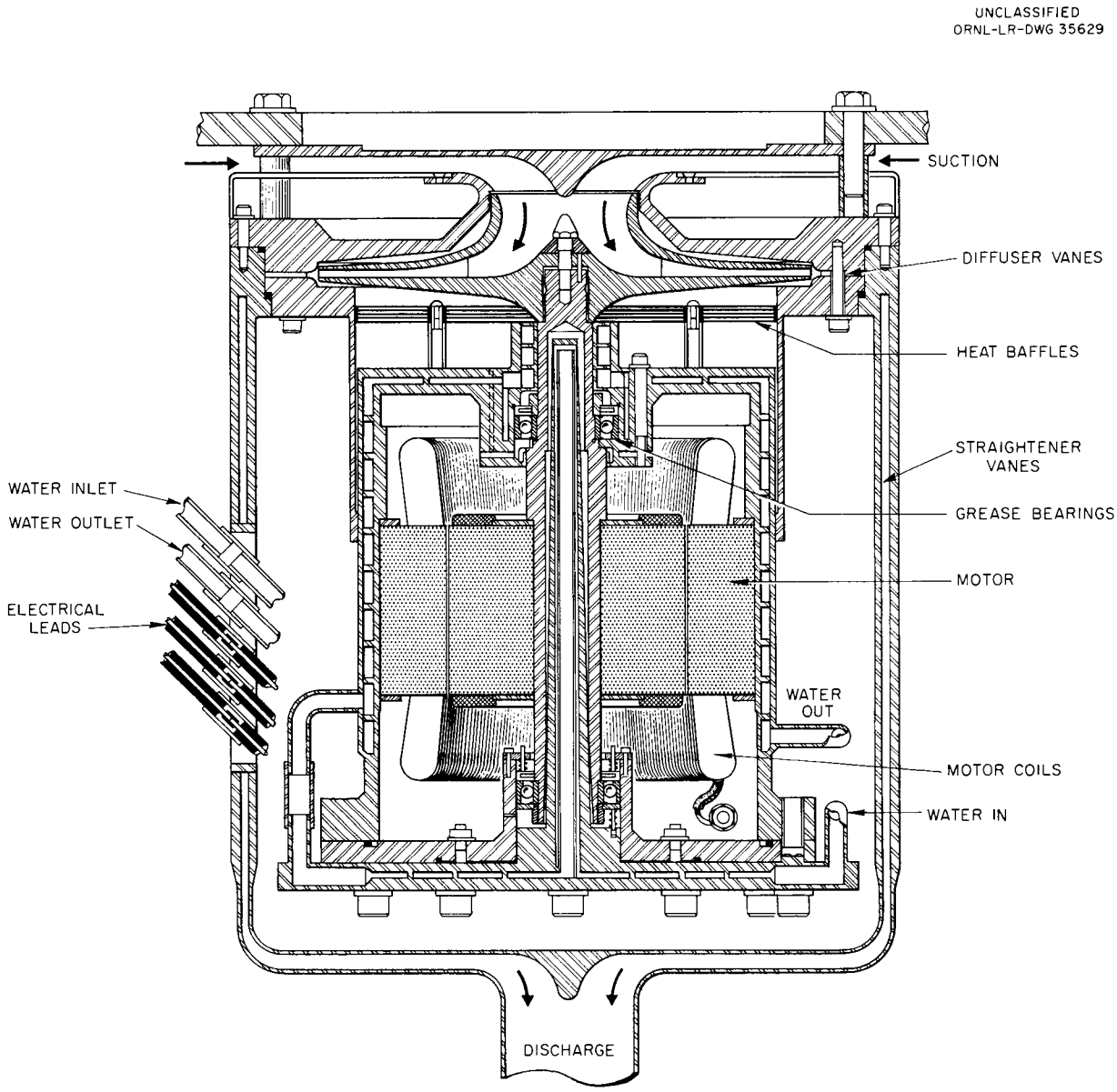

Fig. 8.1. Grease-Lubricated Compressor for Large ORR In-Pile Loop.

experience in this field. Their machine should demonstrate the feasibility of gas bearings and accelerate understanding of design requirements for compressors for high-temperature gas loops.

Parametric studies of pneumodynamic bearings for gas-bearing compressors have been initiated and a tester to confirm computations of bearing minimum film thickness and whirl suppression ability is being designed. Operation of the tester at 75°F and 250 psia with air will permit direct correlation with the compressor operating conditions of 600°F and 400 psig with helium. A search has been instituted for journal and bearing materials suitable for operation at 600°F and, possibly, up to 1000°F.

High-Temperature Electric Motors. A motor operable at 600 to 1000°F for use with gas-bearing compressors is being developed to provide improved compressor reliability through the elimination of water cooling. Three motors, each rated 12 hp at 24,000 rpm, suitable for use at 600°F have been purchased and are to be delivered in January 1959. A group of motorettes (small test units which simulate the insulation in electric motors) with the same insulation system as that to be used in the purchased motors are now under test at temperatures of 800 to 1200°F in helium.

Compressors for Argon Forced-Circulation Loop. A compressor to be used in a laboratory forced-circulation loop filled with argon, which was ordered from the AiResearch Manufacturing Company in June 1958, is to be delivered in February 1959. It is designed to produce a pressure rise of 7.0 psi in argon flowing at a rate of 475 cfm at 600°F under a pressure of 30 psig; it is to operate for 1000 hr without maintenance; and it is to meet the same contaminant requirements as precribed for the in-pile loop compressors. It is a single-stage centrifugal type with a 400-cycle totally enclosed motor and grease-lubricated ball bearings. The motor enclosure and the bearings are water cooled.

Supporting Activities. Three surplus gasoline- or diesel-driven, 400-cycle generators were obtained to supply power to the compressors. An existing area was modified to provide a clean assembly shop. A cold shakedown test stand was completed and a hot test stand was designed.

INTERNAL DISTRIBUTION

1. J. W. Allen
2. M. Bender
3. D. S. Billington
4. E. P. Blizard
5. A. L. Boch
6. C. J. Borkowski
7. W. F. Boudreau
8. G. E. Boyd
9. E. J. Breeding
10. R. B. Briggs
11. C. E. Center (K-25)
12. R. A. Charpie
13. J. H. Coobs
14. J. A. Conlin
15. W. B. Cottrell
16. F. L. Culler
17. H. N. Culver
18. J. H. DeVan
19. L. M. Doney
20. D. A. Douglas
21. L. B. Emlet (K-25)
22. E. P. Epler
23. H. L. Falkenberry
24. J. Foster
25. A. P. Fraas
26. J. H. Frye, Jr.
27. G. A. Garrett (K-25)
28. J. M. Googin (Y-12)
29. B. L. Greenstreet
30. W. R. Grimes
31. E. Guth
32. R. F. Hibbs (Y-12)
33. M. R. Hill
34. H. W. Hoffman
35. A. Hollaender
36. A. S. Householder
37. W. H. Jordan
38. C. P. Keim
39. M. T. Kelley
40. J. A. Lane
41. S. A. Levin (K-25)
42. R. S. Livingston
43. H. G. MacPherson
44. W. D. Manly
45. E. R. Mann
46. W. B. McDonald
47. F. R. McQuilkin
48. A. J. Miller
49. K. Z. Morgan
50. J. P. Murray (Y-12)
51. F. H. Neill
52. M. L. Nelson
53. L. G. Overholser
54. P. Patriarca
55. F. S. Patton (Y-12)
56. A. M. Perry
57. D. Phillips
58. M. E. Ramsay
59. P. M. Reyling
60. A. F. Rupp
61. G. Samuels
62. H. W. Savage
63. A. W. Savolainen
64. O. Sisman
65. E. D. Shipley
66. M. J. Skinner
67. A. H. Snell
68. E. Storto
69. R. D. Stulting
70. J. A. Swartout
71. E. H. Taylor
72. D. B. Trauger
73. E. Von Halle (K-25)
74. C. S. Walker
75. A. M. Weinberg
76. G. C. Williams
77. C. E. Winters
78. J. Zasler

79-82. ORNL - Y-12 Technical Library (4 copies) Document Reference Section

83-122. Laboratory Records Department (40)

123. Laboratory Records Department, R. C. (1)

124-126. Central Research Library (3)

EXTERNAL DISTRIBUTION

127. Division of Research and Development, AEC, ORO

128-710. Given distribution as shown in TID-4500 (14th ed.) under Reactors-Power category (75 copies - OTS)